CHAPTER 5 ENVIRONMENTAL SENSITIVITY OF BIREFRINGENT FIBRES

5.1 Introduction

Environmental factors such as pressure, bends, twists and magnetic fields can considerably modify the intrinsic birefringence of a fibre by detuning (beating) and transferring power (coupling) between the two polarised modes, resulting in a randomly varying output polarisation state.

In coherent detection systems[1, 2], fibre interferometers[3 - 6] and when interfacing to polarisation-sensitive integrated-optical components[7], a high-birefringence fibre is used to provide polarisation immunity from external influences[8]. A single polarised normal mode may be selected and sustained with minimal coupling to the orthogonally-polarised mode. The extinction ratio η of the power transferred from the launched mode to the other compared with the power in the original launched mode quantifies the polarisation-maintenance properties. As shown below, the degradation of this ratio by a disturbance depends on the magnitude as well as the spatial period of the birefringence introduced by the disturbance.

In complete contrast, for polarimetric sensors, fibre sensitivity to a given effect must be enhanced. Induced changes in intrinsic fibre birefringence, i.e. mode-beating, may be used as a measure of a given stimulus[9]. Alternatively, the power coupling between the modes may be exploited as in a Faraday-rotation current sensor[10, 11]. Ultra-low birefringence fibres[12, 13] are particularly suitable in this application. Fibre isolators[14, 15, 16] utilise the periodicity of mode-coupling in a fibre with controlled birefringence to obtain the required forty-five degrees of Faraday rotation.

In this Chapter, coupled-mode propagation[17-22] is studied theoretically to evaluate the performance of polarisation-maintaining fibres and sensors, assuming uniform (length-invariant) fibre disturbances. Although this assumption is valid in many sensor applications, in a real polarisation-maintaining fibre cable installation, the external influences are bound to be random in nature and vary along the fibre length. Detailed analysis of such a system would require statistical information on the likely distribution of disturbances which is not at present available. However, analysis of uniform environmental effects, such as a simple bend or twist, can still usefully provide comparisons and design criteria for polarisation-maintaining fibre cables and fibre sensors.

The present analysis[23,24] is an extension of the twisted-fibre analysis presented in Chapter Four[24, 25] and gives results in agreement with the work reported independently by Sakai and Kimura[18, 19]. In our case, we can present the results in terms of the fibre retardation R, rotation Ω and principal axis orientation ϕ. This is intuitively appealing and allows the analysis to be easily verified experimentally. In addition, we treat the cases of linearly- and circularly-birefringent fibres as well as 'spun' fibres.

Finally the design and use of fibres in practical applications is discussed.

5.2 Uniform Coupled-Mode Effects in Birefringent Fibres

The power exchange and mode beating between the fibre normal modes caused by any uniform (length-invariant) disturbance such as a single bend may be analysed by the approach applied to twisted fibres in Chapter Four.
The versatility and intuitive appeal of this analysis now becomes apparent.

Fibre disturbances may be classified into those inducing linear and circular birefringence (see Chapter Two). In this section we will analyse linearly-birefringent, circularly-birefringent and spun fibres in turn, with respect to these two general types of disturbance.
The general method is summarised as follows. First, the unperturbed fibre is considered as a series of linear retarders (for a linearly-birefringent fibre) or circular retarders (for a circularly-birefringent fibre)[25]. The disturbance in question is then introduced by interspersing the stack with the appropriate retarders or rotators (and any twist). For a disturbance such as a bend, the retarders are introduced with their principal axes oriented in the direction of the applied perturbation[23]. Note that as in Chapter Four, the waveguide modes within the fibre are approximated as plane waves[24]. A local Jones Calculus equation is then drawn up and the two coupled-mode equations obtained. These equations contain terms describing the mode-detuning and mode-coupling introduced[25], and yield a matrix equation describing the properties of the fibre in terms of the linearly polarised x and y electric vectors[24], or after suitable transformation, the circularly-polarised normal modes of a circularly-birefringent fibre. The general form of the eqation is:

$$\begin{bmatrix} A_1\ (z) \\ A_2\ (z) \end{bmatrix} = \begin{bmatrix} G & -H^* \\ H & G^* \end{bmatrix} \cdot \begin{bmatrix} A_1(O) \\ A_2(O) \end{bmatrix} \qquad (5.1)$$

where A_1, A_2 are the electric vectors of the two normal modes, and the asterisk denotes complex conjugation (c.f. equation (4.9))). This is equivalent to a retarder-rotator description of the fibre, as shown in section 4.5.

The performance of the fibre under the influence of the disturbance may be expressed in the form of the extinction ratio $\eta(z)$ when only one of the modes (A_1 (O)) is launched:

$$\eta(z) = \frac{|A_2\ (z)|^2}{|A_1\ (z)|^2} = \frac{q^2 \sin^2 \gamma z}{1 + q^2 \cos^2 \gamma z} \qquad (5.2)$$

where q depends on the ratio of the birefringence due to the disturbance $\delta\beta$, to the intrinsic fibre birefringence $\Delta\beta$ and is known as the "coupling strength"[17]. γ is the phase retardation of the two new normal modes and again depends on the ratio of $\delta\beta$ to $\Delta\beta$.

We now consider the two cases of weak and strong disturbances.

(a) Weak disturbances ($\delta\beta << \Delta\beta$)

In this case, the small birefringence $\delta\beta$ introduced is dominated by the comparatively large intrinsic birefringence $\Delta\beta$. Thus the phase propagation velocities of the two normal modes are largely unperturbed, giving $\gamma \simeq \Delta\beta/2$. The extinction ratio η is shown in Figure 5.1 as a function of fibre length z for $\Delta\beta = 180^\circ/m$ and $q = 0.05$. η oscillates along the fibre and at certain points all the power returns to the original polarised normal mode ($\eta = 0$). These points occur when $z \simeq 2\pi N/\Delta\beta = N L_p$, where N is an integer and L_p is the fibre beat length. Testing a high-birefringence fibre for its polarisation-holding capability under tight bending or twisting can lead to erroneous results if the length of the disturbance is not taken into account; a fibre can apparently exhibit excellent polarisation-holding if the disturbed length is equal to a multiple of the fibre beat length L_p, even though significant power transfer may have occurred in reality[26]. The poorest extinction ratio $\eta_{MIN} \simeq q^2$ occurs for $z \simeq (2N+1)\pi/\Delta\beta$ i.e. periodically at intervals of the fibre beat length L_p, alternating with the points of high extinction ratio. If the sign of $\delta\beta$ reversed every $L_p/2$, the power in the unwanted mode would increase progressively along the fibre[27]. Thus maximum power transfer into the unwanted mode occurs when the spatial period of the disturbance, u, is equal to the fibre beat length[26], a well-known coupled-mode theory result[22].

(b) Strong disturbances ($\delta\beta >> \Delta\beta$)

For a strong disturbance, the fibre birefringence $\Delta\beta$ is dominated by the birefringence $\delta\beta$ introduced, which now effectively governs the propagation to give $\gamma \simeq \delta\beta/2$, η oscillates along the fibre, all the power returning to the original mode after a distance $z \simeq 2\pi N/\delta\beta = Nu$, where u is the beat period of the disturbance. Conversely, maximum power ($\eta = q^2$) occurs at $z = (2N + 1) \pi/\delta\beta$ alternating with the points of zero power transfer[27]. The power transfer no longer depends on the spatial period of the disturbance relative to the intrinsic birefringence.

5.2.1 Linearly-birefringent fibres

(a) *Externally-induced linear birefringence*

Consider a fibre with linear birefringence $\Delta\beta$ subjected to a disturbance introducing a linear birefringence $\delta\beta$ (e.g. a bend) at an angle Θ to the principal axes of the fibre. As shown in Figure 5.2, the fibre is represented as a series of retarder elements interspersed with a second series at an azimuthal angle Θ to the first, which represent the perturbation $\delta\beta$. Each pair of retarders is δz thick. The local Jones Calculus equation for section A is:

$$\left[\bar{E}_A\right] = \begin{bmatrix} m_1 & m_2 \\ m_3 & m_4 \end{bmatrix} \cdot \begin{bmatrix} a_x & \hat{x}_A \\ a_y & \hat{y}_A \end{bmatrix} \qquad (5.3)$$

where

$$m_1 = e^{i\,\beta_x z}\left(\cos\frac{\delta\beta\delta z}{2} + i.\cos 2\Theta \sin\frac{\delta\beta\delta z}{2}\right)$$

$$m_2 = e^{i\,\beta_y z}.i.\sin 2\Theta\,\sin\frac{\delta\beta\delta z}{2}$$

$$m_3 = i.\sin 2\Theta.\sin \frac{\delta\beta\delta z}{2}.\, e^{i\,\beta_x z}$$

$$m_4 = e^{i\,\beta_y z}\left(\cos \frac{\delta\beta\delta z}{2} \quad -i.\cos 2\Theta.\sin \frac{\delta\beta\delta z}{2}\right)$$

and β_x, β_y, a_x, a_y, $\hat{x}_A$ and $\hat{y}_A$ are as defined in section 4.5.

Using equation (4.2) and following the procedure outlined in Section 4.5 we obtain the two coupled-mode equations:

$$\frac{d\,A_x}{dz} - i\beta_x\left(1 + \frac{\delta\beta}{2\beta_x}\cos 2\Theta\right)A_x = i\,\frac{\delta\beta}{2}\sin 2\Theta.\; A_y \qquad (5.4)$$

$$\frac{d\,A_y}{dz} - i\,\beta_y\left(1 - \frac{\delta\beta}{2\beta_y}\cos 2\Theta\right)A_y = \frac{i\,\delta\beta}{2}\sin 2\Theta.\; A_x \qquad (5.5)$$

where A_x, A_y are given by equations (4.7) and (4.8). These coupled-mode equations clearly demonstrate the interesting detuning (mode-beating) and coupling (interchange of power) arising in coupled-mode propagation[28, 29]. The propagation constants β_x and β_y are modified by $\pm \frac{\delta\beta}{2}\cos 2\Theta$, while the two original modes A_x and A_y are coupled with a coefficient $i\,\frac{\delta\beta}{2}\sin 2\Theta$. Thus, depending on the relative inclination Θ, the induced linear birefringence $\delta\beta$ detunes and couples the modes. The new normal modes are linearly-polarised because the coupling coefficient is imaginary[21]. For the trivial case $\Theta = 0^{\circ}$, all the retarder axes along the fibre line up to form a total birefringence $\delta\beta + \Delta\beta$, but the two original linear modes remain uncoupled. Conversely, for $\Theta = 45^{\circ}$, the birefringence $\delta\beta$ is equally inclined to both fibre principal axes resulting in zero detuning or incremental birefringence, while the original modes are maximally coupled.

The equations (5.4) and (5.5) can be solved to give

$$\begin{bmatrix} A_x(z) \\ A_y(z) \end{bmatrix} = \begin{bmatrix} G & -H^* \\ H & G^* \end{bmatrix} \begin{bmatrix} A_x(0) \\ A_y(0) \end{bmatrix} \qquad (5.6)$$

where
$$G = \left(\cos \gamma z + \frac{i\rho}{\sqrt{1+\rho^2}} \sin \gamma z\right) e^{i\beta_s z} \qquad (5.7)$$

$$H = \frac{i \sin \gamma z}{\sqrt{1+\rho^2}} \cdot e^{i\beta_s z} \qquad (5.8)$$

and
$$\beta_s = (\beta_x + \beta_y)/2 \qquad (5.9)$$

$$\rho = \frac{\Delta\beta + \delta\beta \cos 2\Theta}{\delta\beta \sin 2\Theta} = \frac{1}{q} \qquad (5.10)$$

$$\gamma = \tfrac{1}{2} \sqrt{\Delta\beta^2 + 2\delta\beta . \Delta\beta . \cos 2\Theta + \delta\beta^2} \qquad (5.11)$$

If only linearly-polarised light parallel to the x axis is launched, the output extinction ratio $\eta(z)$ becomes:

$$\eta(z) = \frac{|H|^2}{|G|^2} = \frac{q^2 \sin^2 \gamma z}{1+q^2 \cos^2 \gamma z} \qquad (5.12)$$

The matrix equation (5.6) may also be represented by a retarder/rotator model for the disturbed fibre. We obtain the retardation R(z), principal axis position $\phi(z)$ and rotation $\Omega(z)$:

$$R(z) = 2\gamma z \qquad (5.13)$$

$$\phi(z) = \tfrac{1}{2} \tan^{-1} q \qquad (5.14)$$

$$\Omega(z) = 0 \qquad (5.15)$$

Since the disturbed fibre supports two new polarisation eigenstates or normal modes which are linearly-polarised, it appears only as a simple retardation element, with zero net rotation.

Considering the case of a small perturbation i.e. $\delta\beta << \Delta\beta$, the retardation $R(z) \simeq \Delta\beta z$, while $\phi(z) \simeq 0$ i.e. R has principal axes lying parallel to those of the fibre. Thus, as one may expect, the intrinsic birefringence remains unaltered; when evaluating η, mode-beating may be neglected[26] and only mode-coupling considered. Maximum mode-coupling occurs for $\Theta = 45^{o}$, where q is a maximum. In this condition, mode-beating is zero for all $\delta\beta$ values[26]. The poorest exctinction ratio η_{MIN} becomes

$$\eta_{MIN} = q^2 = \frac{\delta\beta^2}{\Delta\beta^2} \qquad (5.16)$$

η_{MIN} for $\Theta = 45^{o}$ is shown in Figure 5.3 with a bend as the perturbation, for a 125µm-diameter fibre with beat lengths L_p of 2, 10 and 30mm respectively at $\lambda = 1.3\mu m$, as a function of bend radius. Even in a so-called "polarisation maintaining" fibre with $L_p = 2mm$, a bend of 5mm radius degrades the extinction ratio to -30dB. This bend need only be $L_p/2 = 1mm$ in length.

For large perturbations i.e. $\delta\beta >> \Delta\beta$, the propagation given by the coupled-mode equations (5.4) and (5.5), is dominated by the induced birefringence $\delta\beta$. The fibre behaves as a retarder $R \simeq \delta\beta z$ with principal axes (aligned) parallel and perpendicular to the plane of the disturbance i.e. $\phi(z) \simeq \Theta$. This "swamping" of the small intrinsic fibre birefringence $\Delta\beta$, by a large bend birefringence $\delta\beta$ is an extremely effective means of providing a controlled fibre retardation with defined principal axes, suitable for sensors[16, 30, 31] polarisation controllers[32] and filters[33].

Experiment

An experiment was performed to verify the analysis presented in this sub-section. A section of the fibre ($\Delta\beta = 122.7^{o}/m$)[12] was bent (assumed sinuoidally) with a mean radius $\overline{R}'$ dependent on the displacement of the two halves of the device shown in Figure 5.4. Using 633nm-light polarised parallel to one of the original fibre principal axes, the output extinction ratio η was measured for the total fibre length as a function of $\overline{R}'$. The fibre sections outside the device were each held straight and untwisted using the vertical bench system described in Section 3.3. These sections therefore supported the two original linearly-polarised normal modes, ensuring that the extinction ratio η at the end of the deformed section was transmitted, without degradation, to the end of the fibre. The experimental results (dots) are shown in Figure 5.5. A value of $\Theta \simeq -52.9^{o}$ was obtained from the relative orientations of the original principal axes of the fibre and the plane of bending. Using the fibre radius of 61μm to calculate the bend birefringence $\delta\beta$[34], the predicted extinction ratio from equation (5.12) was obtained. As shown in Figure 5.5 there is close agreement with the experiments. The experimental curve deviates slightly at small bend radii, where both unavoidable tension in the fibre can significantly affect $\delta\beta$[35] and the area of fibre contact on the former becomes large enough to affect the assumption of sinusoidal bending. At large bend radii the extinction ratio 'saturates' due to the finite extinction of the two polarisers used in the experiment (see section 3.4).

The birefringence properties of the whole fibre were also measured as a function of the mean bend radius. Using a correction based on Jones Calculus, the retardation, principal axis and rotation in the deformed section itself were calculated from these measurements. The measured retardance R is shown in Figure 5.6 (a) (dots) as a function of reciprocal square mean bend radius $(1/\overline{R}')^2$, again closely agreeing with theory (equation (5.13)). At small radii the intrinsic birefringence $\Delta\beta$ is swamped by the bend birefringence $\delta\beta$, so the curve becomes linear with $({}^{1}/\overline{R'})^{2}$ [34]. The coefficient is extremely close to that predicted.[34] Since at large radii $\delta\beta$ is much smaller, R approaches the retardance of the straight fibre. Again a small deviation from linearity occurs at very small bend radii where the assumption of sinusoidal bending breaks down.

The principal axis orientation ϕ measured in the deformed sections is shown in Figure 5.6 (b) (dots), closely agreeing with the theoretical prediction of equation (5.14) (solid line). The principal axis ϕ is initially close to that of the undeformed fibre (0^{o}), but rapidly approaches the plane of bending as the bend radius decreases and bend birefringence becomes dominant. The measured rotation Ω is shown in Figure 5.6 (c) and is thought to originate from the small intrinsic rotation of the fibre and from twists arising within the bending device. This experiment therefore verifies the analysis of a linearly-birefringent fibre subject to a disturbance causing linear birefringence such as bend[34, 36] or side pressure[37, 38].

(b) *Twist and externally-induced circular birefringence*

We now examine the case of a linearly-birefringent fibre with birefringence $\Delta\beta$ subjected to a twist ξ, to circular birefringence α_o and/or Faraday rotation f_o, drawing directly on the analysis presented in Chapter Four. In the coupled-mode equations (4.5) and (4.6) for a twisted fibre (with twist-induced rotation α) the propagation constants β_x and β_y of the two original modes remain un-modified [28]. Therefore twists or rotation produce mode-coupling but zero mode-detuning in a linearly-birefringent fibre[28]. The output extinction ratio $\eta(z)$ for a birefringent fibre with a twist is obtained using equations (4.9) (4.10) and (4.11) as

$$\eta(z) = \frac{q^2 \sin^2 \gamma z}{1 + q^2 \cos^2 \gamma z} \qquad (5.17)$$

where $$q = \frac{2\ (\xi - \alpha)}{\Delta\beta} \tag{5.18}$$

and
$$\gamma = \tfrac{1}{2}\sqrt{\Delta\beta^2 + 4(\xi - \alpha)^2} \tag{5.19}$$

Note that η is referred to, and must be observed in, the *twisted* coordinate system. $\eta(z)$ is oscillatory with length and η_{MIN} occurs at multiples of L_p. Figure 5.7 shows η_{MIN} as a function of twist for beat lengths L_p of 2, 10 and 30mm respectively at $\lambda = 1.3\mu m$. For a "polarisation-maintaining" fibre with a beat length of 2mm, a twist of 8 turns/m will degrade the extinction ratio to -31dB. The new normal modes of the twisted fibre are elliptically-polarised and rotate with the fibre twist (see sub-section 4.6.2).

Any initial fibre rotation α_o may be included in the photo-elastic rotation term α. Moreover, since we are dealing with unidirectional propagation, any Faraday rotation f_o induced by an axial magnetic field is indistinguishable from the rotation α. Consider now a linearly-birefringent fibre subject to a Faraday rotation f_o, but without twist i.e. $\xi = 0, \alpha = 0$. As for a simple twist, induced rotation will couple the two modes without detuning them[28]. Equation (5.17) may be re-written using

$$q' = \frac{2\ f_o}{\Delta\beta} \tag{5.20}$$

$$\gamma' = \tfrac{1}{2}\sqrt{\Delta\beta^2 + 4\ f_o^{\,2}} \tag{5.21}$$

as
$$\eta(z) = \frac{q'^2 \sin^2 \gamma' z}{1 + q'^2 \cos^2 \gamma' z} \tag{5.22}$$

It is however, common practice in Faraday-effect current-transducers to detect the Faraday rotation using the intensities in the orthogonal directions at 45° to fibre principal axes[10, 11, 24], to reduce the effects of source intensity variations. The output, J(z) is then given by[10, 11, 24, 39]:

$$J(z) = \frac{f_o}{\gamma'} \cdot \sin \quad 2\gamma' z \qquad (5.23)$$

J(z) is oscillatory with length so that the maximum interaction length with the field is limited to $L_p/4$. Furthermore, since the maximum value of J for small f_o is $2f_o/\Delta\beta$, a low-birefringence fibre is essential[39, 40] to maximise the interation length and to prevent the linear birefringence from "quenching" the Faraday effect[10, 11, 16, 41].

Next consider the combined effects of twist ξ and Faraday rotation f_o. The parameters q and γ in equation (5.17) become

$$q'' = \frac{2(\xi - \alpha + f_o)}{\Delta\beta} \qquad (5.24)$$

$$\gamma'' = \tfrac{1}{2}\sqrt{\Delta\beta^2 + 4(\xi - \alpha + f_o)^2} \qquad (5.25)$$

A large twist rate will rapidly couple the two modes, effectively averaging the linear birefringence $\Delta\beta$ to zero, (see sub-section 4.6.5) leaving only the rotation $\Omega(z) = (\alpha + f_o)z$ unaltered. Thus the fibre is simple circular retarder, and f_o may be detected as a change in this birefringence[42] (see sub-section 5.2.2 (b)). For completeness, the sensitivity J(z) for a twisted fibre used in a current monitor is[24]:

$$J(z) = \sin\left[2(\delta_1 - \gamma_1)z\right] \cdot \frac{1 + \tan^2 \delta_1 z}{1 + \tan^2 \gamma'' z} \qquad (5.26)$$

$$\text{where } \tan \delta_1 z = \frac{\xi - \alpha + f_o}{\gamma''} \cdot \tan \gamma'' z \qquad (5.27)$$

$$\text{and} \quad \tan \gamma_1 z = \frac{\xi - \alpha}{\gamma} \cdot \tan \gamma z \qquad (5.28)$$

with γ given by equation (5.19).

For small twists i.e. $\xi << f_o, \Delta\beta$, equation (5.26) reduces to the result for an untwisted fibre (equation (5.23)). Conversely, for a large twist i.e. $\xi >> \Delta\beta$ $\gamma_1 \simeq \gamma$ and $\delta_1 \simeq \gamma''$ giving

$$J(z) = \sin 2f_o z \tag{5.29}$$

This is the response of a purely isotropic fibre to a Faraday rotation f_o.

Figure 5.8 shows the magnetic sensitivity of a twisted linearly-birefringent fibre relative to that of an isotropic fibre as a function of the number of turns of twist in the fibre. The curves are plotted for the three different values of net fibre retardation $\Delta\beta z$ shown and for a small Faraday rotation, $2f_o z = 10^o$ [24]

When $\Delta\beta z$ is small i.e. $\pi/2$, the sensitivity at zero twist is relatively high as predicted by equation (5.23). A very small twist is sufficient to produce maximum sensitivity. For large $\Delta\beta z$ values ($7\pi/2$) the sensitivity at zero twist is very low since only the last $\pi/2$ of retardation contributes to the sensitivity[24]. A small twist modifies the overall fibre retardance to an integral multiple of π to give zero sensitivity. Note that since the net retardance of the fibre varies as the twist increases, an oscillatory variation in sensitivity is produced.

From Figure 5.8, provided that at least two turns of twist ξ per beat length L_p exist, a sensitivity approaching that of an isotropic fibre is obtained[42, 43].

5.2.2 Circularly-birefringent fibres

Circularly-birefringent fibres have been proposed for applications requiring polarisation-maintenance[44]. Their main advantage over linear polarisation-maintaining fibres[45] is that azimuthal alignment of fibre joints is not required. Tightly twisting a fibre induces a large circular birefringence suitable for the maintenance of polarisation. In the following analysis the fibre is modelled as a simple circularly birefringent element, ignoring the fact that it is actually a twisted linearly-birefringent fibre (see 5.2.1 (b)).

(a) *Externally-induced linear birefringence*

A circularly-birefringent fibre is modelled as a series of rotation plates each of thickness δz and rotation $\alpha\,\delta z$ where $\alpha = 0.073$ x fibre twist rate[24] as shown in Figure 5.9. External side-pressure or bending introduces a linear birefringence $\delta\beta$, represented by interspersing linear retardation plates each with retardance $\delta\beta\delta z$ and thickness δz. The principal axes of these plates are inclined at an angle Θ determined by the plane of the disturbance with respect to the external co-ordinate system x'y'. For simplicity, coupled-mode analysis is performed in terms of the A_x and A_y modes of the retarder in the x, y co-ordinate system. The results are then translated to x'y' and finally into the circularly-polarised modes A_l, A_r using Jones Calculus[46]. The Jones matrices of the rotators $\alpha\delta z$ are independent of the choice of co-ordinate system. In terms of x, y, the local Jones equation is:

$$[\bar{E}_A] = \begin{bmatrix} \cos\alpha\delta z & -\sin\alpha\delta z \\ \sin\alpha\delta z & \cos\alpha\delta z \end{bmatrix} \cdot \begin{bmatrix} e^{i\beta_x z} & 0 \\ 0 & e^{i\beta_y z} \end{bmatrix} \cdot \begin{bmatrix} a_x \cdot \hat{x} \\ a_y \cdot \hat{y} \end{bmatrix} \tag{5.30}$$

where β_x, β_y are the propagation constants in x, and y directions in the retarder plate and $\hat{x}$ and $\hat{y}$ are unit vectors in x and y directions. Since this equation is identical to equation (4.1), we may follow the analysis described in Section 4.5 exactly, but noting that in the present case there is zero twist of the co-ordinate system along the fibre i.e. $\xi = 0$.

We may immediately obtain the matrix equation in terms of A_x and A_y by setting $\xi - \alpha$ to $-\alpha$ in equations (4.9) to (4.14). Translation of this equation to the co-ordinate system x', y' is performed using Jones Calculus[46] to give:

$$\begin{bmatrix} A'_x\ (z) \\ \\ A'_y\ (z) \end{bmatrix} = \begin{bmatrix} G' & -H'^* \\ \\ H' & G'^* \end{bmatrix} \cdot \begin{bmatrix} A_x'\ (0) \\ \\ A_y'\ (0) \end{bmatrix} \tag{5.31}$$

$$\text{where } G' = (\cos\gamma z + i \frac{\rho}{\sqrt{1+\rho^2}} \sin \gamma z.\cos 2\Theta)\ e^{i\beta_s z} \tag{5.32}$$

$$H = \left[- \frac{1}{\sqrt{1 + \rho^2}} \sin \gamma z + i \frac{\rho}{\sqrt{1+\rho^2}} \sin \gamma z.\sin 2\Theta\right] e^{i\beta_s z} \tag{5.33}$$

$$\rho = q = \frac{\Delta\beta}{-2\alpha} \tag{5.34}$$

$$\gamma = \tfrac{1}{2} \sqrt{\Delta\beta^2 + 4\ \alpha^2} \tag{5.35}$$

$$\text{and } \beta_s = \tfrac{1}{2} (\beta_x + \beta_y) \tag{5.36}$$

This matrix equation (5.31) is further transformed to operate in terms of the left- and right circularly-polarised normal modes of the fibre, A_l and A_r, as described in the Appendix. We obtain:

$$\begin{bmatrix} A_l\ (z) \\ \\ A_r\ (z) \end{bmatrix} = \begin{bmatrix} P & -Q^* \\ \\ Q & P^* \end{bmatrix} \cdot \begin{bmatrix} A_l\ (0) \\ \\ A_r\ (0) \end{bmatrix} \tag{5.37}$$

$$\text{where } P = \cos \gamma z - \frac{i}{\sqrt{1+\rho^2}} \sin\gamma z \tag{5.38}$$

$$Q = \frac{-i\rho}{\sqrt{1+\rho^2}} \sin \gamma z . e^{-2i\Theta} \tag{5.39}$$

The form of the final expression (equation (5.37)) is identical to that for a twisted, linearly-birefringent fibre (equation (4.9)). Thus the induced linear birefringence $\Delta\beta$ couples the two circularly-polarised modes without detuning them[28] (c.f. the twisted linearly-birefringent fibre in sub-section 5.2.1 (b)).

The $e^{-2i\Theta}$ term represents the phase between $A_l(z)$ and $A_r(z)$ arising from our choice of axis system x', y'. The output extinction ratio for a left-circularly polarised light input is:

$$\eta(z) = \frac{|A_r(z)|^2}{|A_l(z)|^2} = \frac{q^2 \sin^2 \gamma z}{1 + q^2 \sin^2 \gamma z} \tag{5.40}$$

where q and γ are given by equations (5.34) and (5.35) respectively.

In this case the fibre is particularly sensitive, since for a 125μm fibre twisted at a maximum practical rate[26, 44] of 50 turns/m, a bend of only radius 45mm at $\lambda = 1.3\mu m$ will degrade η_{MIN} to -31dB[26]. Maintenance of polarisation to better than -40dB for bends of 35mm radius (or 23 Nm^{-1} transverse pressure) requires a twist rate close to the theoretical strength of the glass[23]. We saw in Chapter Four that twists can virtually eliminate *intrinsic* linear birefringence because the birefringence axes are rotated. However *extrinsic* effects have a constant azimuthal direction, so the birefringence is quenched only by virtue of the twist-induced circular birefringence α. Since α is equal to 0.07 x twist rate the rotation alone is an order of magnitude less effective than the twist effect.

Experiment

An experiment was conducted to verify the prediction of equation (5.40). A length (~1m) of low-birefringence fibre (GSB2 of Table 4.1)[12], was twisted at 47.4 rad/m to ensure the rotation α 'swamped' the intrinsic birefringence (~0.05 rad/m). Using left-polarised He-Ne laser input light, the output extinction ratio η was measured as a function of the radius R' of a single loop wound near the midpoint of the 139μm diameter fibre, as shown in the inset of figure 5.10. The straight sections at either side of the loop do not interfere with this measurement. The results are shown in figure 5.10 (dots) and compared with the prediction of equation (5.40) (solid line). It is interesting to note that a single loop of 2.4 cm radius catastrophically degrades the extinction ratio to 0dB. The experiment indeed verifies the predictions derived above.

(b) *Twist and externally-induced circular-birefringence*

Again consider the circularly-birefringent fibre to be made up of a stack of rotator plates δz thick and of rotation $\delta\alpha z$ where α = 0.073 x twist rate[24]. Any induced twist or rotation may be described by twisting the local co-ordinate system or by interspersing rotators respectively. However, the circularly-polarised normal modes of the fibre have a zero overlap integral[44] so that the twist or rotation will induce zero coupling.

Instead, while any fibre twist in itself produces no effect whatsoever, the associated twist-induced rotation, and any other rotation will add to the intrinsic circular birefringence[19, 42], to give a mode-beating effect. This beating may be observed as a rotation of the plane of the linearly-polarised output[42] when both modes are launched using linearly-polarised light.

5.2.3 'Spun' Fibres

In a spun fibre, only small residual average linear polarisation anisotropy is present (equation (4.32)). Thus from the previous sub-sections, we would expect a spun fibre to be extremely evironmentally sensitive. However, since there is still a relatively large (rotating) linear birefringence present on a local scale[47] it is not entirely clear what sensitivity such a fibre will exhibit. This is now evaluated.

(a) *Externally-induced linear birefringence*

As shown in Figure 5.11, a spun fibre is represented as a spiralling series of retardation plates each of thickness δz and retardation $\Delta\beta\ \delta z$. A second set of retardation plates with axes aligned to the x axis is interspersed to represent the induced linear birefringence $\delta\beta$ arising from bends or side pressure. The local Jones equation at a position z along the fibre is:

$$\left[\overline{E_A}\right] = \begin{bmatrix} m_1 & m_2 \\ m_3 & m_4 \end{bmatrix} \cdot \begin{bmatrix} a_x \cdot \hat{x} \\ a_y \cdot \hat{y} \end{bmatrix} \tag{5.41}$$

where

$$m_1 = e^{+i\frac{\delta\beta\delta z}{2}}\left[\cos\frac{\Delta\beta\delta z}{2} + i.\cos 2\xi'z.\ \sin\frac{\Delta\beta\delta z}{2}\right]$$

$$m_2 = e^{-i\frac{\delta\beta\delta z}{2}}\ .i.\sin 2\xi'z.\sin\frac{\Delta\beta\delta z}{2}$$

$$m_3 = e^{i\frac{\delta\beta\delta z}{2}}\ .i.\sin 2\xi'z.\sin\frac{\Delta\beta\delta z}{2}$$

$$m_4 = e^{-i\frac{\delta\beta\delta z}{2}}\left[\cos\frac{\Delta\beta\delta z}{2} - i.\cos 2\xi'z.\sin\frac{\Delta\beta\delta z}{2}\right]$$

and ξ' is the fibre spin rate. It is not possible in this case to use the coupled-mode analysis adopted so far, because the azimuth and hence the mode-coupling if the intrinsic birefringence is length-dependent. However, we may use the formalism of Kapron et al[48] and evaluate the matrix $[M]$ in equation (5.41) as $\delta z \to 0$, neglecting terms of the order δz^2:

$$[M] = \begin{bmatrix} 1 + i\,\frac{\delta\beta\delta z}{2} + i\cos 2\xi' z.\Delta\beta\frac{\delta z}{2} & i.\sin 2\xi' z.\,\frac{\Delta\beta\delta z}{2} \\ i.\sin 2\xi' z.\,\frac{\Delta\beta\delta z}{2} & 1 - i.\frac{\delta\beta\delta z}{2} - i\cos 2\xi' z.\,\frac{\Delta\beta\delta z}{2} \end{bmatrix} \tag{5.42}$$

$$\therefore\ [M] = \begin{bmatrix} a & -b^* \\ b & a^* \end{bmatrix} . \delta z + [I] \tag{5.43}$$

where

$$a = i\left[\frac{\delta\beta}{2} + \cos 2\xi' z.\,\frac{\Delta\beta}{2}\right] \tag{5.44}$$

$$b = i\,.\sin 2\xi' z.\,\frac{\Delta\beta}{2} \tag{5.45}$$

and $[I]$ is the unit matrix.

Following the analysis of Kapron[48] step by step we may write the final matrix $[N(z)]$ for the propagation along a fibre of length z as:

$$[N(z)] = \begin{bmatrix} G & -H^* \\ H & G^* \end{bmatrix} \tag{5.46}$$

where

$$G = \cos\lambda \quad + i\frac{C \sin\lambda}{\lambda} \tag{5.47}$$

$$H = (i\ S + \sigma)\ \frac{\sin\lambda}{\lambda} \tag{5.48}$$

$$\sigma = 0 \tag{5.49}$$

$$S = \int_0^z \frac{\Delta\beta}{2}.\sin\ 2\xi' z.dz = \left[-\frac{\Delta\beta}{4\xi'}.\cos\ 2\xi' z\right]_0^z \tag{5.50}$$

$$C = \int_0^z \left(\frac{\delta\beta}{2} + \frac{\Delta\beta}{2}.\cos 2\xi' z\right) dz = \left[\frac{\delta\beta z}{2} + \frac{\Delta\beta}{4\xi'}.\sin 2\xi' z\right]_0^z \tag{5.51}$$

$$\lambda = (C^2 + S^2 + \sigma^2)^{\frac{1}{2}} \tag{5.52}$$

For a large spin rate $\xi' \gg \Delta\beta$, $S \simeq 0$ and $C \simeq \lambda \simeq \delta\beta\, z/2$ and the matrix elements become:

$$G = e^{i\delta\beta z/2} \tag{5.53}$$

$$H = 0 \tag{5.54}$$

In this condition the new fibre matrix is that of a retarder of retardation $\delta\beta z$ and principal axes along the x and y axes. This is the response of an isotropic fibre to an externally-induced linear birefringence $\delta\beta$. Even though there may be a large local birefringence in the fibre[47], an overall circular symmetry always exists in the guide. The disturbance will upset this symmetry on a local scale to produce a response identical to that of an isotropic fibre.

(b) *Twist and externally-induced circular birefringence*

An applied twist which is small compared to the fibre spin rate ξ' will only slightly change the parameters ρ_1 and γ_1 (equations (4.40) and (4.41)). Thus the overall fibre retardation (equation (4.38)) remains small, while the rotation given by equation (4.39) becomes

$$\Omega(z) = g'\xi z \tag{5.55}$$

where g' is the twist-induced rotation coefficient. As shown in sub-section 4.8.5, in the unlikely case of a large twist opposing the spin, the spin averaging effect is reduced and the fibre becomes linearly-birefringent.

Any rotation, such as a Faraday rotation, of f_o deg/m will induce a rotation

$$\Omega(z) = f_o\, z \tag{5.56}$$

exactly as for twist. This is exactly the response of an isotropic fibre[43], which can also be deduced from the result for a twisted fibre (sub-section 5.2.1 (b)) by setting $\alpha = 0$. The "polarisation transparency" of a spun fibre towards external effects is essential for fibre sensor design, providing in addition a "zero retardation base-line" for the introduction of controlled birefringence for birefringent fibre devices[16, 30, 31, 32, 33].

5.3 Fibres for Polarisation-Maintenance

This section investigates the design requirements for a polarisation-maintaining fibre capable of transmitting a stable polarisation state essential for fibre interferometers[3] and coherent detection systems[1]. In such a fibre one of the 'normal' modes is usually selected as the desired polarisation state, but the other mode may be used as a second independent communication channel with negligible crosstalk[1].

Polarisation-maintenance requires a reduction of the power-coupling induced by environmental factors such as bends. For a uniform disturbance (Section 5.2) this entails minimising the "coupling-strength" q and the worst-case extinction ratio $\eta_{MIN} = q^2$ by (i) reducing the strength of the disturbances (ii) increasing the fibre intrinsic birefringence to 'swamp' the externally-introduced birefringence. Deliberately mismatching the spatial period u of the disturbance with the fibre beat length L_p will also substantially reduce power coupling and hence crosstalk between modes[44, 45].

In a real installation however, the disturbances will vary along the fibre length. Note that from our uniform-coupling analysis, extinction ratio degradation occurs only at the point of disturbance. Any undisturbed section following the disturbance will sustain each normal mode without further coupling. This fact considerably simplifies the study of concatenated localised disturbances. Consider two such disturbances on a single fibre, where, with one of the normal modes launched, each disturbance alone would produce a fibre output extinction ratio of η_1 and η_2 respectively. Assuming the coupling is very weak ($\eta_1, \eta_2 \ll 1$), coupling of the small power in the second mode back into the intended mode is negligible and we obtain the net extinction ratio $\eta \simeq \eta_1 + \eta_2$. Thus the order of the disturbances is arbitrary, while for a series of disturbances $\eta = \sum_{z=0}^{L} \eta(z)$ for a length L of fibre. In practice, the perturbation coupling strengths q(z) will be time variant and random in nature, with an average value $\langle q(z) \rangle = 0$. The z dependence of η can no longer be included easily, so that we assume the worst-case $\eta_{MIN}(z) = q(z)^2$. Again, assuming power is coupled only <u>out</u> <u>of</u> the intended mode continuously along the fibre[17, 22], analysis[17, 22] gives the average extinction ratio:

$$\langle\eta\rangle = \tanh\ (hL)^{49} \tag{5.57}$$

$$\text{where } h = k^2/_4 \ . \ \langle|\Gamma(\Delta\beta)|^2\rangle \tag{5.58}$$

where k is the free-space wavenumber, < > denotes the "ensemble average". $\langle|\Gamma(\Delta\beta)|^2\rangle$ is the average power spectral density of the disturbance q(z) at a spatial frequency (given by $2\pi/u$) of $\Delta\beta$ and is proportional to $(^1/\Delta\beta)^2$ [50]. For polarisation-mainentance the polarisation-holding parameter h must be minimised. This entails minimising $\langle|\Gamma(\Delta\beta)|^2\rangle$ i.e. reducing q(z) by (a) reducing the disturbances or (b) increasing $\Delta\beta$. An additional advantage is gained from (b). Appreciable coupling will only occur when the disturbance contains spatial frequencies close to $\Delta\beta$. However, the spectrum of frequencies for practical disturbances (q(z)) is assumed[17] to be bandwidth-limited at a spatial period of ~ 1mm. Thus reducing L_p to well below 1mm will ensure further reduction of mode-coupling. The spatial frequency dependence of $\langle|\Gamma(\Delta\beta)|^2\rangle$ assumed above has been verified in many types of "polarisation-maintaining" fibres using a polychromatic source[51, 52] to produce a spectral average simulating the ensemble average of the coupled modes.

Thus, the conclusions of uniform and random coupling theory are identical: to produce polarisation-maintenance one must (a) reduce the disturbances as far as possible (b) increase $\Delta\beta$ to both reduce the effect of the disturbances and to pitch $\Delta\beta$ well beyond the highest spatial frequencies present.

High-birefringence fibres are undergoing intensive development. Linearly-birefringent fibres with beat lengths of 0.75mm at 633nm have been produced[53] by using a highly-elliptical core[54, 55]. By increasing the stress anisotropy[17, 55-60] beat lengths as short as 0.87mm at 633nm and fibre losses of 0.8 dB/km at 1.55μm have been obtained [61]. Novel structures using axially non-symmetric refractive index distributions in the core have also been proposed[62, 63] and demonstrated[64, 65]. Circularly-birefringent fibres produced using a tight fibre twist[28] have been proposed[44] to avoid the jointing problems envisaged[45] in linearly-birefringent fibres, but good polarisation-maintenance[23] has yet to be demonstrated. Three excellent reviews of progress in high-birefringence fibres have appeared recently[17, 63, 26].

Very little research has been done into the reduction of random fibre disturbances, mainly because of the difficulty in treating the problem analytically. It is nevertheless clear from the numerical results derived in Section 5.2 for uniform coupling that even for the fibre beat lengths of ~ 1-2mm currently obtained, relativly gentle twists and bends can significantly degrade the extinction ratio under certain conditions. Moreover, a single sharp bend or kink ('hot-spot') can be sufficient to catastrophically reduce the extinction ratio. For polarisation ratios of -30dB or better some considerable care in fibre handling and packaging is required[66]. Our analysis indicates the necessity for the elimination of microbends of less than ~ 5mm radius for a linearly-birefringent fibre and less than 45mm for a circularly-birefringent fibre.

Although uniform-coupling analysis already provides quantified guidelines for polarisation-maintenance, detailed statistical information on the disturbances in real fibre cables is essential before realistic estimates of polarisation performance can be made.

5.4 Fibres for Polarimetric Sensor Applications

Fibre polarimetric (single-fibre) sensors can be broadly classified into "beating-type" and "coupling-type" devices which exploit respectively the mode-beating and mode-coupling effects introduced by a stimulus. These effects have been analysed in detail in Section 5.2.

In the "beating-type" sensor, both fibre modes are launched and the change in fibre birefringence i.e. mode-beating introduced by a stimulus is observed. Small mode-coupling effects introduced by the generally weak stimulus will not significantly affect the high power in each of the modes. Thus, since the sensor is sensitive only to mode-detuning, selective detection of a particular stimulus is possible. For example, a circularly-birefringent effect does not cause any detuning in a linearly-birefringent fibre and vice versa (see Section 5.2). The detection of a given type of birefringence effect requires a fibre with birefringence of the same type and, in the case of linear birefringence, of the same principal axis orientation. One example is the circularly-birefringent (highly-twisted) fibre Faraday rotation ammeter[42]. The large intrinsic circular birefringence will swamp any external linear-birefringence effects such as side pressure or fibre coiling[42], which in any case introduce mode-coupling but not detuning (sub-section 5.2.2 (a)). The device is virtually immune to these effects. Similarly the twist will swamp the intrinsic birefringence (see sub-section 4.6.5), but it is advantageous to use an ultra-low birefringence spun fibre[13].

The linearly-birefringent equivalent is the single-fibre temperature sensor[9], where the change in thermal stress birefringence B_S[59] is exploited as a sensitive measure of temperature. The birefringence B_S is made as high as possible to produce good temperature sensitivity[9]. This also has the advantage of de-sensitising the long fibre length to twists which, without detuning the modes, cause a small amount of power coupling. Another device, proposed as an acoustic or magnetic sensor[30, 31], uses a relatively low-birefringence fibre, tightly coiled on the former to provide a large defined bend-birefringence $\Delta\beta_b$[34] with a known principal axes. An acoustic or magnetic field acts on the former to introduce a tension-bend birefringence[35] with a principal axis parallel

to the bend-birefringence $\Delta\beta_b$, thereby producing a mode-beating effect. The large bend-birefringence provides some immunity from fibre twists and swamps the smaller intrinsic fibre birefringence $\Delta\beta$ (sub-section 5.2.1 (a)). Using an ultra-low birefringence 'spun' fibre[13] is an obvious advantage and guarantees that the fibre coil principal axes lie in the plane of the coil.
These "beating-type" sensors provide sensitivities approaching those of the two-fibre interferometers[5, 67, 68] but are quite temperature sensitive[69, 36]. Special detection schemes to provide maximum sensitivity over a wide temperature range have been reported[70].

"Coupling-type" sensors exploit the power-coupling effect induced by an external stimulus. As shown in Section 5.2, coupling is introduced in a circularly-birefringent fibre only by linear-birefringence $\delta\beta$. In a linearly-birefringent fibre, circular birefringence or a linearly-birefringent disturbance at an angle to the principal axis would cause coupling. To maximise the coupling and hence the device sensitivity, two approaches may be taken; (a) matching the period of the stimulus to the fibre beat length - the "resonant" sensor; and (b) using a very-low birefringence fibre.

An example of the "resonant" sensor is the Faraday isolator[14] which uses a periodic magnetic field spatially matched to the intrinsic fibre beat length L_p[15]. However, L_p varies from fibre to fibre and is strongly temperature-sensitive, making the device extremely difficult to set up and operate. An alternative design[16] uses the controlled birefringence of a coil whose radius is chosen so that the fibre beat length is equal to the coil circumference. This ensures that when the coil is placed in a uniform field resonant coupling will take place[41]. A spun fibre is essential to the attainment of accurately tuned coils (see sub-section 5.2.1 (a)). The device has a useful operating range of at least $\pm$ 10°C [69] and can also act as a spectral filter or magnetic field sensor[16].

A "coupling" device using a low-birefringence fibre is sensitive to virtually all environmental influences (sub- section 5.2.3). For example, a Faraday-rotation current monitor using a low-birefringence fibre has been proposed and demonstrated[10, 11, 39, 43]. However, the introduction of birefringence by coiling the fibre or by side pressure, which typically varies with temperature and time results in a loss of sensitivity[11, 39] and calibration/drift errors. These difficulties can be largely overcome by using novel fibre structures[71], coiling[11] or loose rigid tube coating[37] which *passively* reduce the sensitivity to undesired influences.

5.5 Summary

In this Chapter we have addressed the problem of external influences on birefringent fibres which is a major obstacle in the design of polarisation-maintaining fibres. These effects, however, can be turned to advantage in fibre sensors.

A general analytical method based on coupled-mode theory has been derived to evaluate various types of uniform disturbance in birefringent fibres. It has been shown that both detuning and power transfer (coupling) between the fibre normal modes can occur, depending on the type of disturbance. Essentially a disturbance inducing linear birefringence will "detune" as well as "couple" in a linearly-birefringent fibre, but only "couple" the modes of a circularly-birefringent fibre. Similarly, a circularly-birefringent disturbance will only couple the modes of a linearly-birefringent fibre and only detune those of a circularly-birefringent fibre. The relative importance of detuning and coupling is specific to the problem under consideration.

The uniform mode-coupling analysis has been extended to treat non-uniform disturbances and agrees with the findings of a true random power-coupling analysis applicable to real fibre installations. Appreciable coupling occurs only when the system of disturbances along a fibre contains spatial frequencies close to the birefringence of the fibre. Increasing the birefringence beyond the range of spatial frequencies expected significantly reduces coupling and the development of high-birefringence fibres is receiving considerable attention. Reduction of the magnitude of these disturbances in a cable is necessary although very little is known of their statistical features. Nevertheless, uniform mode-coupling analysis already puts forward approximate guidelines for protective cable structures.

Fibre sensors may exploit either mode detuning or coupling effects as a measure of a given stimulus. In many cases a controlled amount of type of fibre birefringence is essential or at least advantageous and may be obtained by the deliberate introduction of fibre bending or twists. The low intrinsic birefringence of a spun fibre is a useful 'base-line' for many of these sensor designs.

5.6 References

1. Fevre, F., Jeunhomme, L., Joindot, I., Monerie, M., and Simon, J. C.: "Progress towards heterodyne-type single-mode fibre communications systems", IEEE J. Quantum Electron., QE-17, 1981, pp. 897-906.

2. Yamamoto, Y., and Kimura, T.: "Coherent optical fibre transmission systems", IEEE J. Quantum Electron., QE-17, 1981, pp. 919-935.

3. Ulrich, R., and Johnson, M.: "Fibre ring interferometer: Polarisation analysis", Opt. Lett., 4, 1979, pp. 152-154.

4. Schiffer, G., Leeb, W. R., Krammer, H., and Wittman, J.: "Reciprocity of birefringent single-mode fibres for optical gyros", Appl. Optics, 18, 1979, pp. 2096-2097.

5. Sheem, S. K., and Giallorenzi, T. G.: "Polarisation effects on single-mode optical fibre sensors", Appl. Phys. Lett., 35, 19791 pp. 914-917.

6. Ulrich, R.: "Fibre-optic rotation sensing with low drift", Optics Lett., 5, 1980, pp. 173-175.

7. Steinberg, R. A., and Giallorenzi, T. G.: "Performance limitations imposed on optical waveguide switches and modulators by polarisation", Appl. Optics, 15, 1976, pp. 2440-2453.

8. Ramaswamy, V., French, W. G., and Standley, R. D.: "Polarisation characteristics of non-circular core single-mode fibres", Appl. Optics, 17, 1978, pp. 3014-3017.

9. Eickhoff, W.: "Temperature sensing by mode-mode interference in birefringent optical fibres", Optics Lett., 6, 1981, pp. 204-206.

10. Smith, A. M.: "Polarisation and magneto-optic properties of single-mode optical fibre", Appl. Optics, 17, 1978, pp. 52-56.

11. Papp, A., and Harms, H.: "Magneto-optical current transformer. Parts I-III", Appl. Optics, 19, 1980, pp. 3729-3745.

12. Norman, S. R., Payne, D.N., Adams, M.J., and Smith, A.M.: "Fabrication of single-mode fibres exhibiting extremely low polarisation birefringence", Electron. Lett., 15, 1978, pp. 309-311.

13. Barlow, A. J., Payne, D.N., Hadley, M.R., and Mansfield, R.J.: "Production of single-mode fibres with negligible intrinsic birefringence and polarisation mode-dispersion", Electron. Lett., 17, 1981, pp. 725-726.

14. Stolen, R.H., and Turner, E.H.: "Faraday rotation in highly birefringent optical fibres", Appl. Optics, 19, 1980, pp. 842-845.

15. Turner, E.H., and Stolen, R.H.: "Fibre Faraday circulator or isolator", Optics Lett., 6, 1981, pp. 322-323.

16. Day, G.W., Payne, D.N., Barlow, A.J., and Ramskov Hansen, J.J.: "Faraday rotation in coiled monomode optical fibres: isolators, filters and magnetic sensors", Optics Lett., 7, 1982, pp. 238-240.

17. Kaminov, I.P.: "Polarisation in optical fibres", IEEE J. Quantum Electron., QE-17, 7, 1982, pp. 238-240.

18. Sakai, J., and Kimura, T.: "Birefringence and polarisation characteristics of single-mode optical fibres under elastic deformations", IEEE J. Quantum Electron., QE-17, 1981, pp. 1041-1051.

19. Sakai, J., and Kimura, T.: "Polarisation behaviour in multiply perturbed single-mode fibres", IEEE J. Quantum Electron., QE-18, 1981, pp. 59-65.

20. Fujii, Y., and Sano, K.: "Polarisation coupling in twisted elliptical optical fibre", Appl. Optics, 19, 1980, pp. 2602-2605.

21. Monerie, M., and Jeunhomme, L.: "Polarisation mode coupling in long single-mode fibres", Opt. Quantum Electron., 12, 1980, pp. 449-461.

22. Marcuse, D.: "Theory of Dielectric Waveguides", Academic Press, 1974.

23. Barlow, A. J., and Payne, D. N.: "Polarisation maintenance in circularly birefringent fibres", Electron. Lett., 17, 1981, pp. 388-389.

24. Barlow, A. J., Ramskov Hansen, J. J., and Payne, D. N.: "Birefringence and polarisation mode-dispersion in spun single-mode fibres", Appl. Optics, 20, 1981, pp. 2962-2968.

25. McIntyre, P., and Snyder, A. W.: "Light propagation in twisted anisotropic media - application to photoreceptors", J. Opt. Soc. Am., 68, 1978, pp. 149-157.

26. Payne, D. N., Barlow, A. J., and Ramskov Hansen, J.J.: "Development of low- and high-birefringence optical fibres", IEEE J. Quantum Electron., QE-18, 1982, pp. 477-488.

27. Ramskov Hansen, J. J.: University of Southampton, private communication.

28. Ulrich, R., and Simon, A.: "Polarisation optics of twisted single-mode fibres", Appl. Optics, 18, 1979, pp. 2241-2251.

29. Ulrich, R.: "Representation of codirectional coupled waves", Optics Lett., 1, 1977, pp. 109-111.

30. Rashleigh, S. C.: "Acoustic sensing with a single-coiled monomode fibre", Optics Lett., 5, 1980, pp. 392-394.

31. Rashleigh, S. C.: "Magnetic-field sensing with a single-mode fibre", Optics Lett., 6, 1981, pp. 19-21.

32. Lefevre, H. C.: "Single-mode fibre fractional wave devices and polarisation controllers", Electron. Lett., 16, 1980, pp. 778-780.

33. Yen, Y., and Ulrich, R.: "Birefringent optical filters in single-mode fibre", Optics Lett., 6, 1981, pp. 278-280.

34. Ulrich, R., Rashleigh, S. C., and Eickhoff, W.: "Bending-induced birefringence in single-mode fibres", Optics Lett., 5, 1980, pp. 273-275.

35. Rashleigh, S. C., and Ulrich, R.: "High birefringence in tension-coiled single-mode fibres", Optics Lett., 5, 1980, pp. 354-356.

36. Smith, A. M.: "Birefringence induced by bends and twists in single-mode optical fibre", Appl. Optics, 19, 1980, pp. 2606-2611.

37. Smith, A. M.: "Single-mode fibre pressure sensitivity", Electron. Lett., 16, 1980, pp. 773-774.

38. Namihira, Y., Kudo, M., and Mushiake, Y.: "Effect of mechanical stress on the transmission characteristics of optical fibre", Trans. IECE., Japan, 60C, 1977, pp. 391-398.

39. Smith, A. M.: "Optical fibres for current measurement applications", Opt. Laser Techn., Feb. 1980, pp. 25-29.

40. Findakly, T.: "Single-mode fibre isolator in toroidal configuration", Appl. Optics, 20, 1981, pp. 3989-3990.

41. Stanford University, unpublished work.

42. Rashleigh, S. C., and Ulrich, R.: "Magneto-optic current sensing with birefringent fibres", Appl. Phys. Lett., 34, 1979, pp. 768-770.

43. Smith, A. M.: "Polarisation properties of a very low birefringence optical fibre produced by a novel technique", C.E.R.L., Internal report, 1980.

44. Jeunhomme, L., and Monerie, M.: "Polarisation-maintaining single-mode fibre cable design", Electron. Lett., 16, 1980, pp. 921-922.

45. Monerie, M.; "Polarisation-maintaining single-mode fibre cables: influence of joins", Appl. Optics, 20, 1981, pp. 2400-2406.

46. Jones, R. C.: "A new calculus for the treatment of optical systems" (Parts I-VII) J. Opt. Soc. Am., 31, 1941, pp. 488-503; 32, 1942, pp. 486-493; 37, 1947, pp. 107-112; 38, 1948, pp. 671-685.

47. Barlow, A. J., Ramskov Hansen, J. J., and Payne, D. N.: "Anisotropy in spun single-mode fibres", Electron. Lett., 18, 1982, pp. 200-202.

48. Kapron, F. P., Borrelli, N. F., and Keck, D. B.: "Birefringence in dielectric optical waveguides", IEEE J. Quantum Electron., QE-8, 1972, pp. 222-225.

49. Matsumura, H., Katsuyama, T., and Suganuma, T.: "Fundamental study of single-polarisation fibres", Paper presented at Sixth European Conference on Optical Communication, York, UK, 1980.

50. Rashleigh, S. C.: "Polarised light propagation in single-mode fibres", Paper presented at IOOC., San Francisco, 1981.

51. Rashleigh, S. C., Burns, W. K., Moeller, R. P., and Ulrich, R.: "Polarisation holding in birefringent single-mode fibres", Optics Lett., 7, 1982, pp. 40-42.

52. Rashleigh, S. C., and Marrone, M.J.: "Polarisation-holding in a high-birefringence fibre", Electron. Lett., 18, 1982, pp. 326-327.

53. Dyott, R. B., Cozens, J. R., and Morris, D. G.: "Preservation of polarisation in optical-fibre waveguides with elliptical cores", Electron. Lett., 15, 1979, pp. 380-382.

54. Giallorenzi, T. G. et al.: "Optical fibre sensor technology", IEEE J. Quantum Electron., QE-18, 1982, pp. 626-665.

55. Akers, F. I., and Thompson, R. E.: "Polarisation-maintaining single-mode fibres", Appl. Optics, 21, 1982, pp. 1720-1721.

56. Stolen, R. H., Ramaswamy, V., Kaiser, P., and Pleibel, W.: "Linear polarisation in birefringent single-mode fibres", Appl. Phys. Lett., 33, 1978, pp. 699-701.

57. Ramaswamy, V., Kaminov, I. P., and Kaiser, P.: "Single polarisation optical fibres : Exposed cladding technique", Appl. Phys. Lett., 33, 1978, pp. 814-816.

58. Kaminov, I. P., Simpson, J. R., and Presby, H. M.: "Strain birefringence in single polarisation germanosilicate optical fibres", Electron. Lett., 15, 1979, pp. 677-679.

59. Ramaswamy, V., Stolen, R. H., Divino, M. D., and Pleibel, W.: "Birefringence in elliptically clad borosilicate single-mode fibres", Appl. Optics, 18, 1979, pp. 4080-4084.

60. Hosaka, T., Okamoto, K., Sasaki, Y., Miya, T., and Edahiro, T.: "Low-loss single polarisation fibres with asymmetrical strain birefringence", Electron. Lett., 17, 1981, pp. 530-531.

61. Katsuyama, T., Matsumura, H., and Suganuma, T.: "Low loss single-polarisation fibres", Electron. Lett., 17, 1981, pp. 473-474.

62. Okoshi, T., and Oyamada, K.: "Single-polarisation single-mode optical fibre with refractive-index pits on both sides of core", Electron. Lett., 16, 1980, pp. 712-713.

63. Okoshi, T.: "Single-polarisation single-mode optical fibres", IEEE J. Quantum Electron., QE-17, 1981, pp. 871-884.

64. Hosaka, T., Okamoto, K., Sasaki, Y., and Edahiro, T.: "Single-mode fibres with asymmetrical refractive index pits on both sides of core", Electron. Lett., 17, 1981, pp. 191-193.

65. Kitayama, K., Seikai, S., Uchida, N., and Akiyama, M.: "Polarisation-maintaining single-mode with azimuthally inhomogeneous index profile", Electron. Lett., 17, 1981, pp. 419-420.

66. Boscher, D., and Nonclerq, B.: "Ultra-low-loss optical fibre cable design and characterisation", Paper presented at Seventh European Conference on Optical Communication, Copenhagen, Denmark, 1981.

67. Bucaro, J. A., Dardy, H. D., and Carome, E. F.: "Fibre-optic hydrophone", J. Acoust. Soc. Am., 62, 1977, pp. 1302-1304.

68. Dandridge, A., Tveten, A .B., Sigel, F. H., West, E. J., and Giallorenzi, T. G.: "Optical fibre magnetic field sensors", Electron. Lett., 16, 1980, pp. 408-409.

69. Barlow, A. J., and Payne, D. N.: "The stress-optic effect in optical fibres", to be published in IEEE J. Quantum Electron.

70. Rashleigh, S. C.; "Fibre-optic sensors with reduced sensitivity to environmental perturbations", Appl. Optics, 20, 1981, pp. 1498-1499.

71. Payne, D. N.: University of Southampton, Private Communication.

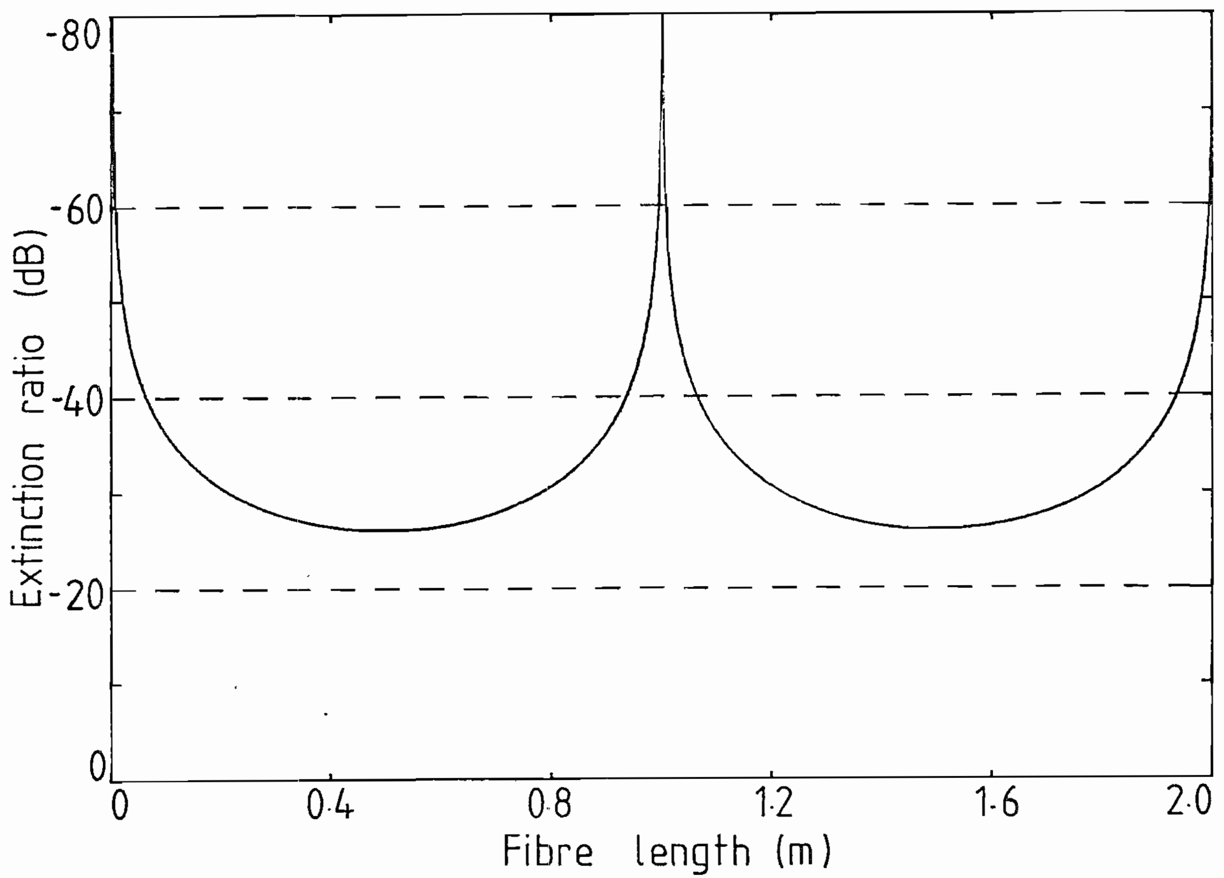

Figure 5.1 Output polarisation extinction ratio $\eta(z)$ as a function of fibre length for a birefringent fibre subjected to a weak uniform disturbance and when only one of the modes is launched; $q = 0.05$, $\Delta\beta = 180^{\circ}/m$.

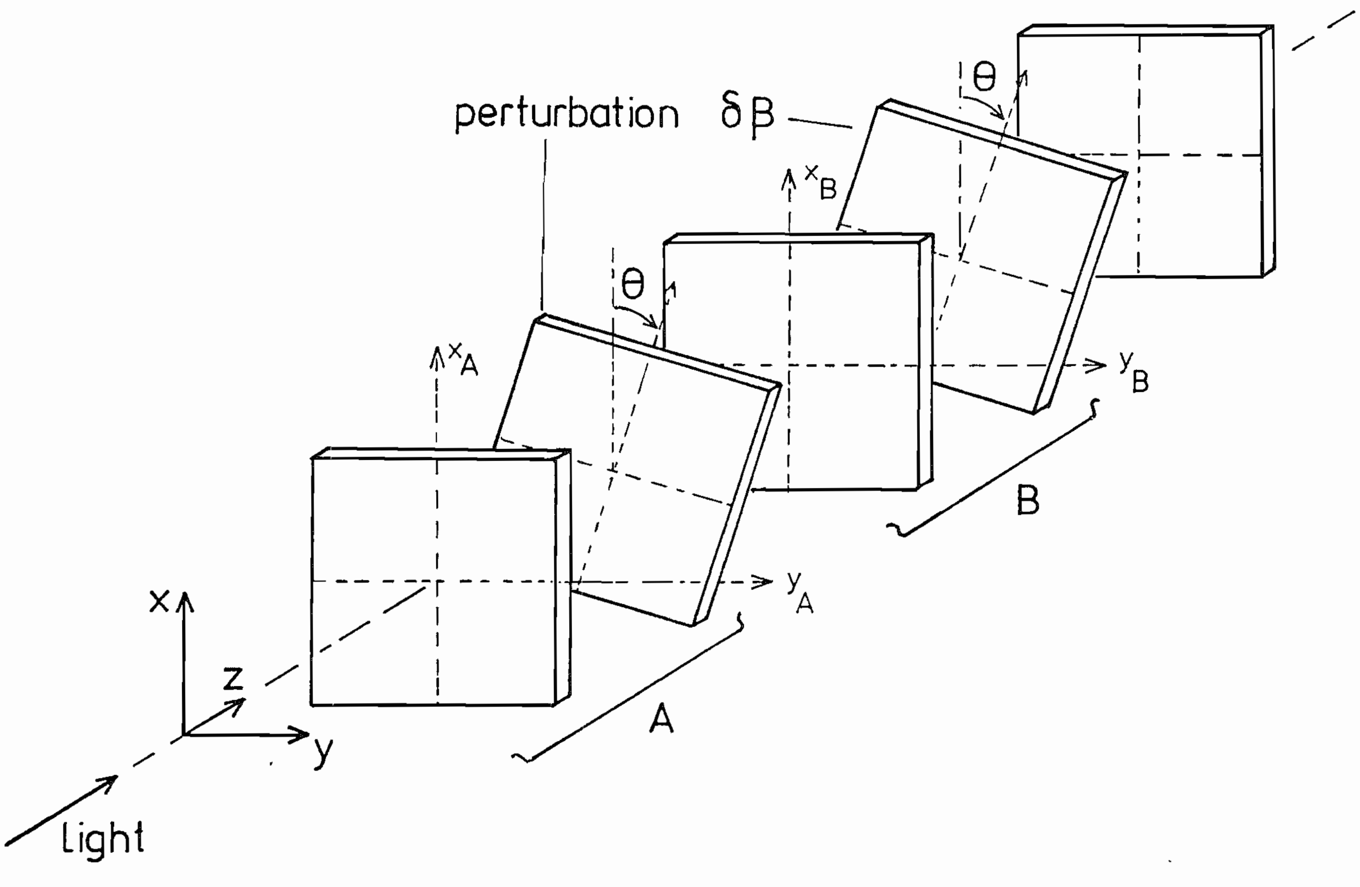

Figure 5.2 Schematic representation of the model used for a linearly-birefringent fibre subject to a linearly-birefringent disturbance, such as a bend, inclined at angle Θ to the fibre principal axes.

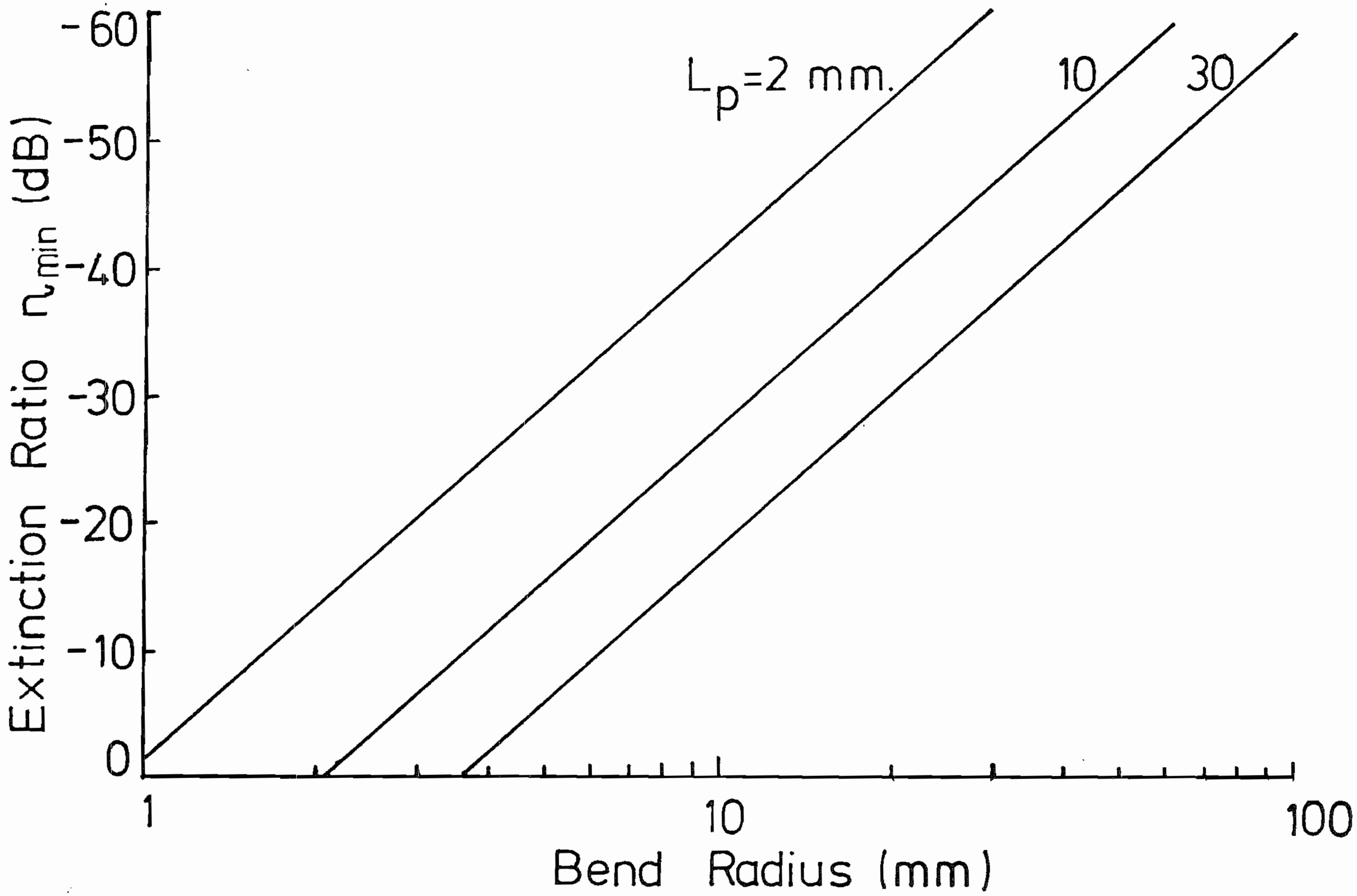

Figure 5.3 Minimum extinction ratio η_{MIN} for linearly-birefringent fibre subject to a bend inclined at 45^{o} to the fibre principal axes shown for various values of L_p(@ 1.3μm). Fibre is 125μm in diameter.

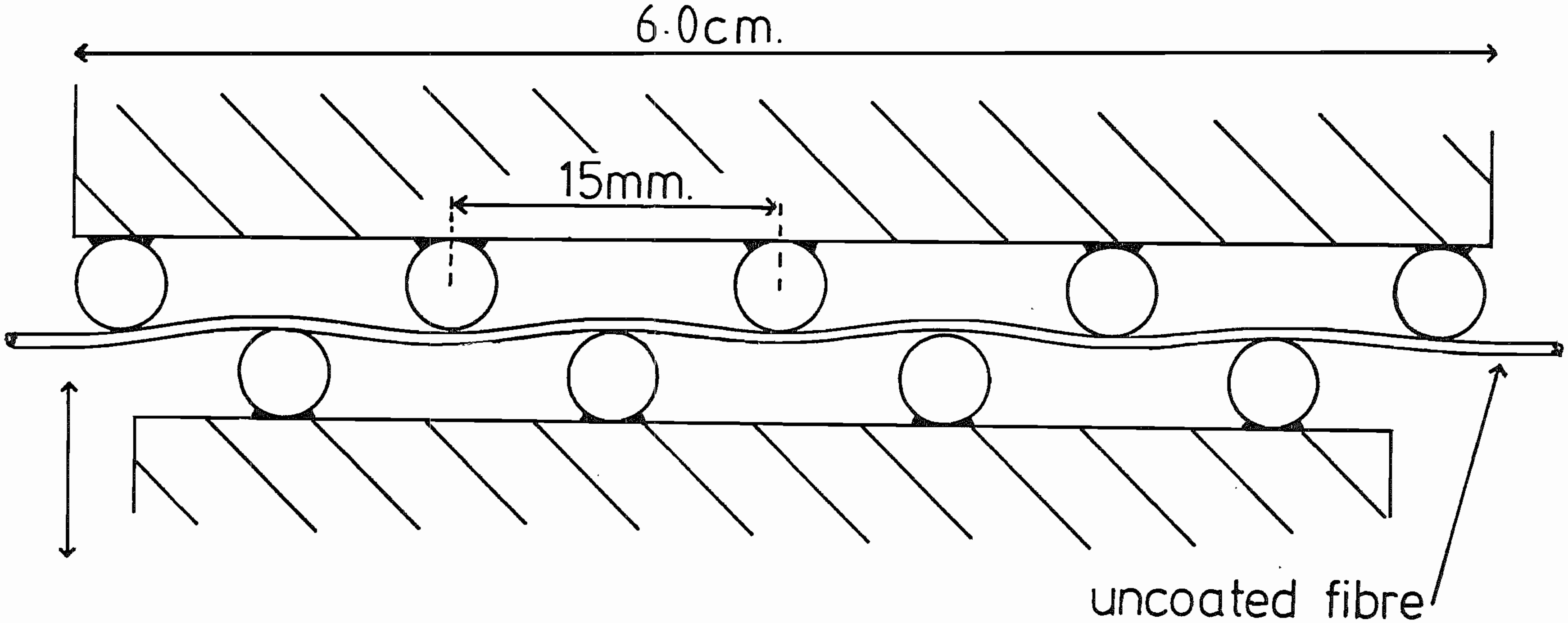

Figure 5.4 "Cockling" device to induce controlled bending into a birefringent fibre.

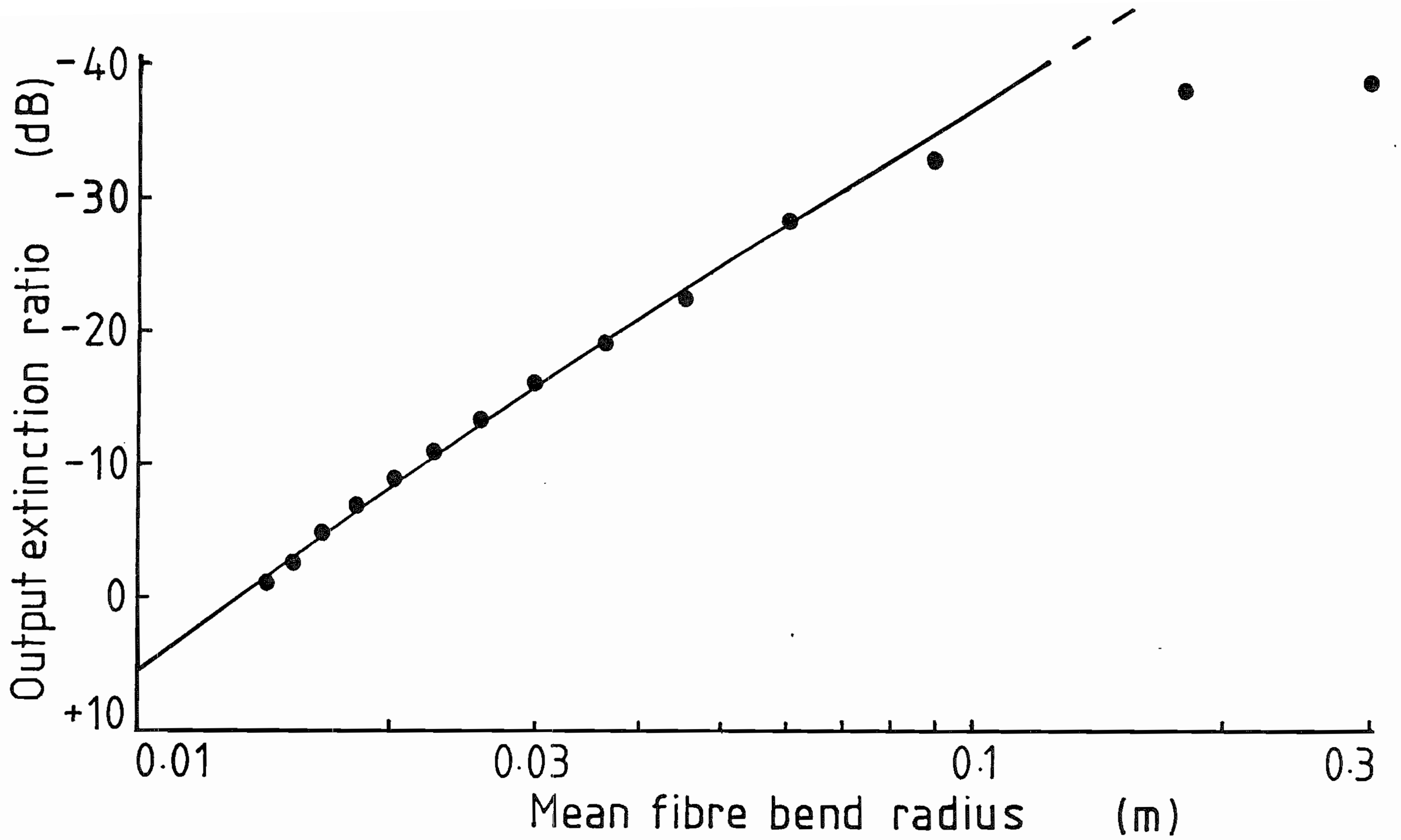

Figure 5.5 Measured output extinction ratio for a linearly-birefringent fibre ($\Delta\beta = 122.7^{o}/m$) as a function of mean fibre bend radius R'. Solid line shows theoretical prediction; $\theta = -52.9^{o}$, fibre radius = 61μm.

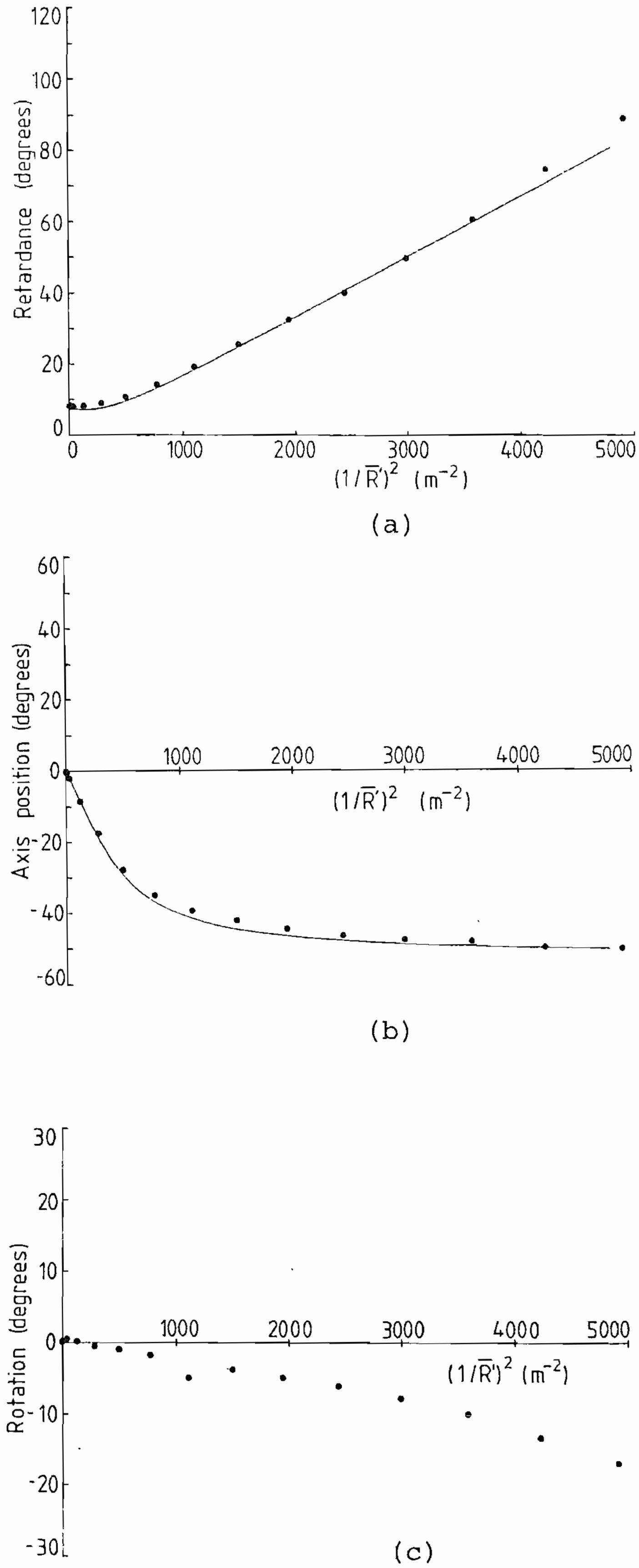

Figure 5.6 Measured birefringence parameters in deformed, linearly-birefringent fibre ($\Delta\beta$=122.7^{o}/m) as a function of reciprocal square mean fibre radius (a) retardance R, (b) principal axis position ϕ (c) rotation Ω. In each case, the solid line is the theoretical prediction for Θ =-52.9^{o}, fibre radius = 61μm.

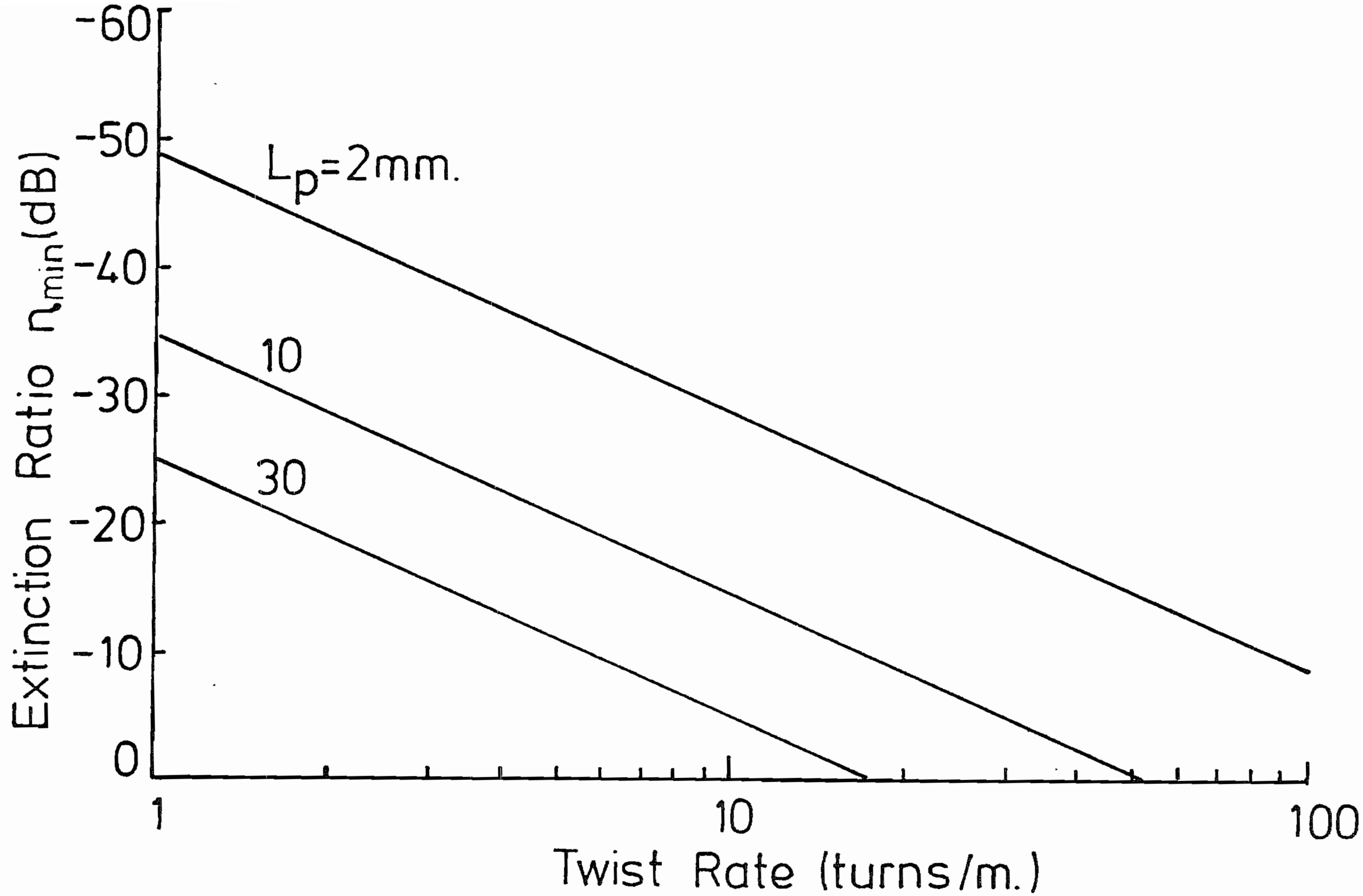

Figure 5.7 Minimum output extinction ratio η_{MIN} for a linearly-birefringent fibre as a function of a uniform applied twist shown for various values of L_p (at 1.3μm).

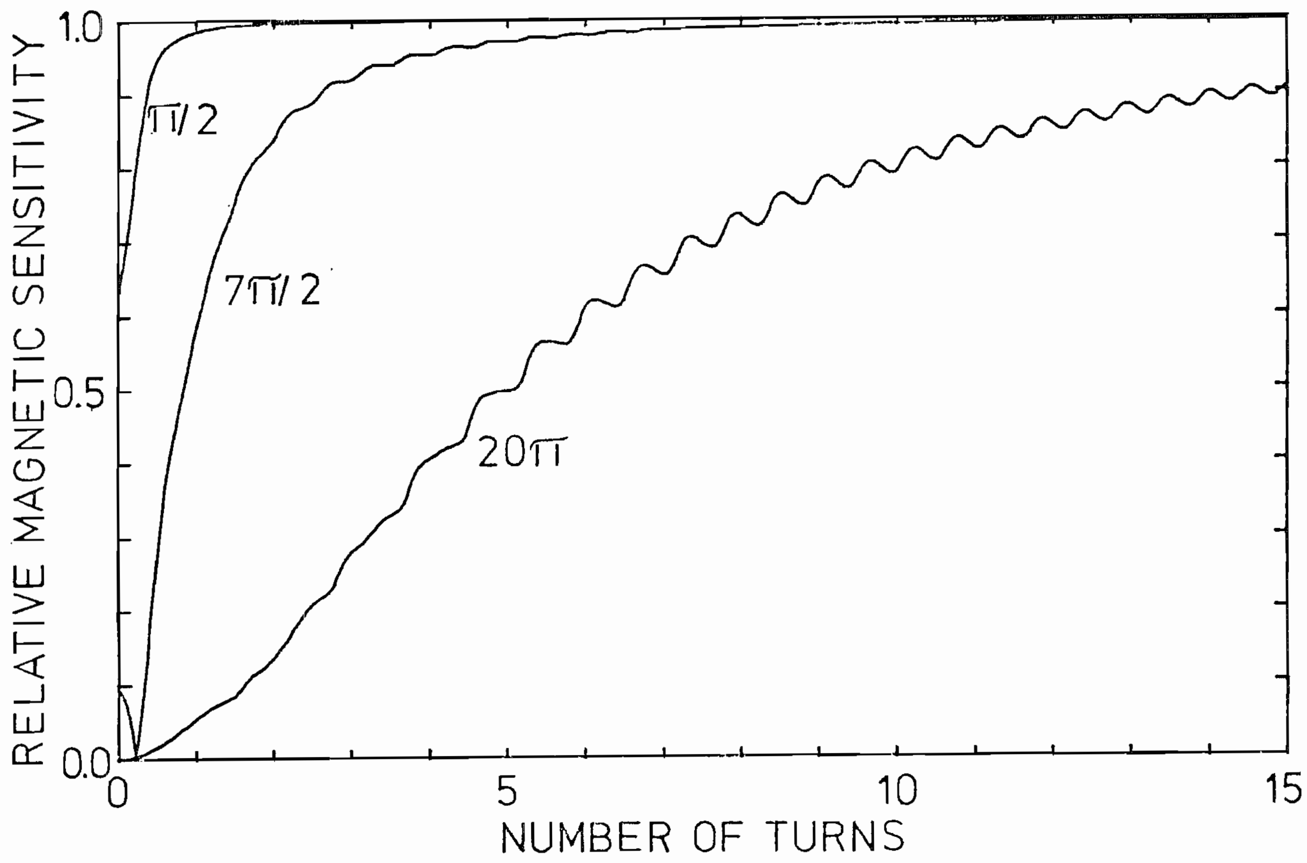

Figure 5.8 Magnetic sensitivity relative to that of an isotropic fibre, for a given length of twisted birefringent fibre as a function of the number of turns in the length. The curves are shown for the values of net retardance $\Delta\beta z$ marked. Faraday rotation angle $2f_o z = 10^o$.

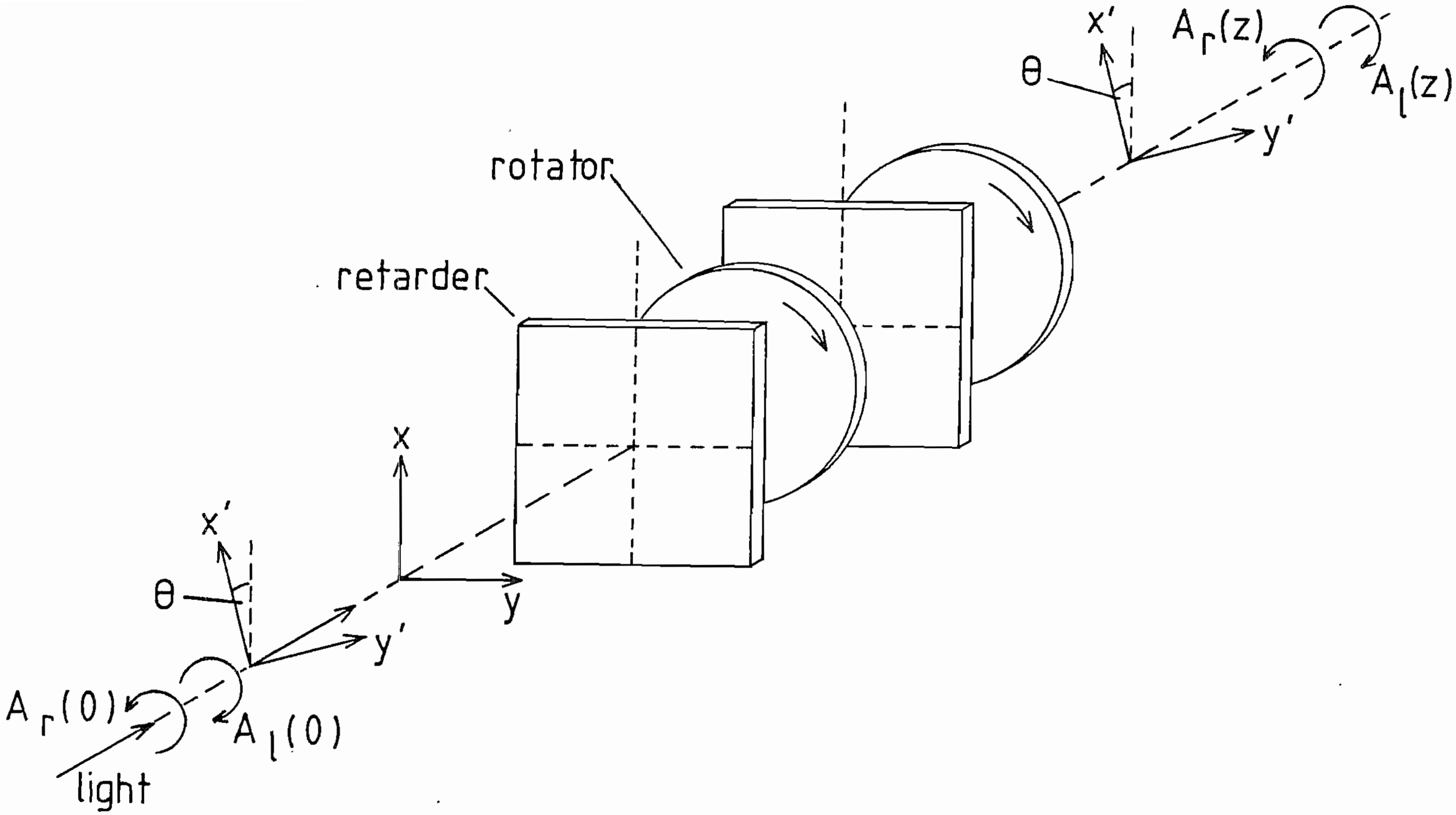

Figure 5.9 Theoretical model used to analayse a circularly-birefringent fibre subjected to a uniform linearly-birefringent disturbance, such as a bend, with an azimuthal angle Θ.

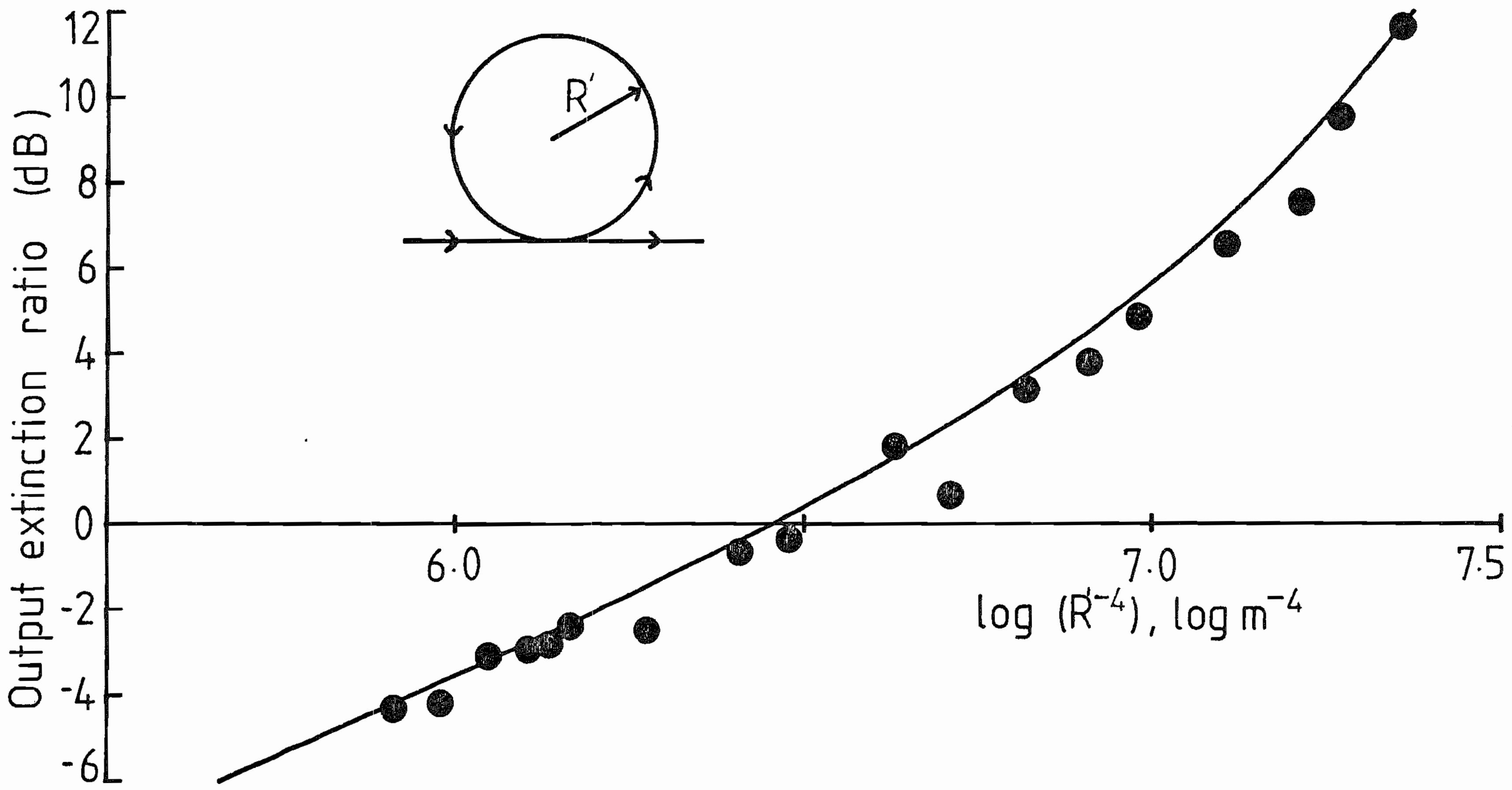

Figure 5.10 Output extinction ratio for a twisted circularly-birefringent fibre as a function of bend radius R′ (see inset). Dots are experimental values: solid line is theoretical prediction.

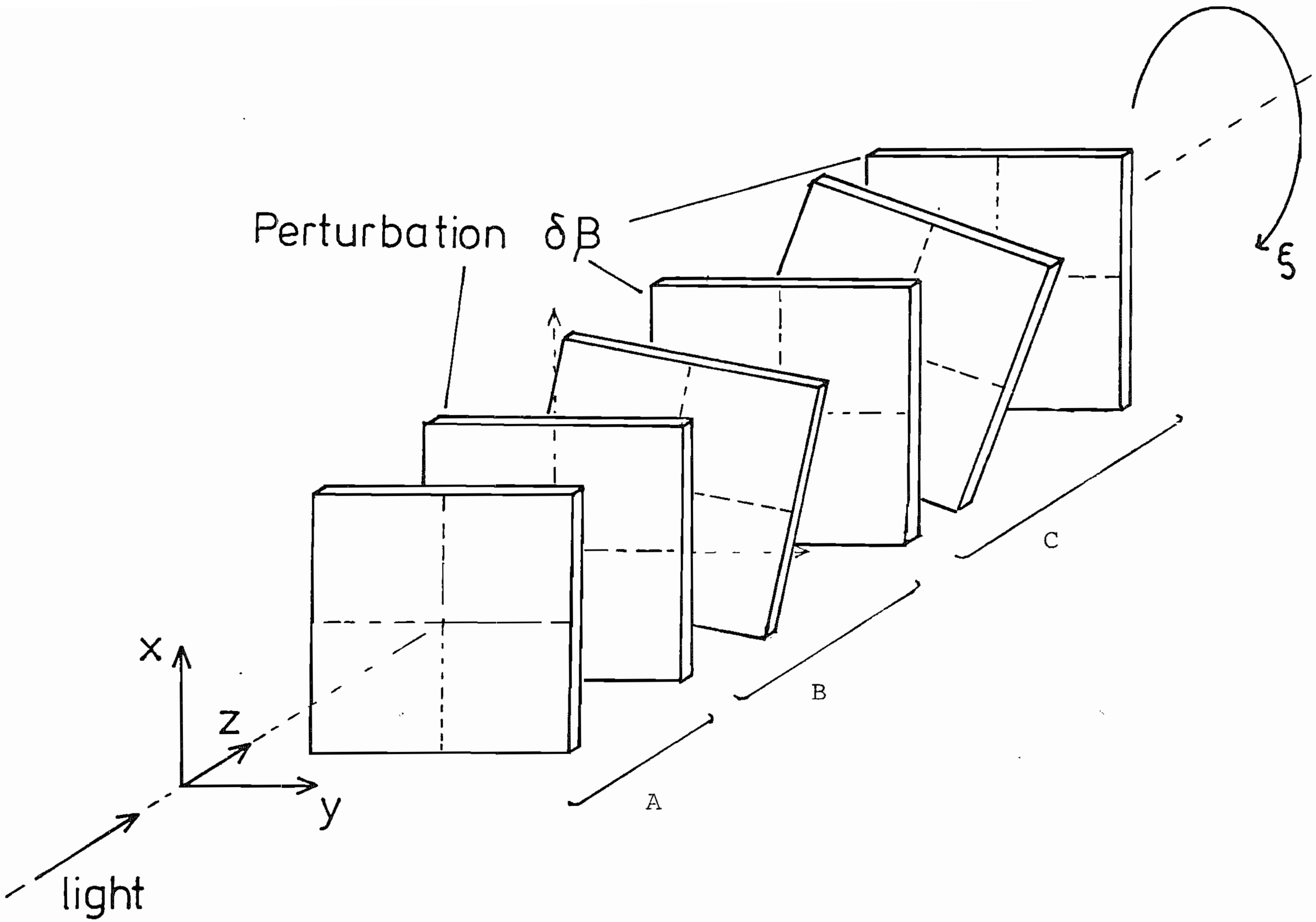

Figure 5.11 Theoretical model used to analyse the effect of a uniform linearly-birefringent disturbance $\delta\beta$, such as bend , on a spun fibre.

CHAPTER 6 THE EFFECT OF WAVELENGTH AND TEMPERATURE IN BIREFRINGENT FIBRES

6.1 Introduction

Fibre birefringence generally varies with the light wavelength, giving rise to a difference in the group-delay between the two orthogonally-polarised fibre modes, an effect known as polarisation mode-dispersion (PMD)[1, 2]. PMD can significantly limit the overall fibre bandwidth[3 - 5], particularly when the first-order chromatic dispersion has either been optimised for the wavelength of operation[6-11], or eliminated by using a highly-monochromatic source, for example in coherent systems[12, 13], and is therefore an extremely important parameter in the design of ultra-high bandwidth fibres.

Polarisation-dispersion is generally higher in high birefringence (polarisation-maintaining) fibres, with any weak mode-coupling resulting in a severe bandwidth reduction. Conversely, stronger coupling between the modes can improve the fibre bandwidth by an averaging effect on the respective pulse transit times, particularly in long fibres[2, 14].

High bandwidth can be ensured only in a fibre with an intrinsically-low PMD, that is, generally a low-birefringence fibre, or preferably a 'spun' fibre[15] with its ultra-low birefringence and PMD (see Section 4.8). In conjunction with a polarisation-controller[16, 17], a low-birefringence fibre is a viable alternative to a polarisation-maintaining fibre for communications (see Section 2.6).

The intrinsic birefringence of a fibre with photo-elastic stress-birefringence varies substantially with ambient temperature. The resultant change in output polarisation state may prove troublesome in coherent systems and fibre interferometers[18] but can be turned to advantage in temperature sensors[19]. In addition, externally-induced birefringence based on the photo-elastic effect, such as bending or twist, will vary with temperature affecting the stability and operation of fibre sensors[20-22] and controlled-birefringence fibre devices[23-27].

In this Chapter, the effects of both wavelength and temperature on fibre birefringence[28] will be examined. First, the polarisation mode-dispersion arising in a linearly-birefringent fibre is discussed. The effects of mode-coupling on this dispersion will be examined qualitatively. A subsequent section will describe a technique for polarisation-dispersion measurements. It will also be shown theoretically and experimentally that polarisation-dispersion can be dramatically reduced in spun fibres.

The effect of temperature on birefringence and sensor devices will be examined. Some techniques for separating and evaluating the stress and waveguide contributions in a birefringent fibre utilising the temperature and wavelength effects are presented. These techniques provide valuable diagnostic information for fibre fabrication and further the understanding of the combination of stress and waveguide effects in a fibre.

6.2 Polarisation Mode-Dispersion

In the absence of chromatic dispersion[3, 6-9, 29] or with a monochromatic source[30], polarisation mode-dispersion becomes the primary limit on fibre bandwidth. For poly-chromatic sources, the group-delay difference will cause output depolarisation[2]. The magnitude of PMD must therefore be considered.

6.2.1 Polarisation-dispersion in linearly-birefringent fibres

In a fibre with stress and waveguide shape linear birefringence B_S and B_G respectively, a group-delay difference $\Delta\tau_o$ arises between the two orthogonally-polarised normal modes. This delay-difference or polarisation mode-dispersion is given by the derivative of the retardance $\Delta\beta$ with respect to the free-space wavenumber, k:

$$\Delta\tau_o = \frac{z}{c} \cdot \frac{d(\Delta\beta)}{dk} = \frac{z}{c}\frac{d}{dk}\,(k(B_G + B_S)) \tag{6.1}$$

$$= \frac{z}{c}\cdot\left[B_G + k\,\frac{dB_G}{dk} + B_S\,(1 + \frac{k}{C}\frac{dC}{dk})\right] \tag{6.2}$$

where z is the fibre length, c is the velocity of light and the stress birefringence B_S is proportional to the photo-elastic constant C. The last term in equation (6.2) represents the dispersion contribution arising from the variation of C with wavelength[28, 31] (see sub-section 6.2.3). The retardance $\Delta\beta_s$ arising from the stress-birefringence varies almost linearly with fibre V-value[32]. The dispersion due to B_S is thus almost constant for all fibre V values, the photo-elastic dispersion contributing about 5-10% to this dispersion[28].

The retardation $\Delta\beta_G$ arising in an elliptical-core step-index fibre is a function of fibre V-value[33,34, 35]. The resultant polarisation-dispersion contribution $\frac{z}{c}\cdot(B_G + k\,\frac{dB_G}{dk})$, is shown in Figure 6.1 for a fibre with a small ellipticity of $(\frac{a}{b} - 1) = 4.3\%$, where a, b are the core semimajor and semiminor axis dimensions, and index difference $\Delta' = 0.5\%$. Note that at $V \simeq 2.48$, close to the second-order mode cut-off, the polarisation dispersion falls to zero[33, 34]. For higher fibre ellipticities this point shifts to higher V value (V is referred to the semimajor axis a in this case)[34, 36] but remains close to the cut-off V-value[34].

The net dispersion $\Delta\tau_o$ calculated for a typical telecommunications fibre (VD319) is shown in Figure 6.2 for $\Delta' = 0.5\%$ and ellipticity $(\frac{a}{b} - 1) = 4.3\%$ and $B_S = 7.13 \times 10^{-7}$ at $\lambda = 1.06\mu m$; the effect of dC/dk was calculated using ref. 28 (see sub-section 6.2.3). The values were chosen to fit data (dots) obtained in an experiment to be described later. Figure 6.2 clearly shows the relative importance of the stress and shape contributions. At the higher order mode cut-off ($V = 2.4$ for this value of ellipticity), the shape contribution is small, vanishing entirely at $V = 2.48$. Fibres designed for operation at 1.3μm typically have V-values close to 2.4 [3] so that any PMD arises largely from the stress effect. However, a much lower V-value (typically 1.5-1.8) [3, 6] is required for zero chromatic dispersion for 1.55μm operation so the waveguide PMD component will then be significant.

The results shown in Figure 6.2 are typical of nominally circular telecommunications grade fibres where $\Delta\tau_o$ is generally 5-10 ps/km. In a long-haul link even this apparently small figure will result in about a nanosecond of dispersion. Therefore operation at 1-10 Gbits/sec over long distances generally requires very low core-ellipticities and stress-birefringence beat lengths greater than 50m, in addition to accurate matching of the chromatic dispersion[3, 4].

Polarisation immunity to external effects[37] may be achieved using a high-birefringence fibre[38, 39]. Assuming the stress component B_S to be dominant, a fibre with a beat length $L_p = 2$mm at $\lambda = 1.3$μm would have $\Delta\tau_o \approx 2.2$ns/km, which becomes active when power transfer into the unwanted mode takes place (see sub-section 6.2.2) thus reducing the bandwidth. Fibres with balanced stress and core ellipticity to produce a small PMD while retaining high birefringence have been proposed recently[36, 40].

6.2.2 Role of mode-coupling

Power coupling between the two orthogonally-polarised modes has a profound effect on the overall fibre bandwidth. With no coupling, the two modes are independent and with only one mode launched, the polarisation dispersion $\Delta\tau_o$ is of no concern.

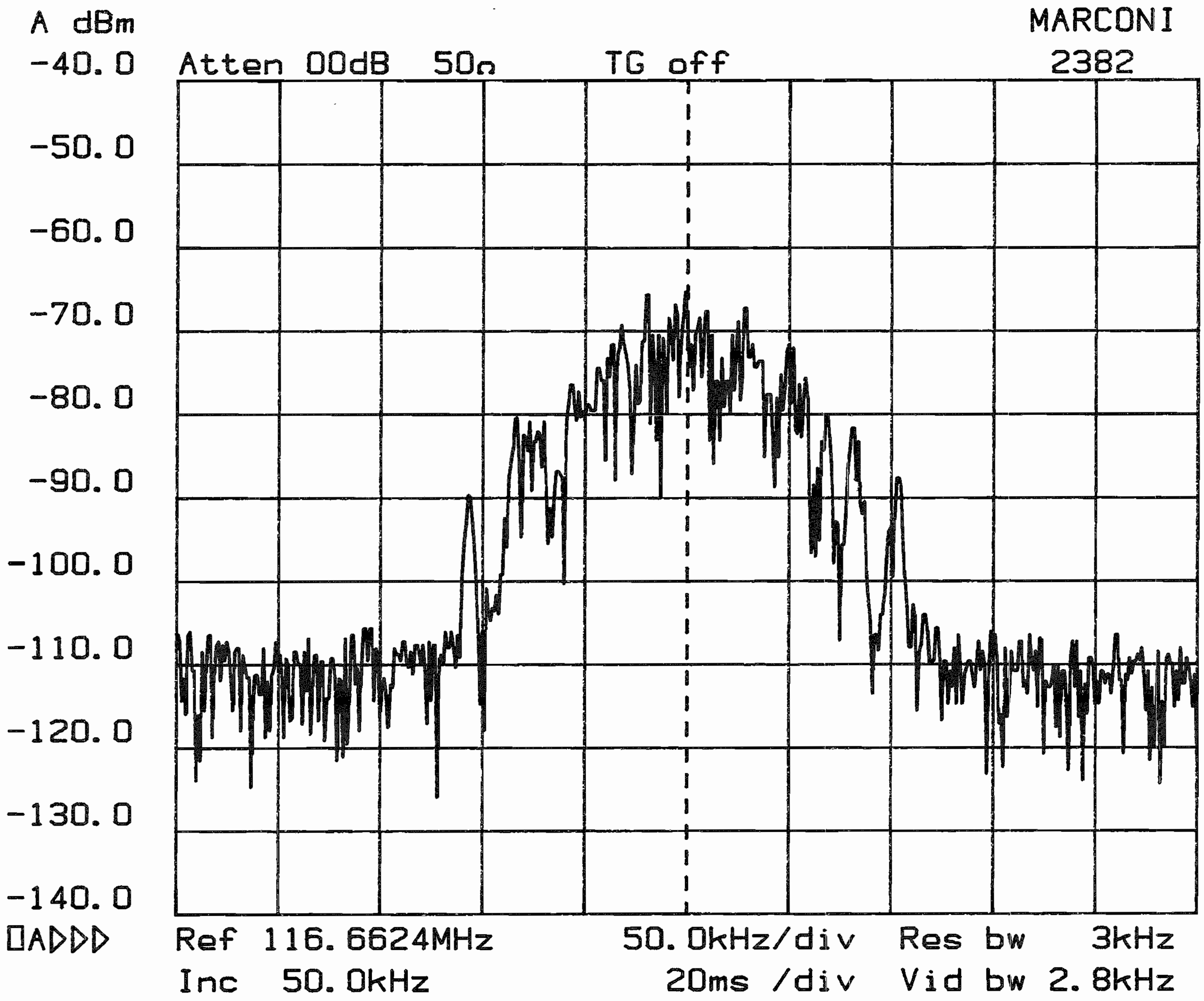
A dBm
-40.0
-50.0
-60.0
-70.0
-80.0
-90.0
-100.0
-110.0
-120.0
-130.0
-140.0
Atten 00dB 50Ω
TG off
MARCONI
2382
Ref 116.6624MHz
Inc 50.0kHz
50.0kHz/div
20ms /div
Res bw 3kHz
Vid bw 2.8kHz

In a long fibre, however, some random coupling will inevitably occur. The normal modes and hence pulse-delay can then only be defined locally within the concatenated local sections making up the fibre, and equation (6.1) breaks down. The net group delay is the sum of the individual delays[14]. Therefore weak mode-coupling or polarisation conversions on a local scale can result in a bandwidth reduction[14] over the zero-coupling cases. Stronger coupling transfers power back and forth continuously along the fibre to statistically equalise the net transit times for any input polarisation. The delay for random coupling is proportional to $(\text{length})^{\frac{1}{2}}$ [2]. However, it is far from clear whether the coupling would be truly random in practice[41]. Further study of the nature of external fibre perturbations is needed before realistic predictions of long fibre bandwidths[42] can be made.

Uniform mode-coupling between the linearly-polarised modes sets up two new normal modes and reduces $\Delta\tau_o$ [43,44] (sub-section 6.2.5).

6.2.3 Dispersion of the stress-optic effect in fibres

The photo-elastic constant C governs fibre birefringence arising from thermal stress[45], bending[37], side pressure[46, 47] and torsion[48]. C is generally assumed invariant with wavelength[25, 32, 49-51], despite measurements of the dispersion of C in bulk glasses[52-58]. The dispersion of C contributes to both intrinsic PMD (equation (6.2)) and to the spectral properties of fibre devices using externally-induced birefringence[28].

In bulk silica the variation of C as a function of wavelength follows a known dispersive law[57, 28].

$$\frac{C(\lambda)}{n_s(\lambda)} = C(\lambda_o) \cdot \left[\frac{n_s(\lambda_o)}{n_s^2(\lambda)} \cdot \frac{\lambda^2}{\lambda_o^2} \cdot \frac{\lambda_o^2-\lambda_1^2}{\lambda^2-\lambda_1^2} \cdot \frac{\lambda^2-\lambda_2^2}{\lambda_o^2-\lambda_2^2} \right] \tag{6.3}$$

where

$n_s(\lambda)$ = refractive index at wavelength λ

λ_o = normalising wavelength

λ_1 = 0.1215μm

λ_2 = 6.900μm

$C(\lambda_o)$ is the value of C at λ_o
C is -3.30×10^{-11} m^2kg^{-1} at λ_o = 633nm [54] and n_s and $dn_s/d\lambda$ are obtained from the data of Malitson[59]. The derivative of equation (6.3) yields $dC/d\lambda$. The results for C and $dC/d\lambda$ are shown in Figures 6.3 and 6.4 respectively.

The dispersion of C in doped-silica is largely unknown, particularly in fibres. Measurement of C in a fibre could be performed by observing the stress-birefringence B_S variation with wavelength (see equation (6.2)). However, the strong dependence of B_S on ambient temperature[19] as well as the likely presence of a shape contribution B_G and externally-induced birefringence make this method unreliable. In contrast, a spun fibre has negligible birefringence of its own, and a controlled stress-induced birefringence may be introduced, by bending or twisting the fibre. Bending requires winding the fibre under tension which introduces further undesired birefringence, whereas twisting is easier to control. For a twist rate ξ a rotation of α of the plane of polarisation is introduced[48]:

$$\alpha = g'\xi = -\frac{R_o C}{n_c}\xi \tag{6.4}$$

where g' is the stress-optic rotation coefficient, n_c the core refractive index and R_o the modulus of rigidity. Differentiation yields:

$$\frac{dC}{d\lambda} = -\frac{1}{R_o}\left[g'\frac{dn_c}{d\lambda} + n_c(\lambda)\frac{dg'}{d\lambda}\right] \tag{6.5}$$

$\frac{dC}{d\lambda}$ was obtained by measuring g' as a function of wavelength in a spun fibre (VD319) [15] with 0.9cm pitch, a silica core doped with 3.4^{m}/o GeO_2, and B_2O_3/SiO_2 cladding. The overall index difference was ~ 0.5% and the cut-off wavelength was 0.95μm. Five turns of twist were applied to the 1.3m-long fibre. The rotation α (equation (6.4)) was measured as described in Chapter Three using the tunable-wavelength Raman source. The results for g' are shown in Figure 6.5 (dots) with a fitted 2nd-order Chebyskev curve (dashed). The expected variation of g' in bulk silica obtained from equations (6.3) and (6.4) [58, 59] is also shown for comparison. The fibre value is ~ 5% higher and only slightly more dispersive.

Evaluation of $dC/d\lambda$ using equation (6.5) requires values of n_c and $dn_c/d\lambda$. It has been shown[28] that for the small GeO_2 concentration used in this fibre (3.4^{m}/o), these values differ by less than ~ 1% from those for bulk silica obtained in ref. 59. The computed results for C and $dC/d\lambda$ are shown in Figures 6.3 and 6.4 respectively. Referring to Figure 6.3, the value of C in the fibre is slightly higher than that extrapolated for bulk silica and is in close agreement with other measurements of C in fibres[49]. The presence of small amounts of GeO_2 does not appear to alter the stress-optic coefficient significantly. In addition, from Figure 6.4, the value of $dC/d\lambda$ in the fibre is ~10% higher than in bulk silica and tends to follow the dispersive law for C given in equation (6.3). Table 6.1 summarises the results for C obtained in the spun fibre.

The variation of C with wavelength must be taken into account when considering the intrinsic polarisation properties of a fibre[60, 61, 32]. For example the variation of fibre stress-birefringence $\Delta\beta_s$ with fibre V-value [32] will become non-linear. However, because $dC/d\lambda$ is small and almost constant, the inclusion of $C(\lambda)$ will only alter the slope of the variation of $\Delta\beta_s$ by some 10%. This can have a marked effect on the intercept of $\Delta\beta_s$ at zero V-value which in fact provides a measure of any shape contribution B_G in the fibre as well as the effect of cladding stresses on stress-birefringence[60, 61]. Correct evaluation of the dispersion of birefringence therefore requires inclusion of the variation of C.

The variation of C will also contribute to the overall PMD in a fibre with stress birefringence B_S, as indicated in equation (6.2). Evaluation of $k/C.\ dC/dk$ from Figures 6.3 and 6.4 yields a value of 9.5×10^{-2} at 1.3μm. The stress-optic effect increases the polarisation mode-dispersion due to stress by ~9.5%.

The dispersion of C will also give rise to dispersion in fibres or devices[16-27] where an external elasto-optic birefringence is introduced[46-48], for example by bending[37]. The polarisation-dispersion in twisted circularly-birefringent fibres will be discussed in sub-section 6.2.5. The dispersive behaviour of C will be particularly important when designing spectral filters[24, 25, 32].

A small chromatic dispersion ($<10^{-15}$ sec nm^{-1} km^{-1}) will arise from the second derivative $d^2C/d\lambda^2$. This dispersion is negligible compared to material and waveguide chromatic dispersion[3] even in highly-stressed polarisation-maintaining fibres.

6.2.4 Measurement of polarisation-dispersion

It is difficult to measure the polarisation mode-dispersion $\Delta\tau_o$ in a linearly-birefringent fibre directly in the time-domain because of its very small value. However, according to the definition of $\Delta\tau_o$ given by equation (6.1), $\Delta\tau_o$ may be obtained by measuring fibre birefringence $\Delta\beta$ as a function of wavelength[15, 31, 49, 50]. Thus:

$$\Delta\tau_o = -\frac{\lambda^2}{c} \cdot \frac{1}{1000} \cdot \quad \frac{1}{360} \cdot \frac{d(\Delta\beta)}{d\lambda} \quad \text{pskm}^{-1} \tag{6.6}$$

where

λ = wavelength in microns

c = velocity of light (ms^{-1})

L = length of fibre used (m)

$\Delta\beta$ = birefringence of fibre in degrees m^{-1}.

Measurements based on this approach were carried out in fibre sections about 1.5m long using the tunable Raman system described in sub-section 3.5.2. Typical birefringence results obtained in two nominally-round telecommunications-grade fibres BP01 and VD319, are shown in Figres 6.6 and 6.7 respectively. For each fibre the linear birefringence $\Delta\beta$ is shown. A small rotation attributable to frozen-in twist was observed but its effect neglected on the grounds that the birefringence is little changed by such small twists (see sub-section 4.6.4).

In each case, the second-order Chebyshev fit is shown. The birefringence of BP01 is relatively small and yields a polarisation-dispersion from equation (6.6) of only 0.26 $pskm^{-1}$ at $\lambda = 1.1\mu m$. By contrast, the birefringence of VD319 is much higher, yielding a polarisation dispersion of 5.15 $pskm^{-1}$ at $1.3\mu m$. The polarisation-dispersion as a function of wavelength for this fibre is shown in Figure 6.2 (dots).

Similar experiments to measure the wavelength dependence of birefringence to obtain polarisation-dispersion have been reported in a fibre with an ellipticity of 0.35[49] and in twisted fibres[32].

The values of dispersion measured in VD319 and BP01 ($\leqslant$5ps/km) are typical of nominally-round telecommunications-grade fibres with low core-cladding index differences[62]. However, in a long length of fibre, random mode-coupling may average this dispersion to give a much smaller effective value over the fibre length (see sub-section 6.2.2). In this instance, the polarisation-dispersion is no longer proportional to length[63, 64, 2] and measurements using the above method encounter difficulty as indicated in ref. 50. Measurements of polarisation-dispersion in fibres with mode-coupling or length-invariant properties cannot be performed by observing the output polarisation state. Instead, we must observe the temporal coherence of the fibre output as the input state is varied, thus effectively "integrating" the dispersion over the whole fibre length. Either a modulated light source[65], or an interferometer to compensate for the relative group-delays at the output[66, 67]. The depolarisation of the output[65, 68, 69] as a function of the source spectral-width may be utilised[2].

Measurements using these techniques[50, 66] in telecommunications-grade fibres give $\Delta\tau_o \simeq 1\text{pskm}^{-1}$, a value considerably lower than that measured in short lengths - indicating that mode-coupling does indeed occur. In contrast, measurements in 1km-long high-birefringence fibres[65, 67] produce $\Delta\tau_o$ values of ~ 0.1ns/km which are proportional to fibre length, indicating negligible coupling. Although one mode may be transmitted, any coupling into the unwanted mode at bends, twists or at joints with misaligned principal axes[70] can severely limit the fibre bandwidth.

6.2.5 Polarisation-dispersion in twisted and spun fibres

As shown in Chapters Four and Five, twisting or spinning a linearly-birefringent fibre uniformly couples the two linearly-polarised modes. These modes exchange power along the fibre (see equations (4.5) and (4.6)). Because the coupling is deterministic and length-invariant, new fibre normal modes may be found[32, 48, 71]. These new eigenstates are elliptically-polarised[65] and are given by equation (4.22) [72].

$$U_{1,2} = \left[\hat{x}(z) - i(\rho \pm \sqrt{1+\rho^2})\hat{y}(z)\right].\exp\left[i(\beta_S \pm \gamma)z\right] \tag{6.7}$$

where

$$\rho = \frac{\Delta\beta}{2(\xi-\alpha)} \tag{6.8}$$

$$\gamma = \tfrac{1}{2}\sqrt{\Delta\beta^2 + 4(\xi-\alpha)^2} \tag{6.9}$$

and $\Delta\beta$ is the intrinsic birefringence of the fibre, ξ the twist rate, α the twist-induced rotation $= g'\,\xi$ and $\hat{x}(z)$ and $\hat{y}(z)$ are unit vectors along the x and y axes in the twisted co-ordinate system. β_S is a common phase factor given by $\beta_S = \tfrac{1}{2}(\beta_x + \beta_y)$ where β_x, β_y are the propagation constants for the two linear modes of the untwisted fibre.

The normal modes define the polarisation mode-dispersion for a twisted or spun fibre. To first order, the variation in the ellipticity of these modes due to the dispersion of $\Delta\beta$ and α is negligible, particularly at high twist rates ($\rho \ll 1$) when these modes are almost circularly-polarised. The modes may be considered to have a fixed polarisation state with a relative difference in propagation constants of 2γ. The polarisation-dispersion becomes:

$$\Delta\tau = \frac{z}{c}.\frac{d(2\gamma)}{dk} \tag{6.10}$$

$$\therefore \quad \Delta\tau = \frac{\left[\rho\,\Delta\tau_o - 2\,\frac{z}{c}.\frac{d\alpha}{dk}\right]}{\sqrt{1+\rho^2}} \tag{6.11}$$

The final term represents the dispersion of the stress-optic twist-induced rotation α (see sub-section 6.2.3). $\Delta\tau_o$ is the dispersion in the untwisted linearly-birefringent fibre given by equation (6.1).
For a large twist or spin rate ($\xi >> \Delta\beta$) we obtain, using equation (6.4):

$$\Delta\tau = \frac{\Delta\beta}{2(\xi-\alpha)} . \Delta\tau_o - \frac{2z}{c} . \frac{d\alpha}{dk} \qquad (6.12)$$

Spun Fibres:

For a spun fibre $\alpha = 0$ and equation (6.12) becomes (for $\xi >> \Delta\beta$).

$$\Delta\tau = \frac{\Delta\beta}{2\xi} . \quad \Delta\tau_o \qquad (6.13)$$

Because the modes of a tightly-spun fibre are circularly-polarised, this expression also follows directly from equation (4.33) by differentiating the rotation $\Omega(z)$ in a spun fibre.

Therefore spinning a fibre to produce low-birefringence gives the additional advantage that the polarisation mode-dispersion may be reduced by up to two orders of magnitude in inverse proportion to the spin rate.

The result predicted by equation (6.13) represents the reduction in dispersion to be expected in any two-mode guide with deterministic mode-coupling[43].

Measurements of polarisation-dispersion in a spun section of fibre VD319 were performed as described in sub-section 6.2.3. Figure 6.7 shows the linear birefringence as a function of wavelength for both unspun and spun sections of this fibre. The linear birefringence of the spun fibre remains small at all wavelengths. The circular rotation (not shown) is also small. Because the normal modes of a spun fibre are circularly-polarised, the derivative of the rotation was used to evaluate the polarisation-dispersion, as previously discussed. In this fibre $\Delta\tau$ was estimated to be ~0.06 ps/km. This is a dramatic reduction compared with the value of 5.15 ps/km at 1.3μm in the unspun fibre.

A spun fibre is evidently highly suitable for high-bandwidth communication.

Twisted Fibres:

Twisting a fibre influences the dispersion $\Delta\tau_o$ in the same way as spinning. However, the photo-elastic dispersion now becomes significant. In a highly-twisted fibre the linear birefringence is quenched to give:

$$\Delta\tau_c \simeq \frac{-2z}{c} \cdot \frac{d\alpha}{dk} \tag{6.14}$$

$$\Delta\tau_c \simeq \frac{-2z}{c} \cdot \xi \cdot \frac{dg'}{dk} = -2\,\frac{z}{c} \cdot \frac{d(C/n)}{dk} \cdot \frac{\alpha n}{C} \tag{6.15}$$

Figure 6.8 shows the dispersion $|\Delta\tau_c|$ calculated using the results for g' (Figure 6.5) obtained in a twisted, spun fibre. For comparison, the results for bulk silica calculated from equations (6.3) and (6.4) are also shown.

A dispersion of ~2.2ps/km is found in a twisted fibre at λ = 1.3μm which is comparable with the dispersion in a nominally-round telecommunications-grade fibre. Thus far from reducing the dispersion of conventional fibres[73], a twisting produces considerable dispersion which, since these fibres have poor polarisation-maintenance properties[74], will result in significant bandwidth reduction.

6.3 Temperature Dependence of Birefringence

The temperature stability of a fibre sensor device or isolator is heavily dependent on the variation of fibre birefringence with temperature[27, 28, 75].

The thermal expansion-coefficient of silica and doped silica is extremely small ($\sim 10^{-7} - 10^{-6}\ K^{-1}$)[76], while the change in refractive index with temperature is of the order $\sim 10^{-5}\ K^{-1}$[59]. The birefringence B_G due to core ellipticity, which is defined by the core dimensions and core-cladding refractive-index difference is therefore not expected to be temperature dependent. On the other hand, the stress giving rise to birefringence B_S is a strong function of temperature.

The stress contribution B_S can be expressed as[31]

$$B_S = \frac{CE}{1-\nu}(\alpha_1-\alpha_2)\Delta T \cdot [X] \tag{6.16}$$

where

E	=	Young's modulus,
$\alpha_{1,2}$	=	expansion coefficients of stress-inducing glasses,
ΔT	=	difference between room temperature T_r and T_s, the lowest fictive temperature of the constituent glasses of the fibre.
$[X]$	=	a factor depending on the fibre geometry,
ν	=	Poisson's ratio, assumed constant.

The temperature coefficient of stress-birefringence is obtained by differentiation:

$$\frac{dB_S}{dT}\Big/ B_S = \frac{1}{C}\frac{dC}{dT} + \frac{dE}{dT}\frac{1}{E} + \frac{1}{\Delta T} + \frac{1}{(\alpha_1-\alpha_2)}\cdot\frac{d(\alpha_1-\alpha_2)}{dT} \tag{6.17}$$

Data on α_1 and α_2 in fibre glasses is scarce and it is frequently assumed that the expansion coefficient of a doped silica glass is proportional to the dopant concentration as in bulk samples[76]. However, the vastly different thermal history of glasses in fibres compared to bulk samples can be expected to have a marked effect on thermal expansion coefficient. Furthermore, the dopant concentration in a fibre fabricated by the CVD technique is not accurately known (see Section 4.2). The values of ΔT is particularly sensitive to thermal history and is largely unknown in fibres and is frequently estimated[77] from bulk sample values[45, 78, 79].

Since the elastic properties of doped-silica are generally assumed not to depend sensitively on doping[45], the bulk silica values for Young's modulus E[58] and its derivative dE/dT[80] are considered to be good estimates of the parameters for fibres. Due to the lack of data on the temperature dependence of C in glasses, the temperature variation of the twist-induced rotation g' was measured in a twisted, spun fibre,[28] using the procedure described in sub-section 6.2.3. The temperature dependence of C may be obtained from measurements of g' versus temperature, using the derivative of equation (6.4):

$$\frac{dC}{dT} = \frac{-1}{R_0}\left[g'\cdot\frac{dn_c}{dT} + n_c(T)\cdot\frac{dg'}{dT}\right] \qquad (6.18)$$

The variation of g' with temperature was determined at a wavelength of 1.06μm in the same length of spun fibre used to measure g' versus wavelength in sub-section 6.2.3. As previously, five turns of twist were applied to the fibre. The tube furnace described in Chapter Three was used to vary the average temperatures along the fibre from 20-180°C. The measured variation of g' is shown in Figure 6.9, with a first-order Chebyshev fit. The stress-optic rotation coefficient g' varies linearly with temperature over the range shown, with a slope dg'/dT of $8.95 \times 10^{-6}\ K^{-1}$. This yields a temperature coefficient

$1/g' . dg'/dT$ of 1.27×10^{-2} % K^{-1}, which compares well with the value of 0.96×10^{-2} % K^{-1} reported previously on a very similar fibre[81].

In equation (6.18) the bulk silica values for $n_c(T)$ and dn_c/dT may be used because the fibre core has a very low dopant concentration ($3.4^m/o$) [28]. From Malitson[59] $dn_c/dT = 10.93 \times 10^{-6}$ K^{-1} at $T = 25^oC$ and $1.064\mu m$. This yields from equation (6.18), $\frac{dC}{dT} = -4.31 \times 10^{-15}$ m^2 kg^{-1} K^{-1} at $\lambda = 1.064\mu m$ and $T = 25^oC$. The only other published value of $\frac{dC}{dT}$ known to the author is -3.34×10^{-15} m^2 kg^{-1} K^{-1} for a high silica bulk glass with composition 67.5% SiO_2 15.4% B_2O_3, 16.7% K_2O, 0.4% MgO [82]. The result obtained here indicates that neither doping nor thermal history significantly affect the value of dC/dT. The results for C and g' are summarised in Table 6.1.

The variation of stress-birefringence with temperature given by equation (6.17) has been measured experimentally in silica-core stress-birefringent fibres as $\simeq -0.2$% K^{-1} [83]. However, the percentage change in C, $^1/C.\ dC/dT$ is + 0.0134% K^{-1} from our results. The temperature dependence of C makes a small negative contribution to the variation of B_s with temperature[84]. In fact, insertion of these values and the values for bulk silica of $E = 7.45 \times 10^9$ kgm^{-2} [58] and $dE/dT = 1.03 \times 10^6$ kg m^{-2} K^{-1} [80], and $\Delta T = -1000^oC$ [45] into equation (6.17) reveals that the variation in expansion coefficient difference $\alpha_1 - \alpha_2$ is a significant contribution to the temperature dependence of B_s. Unfortunately, the scant knowledge of expansion coefficients in doped silica glasses prevents confirmation of this.

The temperature variation of birefringence affects most fibre sensor applications[28]. Although a spun fibre has no temperature sensitivity of its own, the bending and twist used to provide controlled birefringence for sensing (see Chapter Five) are temperature sensitive. For example, controlled bending is used in isolators[75], polarisation controllers[23], filters[24] and sensors[20, 21]. The bend birefringence $\delta\beta_B$ for a fibre of outer radius r bent to a radius R′ is

$$\delta\beta_B = \frac{\pi EC}{\lambda} \cdot \left(\frac{r}{R'}\right)^2 \qquad (6.19)$$

from which the fractional change in bend birefringence is obtained:

$$\frac{d}{dT}(\delta\beta_B) \cdot \frac{1}{\delta\beta_B} = \left(\frac{1}{C}\frac{dC}{dT} + \frac{1}{E}\frac{dE}{dT}\right) \qquad (6.20)$$

Evaluation of equation (6.20) at 1.064μm [28, 80] gives 0.027% K^{-1} which is considerably less than the value of 0.063% K^{-1} previously reported in a similar fibre[81] at λ = 0.633 μm. However , the former result is confirmed by measurements of bend birefringence in a 40 turn Faraday isolator coil[74,85] at .633μm. The temperature dependence of bend birefringence gives an operating range for the isolator of about 20°C. The variation will similarly affect the operation of other fibre devices based on controlled bend-birefringence.

Fibre devices based on twisting a fibre such as the twisted fibre Faraday-effect current transducer[22] are also temperature sensitive. The variation in g' with temperature given in Figure 6.9 should result in a substantial zero drift[22] in this current transducer.

A 10.37m coil with 15 turns/m twist[22] would, from our results, exhibit a variation of the output plane of rotation of 0.5 ° K^{-1}. The variation observed in practice was considerably higher and thought to arise from the fibre coating used[86]. A twisted fibre which maintains circular polarisation[73] will also exhibit a variation in the output polarisation direction with temperature. This is expected to cause severe operational problems in coherent transmission systems[12] and interferometers[18].

6.4 The Separation of Stress and Waveguide Birefringence

Isolation of the relative contributions to intrinsic birefringence due to stress and waveguide effects can further the understanding of birefringent fibres and assist in their design and fabrication. The total birefringence is the algebraic sum of the two effects. However, whereas the sign of B_G is a fixed relative to the core minor axis, B_S can have either sign[41].

Fibre geometry and refractive-index profile measurements provide an obvious means of calculating B_G and B_S [87]. These techniques, however, have severe drawbacks because the accurate determination of core ellipticity, particularly at low ellipticity values, is difficult and an accurate knowledge of the core-cladding index grading, the fibre V-value[88] and Δ' value as well as a detailed thermal stress-model for the fibres are required[77, 78, 79].

More viable alternatives for isolating the stress and waveguide effects may be obtained by exploiting their respective dependences on temperature and wavelength. Since the waveguide-birefringence B_G is virtually independent of temperature, measurements of fibre birefringence as a function of temperature in principle yields B_S via equation (6.17). However, the scant knowledge of the thermal properties of the fibre preclude obtaining quantitative results. Nevertheless, estimates of the magnitudes of B_S and hence B_G as well as their signs may be obtained, by observing the trend of total fibre birefringence B with temperature since B_S generally decreases with temperature[83] — which must be kept below 200°C to avoid altering the structure[83]. The expected trends of B measured relative to the fibre core minor axis are shown in Table 6.2, for various possible combinations of B_S and B_G. Note that B_G is always positive with respect to the minor axis, while B_S can be of either sign. When B_S is positive B falls as the temperature increases (cases 1 and 3). In contrast B rises towards more positive values with increasing temperature if B_S has the opposite sign to B_G (cases 2 and 4). The overall sign of B or the trend in $|B|$ distinguishes between cases 2 and 4.

Figure 6.10 shows the birefringence observed as a function of temperature in an elliptical-core high-birefringence fibre[39] (the cross-section is shown in Figure 4.11 (b)). The least squares fit shown clearly indicates that case 1,2 or 3 of Table 6.2 applies. However, the fibre geometry predicts a value for B_G only 15% below the overall birefringence measured[31]. This would seem to indicate that B_S is a relatively small contribution and that case 1 applies.

Another result, obtained in a low-birefringence fibre (BP01) [89], is shown in Figure 6.11. In this case $|B|$ rises with an increase in temperature indicating that this fibre must be classified under case 4. The result therefore suggests simply that the stress birefringence partially cancels a much larger waveguide effect.

The different variations of $\Delta\beta_S$ and $\Delta\beta_G$ with fibre V-value (or wavelength) shown in Figure 6.12 can provide a quantitative means of isolating the two effects in a fibre[32, 49]. Measurements of fibre birefringence are usually taken over a limited wavelength range and it is assumed that $\Delta\beta_S$ and $\Delta\beta_G$ are both linear functions of V-value[32, 50]. The subsequent separation of $\Delta\beta_G$ and $\Delta\beta_S$ using this assumption relies heavily on both the accuracy of the measurement and careful interpretation of the data[31, 50]. Alternatively, $\Delta\beta_G$ may be assumed constant over the range of wavelengths used[32]. $\Delta\beta_S$ is evaluated by extrapolating the curve for B to zero V-value[60, 32]. This not only magnifies experimental errors but also endangers the validity of the assumption of constant $\Delta\beta_G$.

An alternative technique has been developed[31] which exploits the zero polarisation-dispersion due to B_G (see Figure 6.1). This point occurs at a V-value just beyond the second-order mode cut-off depending on the core ellipticity[34, 36], close to the normal range of V values used in PMD measurements and requires only a small extrapolation of the PMD data obtained by differentiating the birefringence vs. wavelength results (sub-section 6.2.4). The technique however, has several disadvantages:

(i) differentiating birefringence is particularly susceptible to experimental error;

(ii) the estimate of the fibre V-value may be inaccurate[88]

(iii) the core ellipticity is required and

(iv) a step-index fibre is assumed.

However precise ellipticity measurements are unnecessary for values less than ~10% since the zero-dispersion point is always close to V = 2.47 in such cases.

Having determined zero-dispersion point, B_S may be evaluated using equation (6.2). The theoretical curve for PMD due to the waveguide effect (Figure 6.1) is then fitted to the PMD data to obtain B_G. A typical result for PMD in a fibre (VD319) is shown in Figure 6.2 (dots). This fibre had a core-ellipticity below 10% and so the zero-dispersion point could be evaluated directly from the cut-off V value, obtained by the polarisation-extinction method[90]. Extrapolation of the dispersion data to V = 2.47 yields a dispersion of 2.565 ps/km giving a stress birefringence $B_S = 7.2 \times 10^{-7}$ at $\lambda = 0.93\mu m$, from equation (6.3) and Figure 6.4.

Note that because the dispersion at V = 2.47 is positive, B_S is positive i.e. its fast axis lies parallel to the core minor axis. Had the dispersion been negative, B_S would also have been negative. The upward trend of dispersion from the "zero point" with decreasing V value indicates that the ellipticity birefringence is also positive as expected. The solid line shown on the Figure was obtained using the value for Δ' of 0.5% from the refractive-index profile and predicted a core ellipticity of 4.3%, compared with the measured ellipticity of ~ 3 per cent. At a V value of 1.82 (λ = 1.3μm) the stress and ellipticity contributions are calculated to be $B_S = 7.0 \times 10^{-7}$ and $B_G = 1.8 \times 10^{-7}$.

6.5 Summary

This Chapter has examined the effect of source wavelength and ambient temperature on the properties of birefringent fibres. The variation of fibre birefringence with wavelength gives rise to polarisation mode-dispersion (PMD) which can limit the overall bandwidth, particularly in the absence of chromatic dispersion, or when using a monochromatic source. PMD can be reduced or eliminated by using an ultra-low birefringence fibre, or a strongly-birefringent, polarisation-maintaining fibre. It has been shown that the stress-optic effect, upon which so many fibre birefringence phenomena depend, is also dispersive, contributing about 10% to the dispersion of a stress-birefringent fibre. In contrast, the dispersion in a twisted circularly-birefringent fibre is entirely due to the stress-optic effect.

Mode-coupling plays an extremely important role in determining the polarisation mode-dispersion. Random mode-coupling causes a sub-linear dependence of PMD on fibre length. On the other hand, uniform deterministic mode-coupling, introduced for example, by fibre twisting, redefines the fibre normal modes. The dispersion between the new modes is linear and is reduced compared to the untwisted fibre by a factor proportional to the fibre twist.

As already indicated, twist introduces a stress-optic dispersion. However in a spun fibre no such dispersion exists resulting in a negligibly-low PMD value. These fibres are expected to find considerable applications in high-bandwidth communication systems.

A novel technique for PMD measurement, based on the variation of fibre birefringence with wavelength, has been described. In the presence of mode-coupling this method is no longer applicable and other measurement techniques must be used.

The variation of fibre birefringence with temperature arises from changes in stress and the temperature dependence of the stress-optic coefficient C. The latter can considerably affect the operating temperature range of many fibre devices or sensors based on controlled birefringence.

Finally, several techniques to isolate the waveguide and thermal stress contributions to fibre intrinsic birefringence have been discussed and demonstrated in principle. These methods exploit the temperature and wavelength effects already discussed in this Chapter. It appears that these techniques, which are currently subject to considerable error, could be made sufficiently accurate to yield quantitative results. However , at present the diagnostic information produced by these techniques is invaluable for the understanding of fibre birefringence and in the improvement of the production of birefringent fibres.

6.6 References

1. Schlosser, W. O.: "Delay Distortion in weakly guiding optical fibres due to elliptic deformation of the boundary", Bell Syst. Tech. J., 51, 1972, pp. 487-492.

2. Rashleigh, S. C., and Ulrich, R.: "Polarisation mode-dispersion in single-mode fibres", Optics Lett., 3, 1978, pp. 60-62.

3. Marcuse, D., and Lin, C.: "Low dispersion single-mode fibre transmission - the question of practical versus theoretical maximum transmission bandwidth", IEEE J. Quantum Electron., QE-17, 1981, pp. 869-878.

4. Tsuchiya, H., and Imoto, N.: "Dispersion-free single-mode fibre in 1.5μm wavelength region", Electron. Lett., 15, 1979, pp. 476-478.

5. Adams, M. J., Payne, D. N., and Ragdale, C. M.: "Birefringence in optical fibres with elliptical cross-section", Electron. Lett., 15, 1979, pp. 298-299.

6. Gambling, W. A., Matsumura, H., and Ragdale, C. M.: "Mode dispersion, material dispersion and profile dispersion in graded-index single-mode fibres", Microwaves, Optics and Acoustics, 3, 1979, pp. 239-246.

7. Snyder, A. W., and Sammut, R. A.: "Dispersion in graded single-mode fibres", Electron. Lett., 15, 1979, pp. 269-271.

8. White, K. I., and Nelson, B. P.: "Zero total dispersion in step-index monomode fibres at 1.30 and 1.55μm", Electron. Lett., 15, 1979, pp. 396-397.

9. Chang, C. T.: "Minimum dispersion at 1.55μm for single-mode step-index fibres", Electron. Lett., 15, 1979, pp. 765-767.

10. Kawana, A., et al.: "Pulse broadening in long-span single-mode fibres around a material-dispersion-free wavelength", Optics Lett., 2, 1978, pp. 106-108.

11. Kawana, A., Miya, T., Imoto, N., and Tsuchiya, H.: "Pulse broadening in long-span dispersion free single-mode fibre at 1.5μm", Electron . Lett., 16, 1980, pp. 188-189.

12. Fevre, F., Jeunhomme, L., Joindot, I., Monerie, M., and Simon, J. C.: "Progress towards heterodyne-type single-mode fibre communications systems", IEEE J. Quantum Electron., QE-17, 1981, pp. 897-906.

13. Yamamoto, Y., and Kimura, T.: "Coherent optical fibre transmission systems", IEEE J. Quantum Electron., QE-17, 1981, pp. 919-935.

14. Eve, M.: "Bandwidth of long monomode fibre links in the presence of weak mode coupling", Electron. Lett., 16, 1980, pp. 80-81.

15. Barlow, A. J., Payne, D. N., Hadley, M. R., and Mansfield, R. J.: "Production of single-mode fibres with negligible intrinsic birefringence and polarisation mode-dispersion", Electron. Lett., 17, 1981, pp. 725-726.

16. Ulrich, R.: "Polarisation stabilisation on single-mode fibre", Appl. Phys. Lett., 35, 1979, pp. 840-842.

17. Kidoh, Y., Suematsu, Y., and Furuya, K.: "Polarisation control on output of single-mode optical fibres", IEEE J. Quantum Electron., QE-17, 1981, pp. 991-994.

18. Ulrich, R., and Johnson, M.: "Fibre ring interferometer: Polarisation analysis", Opt. Lett., 4, 1979, pp. 152-154.

19. Eickhoff, W.: "Temperature sensing by mode-mode interference in birefringent optical fibres", Optics Lett., 6, 1981, pp. 204-206.

20. Rashleigh, S. C.: "Acoustic sensing with a single-coiled monomode fibre", Optics Lett., 5, 1980, pp. 392-394.

21. Rashleigh, S. C.: "Magnetic-field sensing with a single-mode fibre", Optics Lett., 6, 1981, pp. 19-21.

22. Rashleigh, S. C., and Ulrich, R.: "Magneto-optic current sensing with birefringent fibres", Appl. Phys. Lett., 34, 1979, pp. 768-770.

23. Lefevre, H. C.: "Single-mode fibre fractional wave devices and polarisation controllers", Electron. Lett., 16, 1980, pp. 778-780.

24. Johnson, M.: "Single-mode fibre birefringent filters", Optics Lett., 5, 1980, pp. 142-144.

25. Yen, Y., and Ulrich, R.: "Birefringent optical filters in single-mode fibre", Optics Lett., 6, 1981, pp. 278-280.

26. Stolen, R. H., and Turner, E. H.: "Faraday rotation in highly birefringent optical fibres", Appl. Optics, 19, 1980, pp. 842-845.

27. Turner, E. H., and Stolen, R. H.: "Fibre Faraday circulator or isolator", Optics Lett., 6, 1981, pp. 322-323.

28. Barlow, A. J., and Payne, D. N.: "The stress-optic effect in optical fibres", to be published in IEEE J. Quantum Electron.

29. Cohen, L. G., Lin, C., and French, W. G.: "Tailoring zero chromatic dispersion into the 1.5-1.6μm low-loss spectral region of single-mode fibres", Electron. Lett., 15, 1979, pp. 334-335.

30. Fevre, F., and Le Guen, D.: "High frequency stability of laser diode for heterodyne communication systems", Electron. Lett., 16, 1980, pp. 709-710.

31. Payne, D. N., Barlow, A. J., and Ramskov Hansen, J.J.: "Development of low- and high-birefringence optical fibres", IEEE J. Quantum Electron., QE-18, 1982, pp. 477-488.

32. Eickhoff, W., Yen, Y., and Ulrich, R.: "Wavelength dependence of birefringence in single-mode fibre", Appl. Optics, 20, 1981, pp. 3428-3434.

33. Tjaden, D. L. A.: "Birefringence in single-mode optical fibres due to core ellipticity", Philips J. Res., 33, 1978, pp. 254-263.

34. Dyott, R. B., Cozens, J. R., and Morris, D. G.: "Preservation of polarisation in optical-fibre waveguides with elliptical cores", Electron. Lett., 15, 1979, pp. 380-382.

35. Yeh, C.: "Elliptical dielectric waveguides", J. Appl. Phys., 33, 1962, pp. 3235-3243.

36. Okamoto, K., Hosaka, T., and Sasaki, Y.: "Linearly single-polarisation fibres with zero polarisation mode dispersion", IEEE J. Quantum Electron., QE-18, 1982, pp. 496-503.

37. Ulrich, R., Rashleigh, S. C., and Eickhoff, W.: "Bending-induced birefringence in single-mode fibres", Optics Lett., 5, 1980, pp. 273-275.

38. Katsuyama, T., Matsumura, H., and Suganuma, T.: "Low loss single-polarisation fibres", Electron. Lett., 17, 1981, pp. 473-474.

39. Birch, R. D.: Private Communication.

40. Sasaki, Y., Okamoto, K., Hosaka, T., and Shibita, N.: "Polarisation maintaining and absorption-reducing fibres", Paper presented at Topical Meeting on Optical Fibre Communication, Pheonix, USA, April, 1982.

41. Kaminov, I. P.: "Polarisation in optical fibres", IEEE J. Quantum Electron., QE-17, 1981, pp. 15-22.

42. Petermann, K.: "Non linear transmission behaviour of a single-mode fibre transmission line due to polarisation coupling", J. Opt. Comm., 2, 1981, pp. 59-64.

43. Crosignani, B., Papas, C. H., and Di Porto, P.: "Modal dispersion in light guides in the presence of strong coupling", J. Opt. Soc. Am., 68, 1978, pp. 1586-1591.

44. Ramskov Hansen, J. J.: University of Southampton, Private Communication.

45. Kaminov, I. P., and Ramaswamy, V.: "Single-polarisation fibres : Slab model", Appl. Phys. Lett., 34, 1979, pp. 268-270.

46. Smith, A. M.: "Single-mode fibre pressure sensitivity", Electron. Lett., 16, 1980, pp. 773-774.

47. Johnson, M., "In-line fibre-optical polarisation transformer", Appl. Optics, 18, 1979, pp. 1288-1289.

48. Ulrich, R., and Simon, A.: "Polarisation optics of twisted single-mode fibres", Appl. Optics, 18, 1979, pp. 2241-2251.

49. Imoto, N., Yoshizawa, N., Sakai, J., and Tsuchiya, H.: "Birefringence in single-mode optical fibre due to elliptical core deformation and stress anisotropy", IEEE J. Quantum Electron., QE-16, 1980, pp. 1267-1271.

50. Imoto, N., and Ikeda, M.: "Polarisation dispersion measurement in long single-mode fibres with zero dispersion wavelength at 1.5μm", IEEE J. Quantum Electron., QE-17, 1981, pp. 542-545.

51. Yoshizawa, N., Yabuta, T., Kojima, N., and Negishi, Y.: "Jacketed optical fibre characteristics under lateral pressure", Appl. Optics, 20, 1981, pp. 3146-3151.

52. Filon, L. N. G., and Harris, F. C.: "The Photo-elastic dispersion of vitreous silica", Proc. Roy. Soc., A130, 1931, pp. 410-431.

53. Coker, E. G., and Filon, L. N. G.: "Photelasticity", C. U. P., 1957.

54. Jog, E. S.: "The dispersion of the stress-optical coefficient of vitreous silica", J. Indian Inst. Sci. A, 39, 1957, pp. 93-100.

55. Heymans, P., and Allis, W. P.: "The photo-elastic constants of celluloid, glass and fused quartz", J. Maths. Phys., 2, 1923, pp. 216-233.

56. Primak, W., and Post, D.: "Photo-elastic constants of vitreous silica and its elastic coefficient of refractive index", J. Appl. Phys., 30, 1959, pp. 779-788.

57. Sinha, N. K.: "Normalised dispersion of birefringence of quartz and stress optical coefficient of fused silica and plate glass", Phys. Chem. Glasses, 19, 1978, pp. 69-77.

58. Borrelli, N. F., and Miller, R. A.: "Determination of the individual strain-optic coefficients of glass by an ultrasonic technique", Appl. Optics, 7, 1968, pp. 745-750.

59. Malitson, I. H.: "Interspecimen comparison of the refractive index of fused silica", J. Opt. Soc. Am., 55, 1965, pp. 1205-1209.

60. Rashleigh, S. C., and Marrone, M.J.: "Polarisation-holding in a high-birefringence fibre", Electron. Lett., 18, 1982, pp. 326-327.

61. Barlow, A. J., and Varnham, M. P.: unpublished work.

62. Ainslie, B. J., Beales, K. J., Day, C. R., and Rush, J.D.: "The design and fabrication of monomode optical fibre", IEEE J. Quantum Electron., QE-18, 1982, pp. 514-523.

63. Okoshi, T.: "Single-polarisation single-mode optical fibres", IEEE J. Quantum Electron., QE-17, 1981, pp. 871-884.

64. Personick, S. D.: "Time dispersion in dielectric waveguides", Bell Syst. Tech. J., 50, 1971, pp. 843-859.

65. Monerie, M., Lamouler, P., and Jeunhomme, L.: "Polarisation mode dispersion measurements in long single-mode fibres", Electron. Lett., 16, 1980, pp. 907-908.

66. Mochizuki, K., Namihira, Y., and Wakabayashi, H.: "Polarisation mode dispersion measurements in long single-mode fibres", Electron. Lett., 17, 1981, pp. 153-154.

67. Shibata, N., Tateda, M., and Seikai, S.: "Polarisation mode dispersion measurement in elliptical core single-mode fibres by a sptial technique", IEEE J. Quantum Electron., QE-18, 1982, pp. 53-58.

68. Monerie, M., and Jeunhomme, L.: "Polarisation mode coupling in long single-mode fibres", Opt. Quantum Electron., 12, 1980, pp. 449-461.

69. Crosignani, B., and Di Porto, P.: "Degree of polarisation in a birefringent single-mode optical fibre", Electron. Lett., 18, 1982, pp. 15-16.

70. Monerie, M.: "Polarisation-maintaining single-mode fibre cables: influence of joins", Appl. Optics, 20, 1981, pp. 2400-2406.

71. Barlow, A. J., Ramskov Hansen, J. J., and Payne, D. N.: "Birefringence and polarisation mode-dispersion in spun single-mode fibres", Appl. Optics, 20, 1981, pp. 2962-2968.

72. McIntyre, P., and Snyder, A. W.: "Light propagation in twisted anisotropic media - application to photoreceptors", J. Opt. Soc. Am., 68, 1978, pp. 149-157.

73. Jeunhomme, L., and Monerie, M.: "Polarisation-maintaining single-mode fibre cable design", Electron. Lett., 16, 1980, pp. 921-922.

74. Barlow, A. J., and Payne, D. N.: "Polarisation maintenance in circularly birefringent fibres", Electron. Lett., 17, 1981, pp. 388-389.

75. Day, G. W., Payne, D. N., Barlow, A.J., and Ramskov Hansen, J. J.: "Faraday rotation in coiled, monomode optical fibres: isolators, filters and magnetic sensors", Optics Lett., 7, 1982, pp. 238-240.

76. Miller, S. E., and Chynoweth, A. G.: "Optical Fibre Telecommunications", Academic Press, 1979.

77. Namihira, Y., Ejiri, Y., and Mochizuki, K.: "Birefringence in elliptical-cladding single-polarisation fibres", Electron. Lett., 18, 1982, pp. 89-91.

78. Okamoto, K., Hosaka, T., and Edahiro, T.: "Stress analysis of optical fibres by a finite element technique", IEEE J. Quantum Electron., QE-17, 1981, pp. 2123-2129.

79. Varnham, M. P.: University of Southampton, Private Communication.

80. Spinner, S.: J. Am. Ceramic Soc., 39, 1956, pp. 113.

81. Smith, A. M.: "Birefringence induced by bends and twists in single-mode optical fibre", Appl. Optics, 19, 1980, pp. 2606-2611.

82. Morey, G. W.: "Properties of Glass", Reinhold, 1938, pp. 430-431.

83. Ramaswamy, V., Stolen, R. H., Divino, M. D., and Pleibel, W.: "Birefringence in elliptically clad borosilicate single-mode fibres", Appl. Optics, 18, 1979, pp. 4080-4084.

84. Cohen , L. G., and Fleming, J. W.: "Effect of temperature on transmission in light guides", Bell Syst. Tech. J., 58, 1979, pp. 945-951.

85. Day, G. W., Payne, D. N., Barlow, A. J., and Ramskov Hansen, J. J.: "Faraday rotation in tuned optical fibre coils", Paper presented at colloquium on "Optical Fibre Sensors", IEE, London, May, 1982.

86. Rashleigh, S. C.: Private Communication.

87. Sasaki, I., Payne, D. N., and Adams, M. J.: "Measurement of refractive index profiles in optical fibre preforms by spatial filtering technique", Electron. Lett., 16, 1980, pp. 219-221.

88. Marcuse, D.: "Principles of Optical Fibre Measurements", Academic Press, 1981.

89. The fibre was kindly supplied by BTRL, Ipswich.

90. Kato, Y., Kitayama, K., Seikai, N., and Uchida, N.: "Novel method for measuring cut-off wavelength of HE_{21}-, TE_{01} -, and TM_{01} modes", Electron. Lett., 15, 1979, pp. 410-411.

Parameter	Symbol	Units	Value at 1.064μm	Value at 1.3μm
Stress-optic coefficient	C	$m^2\ kg^{-1}$	-3.22×10^{-11}	-3.17×10^{-11}
Wavelength dispersion in C	$dC/d\lambda$	$m^2\ kg^{-1} nm^{-1}$	2.34×10^{-15}	2.32×10^{-15}
Relative dispersion in C	$1/C.\ dC/d\lambda$	$\%\ nm^{-1}$	-0.00729	-0.00734
Temperature coefficient of C	dC/dT	$m^2\ kg^{-1}\ K^{-1}$	-4.31×10^{-15}	-
Relative temp. coefficient of C	$1/C\ \ dC/dT$	$\%\ K^{-1}$	0.0134	-
Stress-optic rotation coefficient	g'	-	0.0706	0.0696
Wavelength dispersion in g'	$dg'/d\lambda$	nm^{-1}	-4.56×10^{-6}	-4.56×10^{-6}
Relative dispersion in g'	$1/g'.\ dg'/d\lambda$	$\%\ nm^{-1}$	-0.0065	-0.0066
Temperature coefficient of g'	dg'/dT	K^{-1}	8.95×10^{-6}	-
Relative temp. coefficient of g'	$1/g'.\ dg'/dT$	$\%\ K^{-1}$	0.0127	-

Table 6.1 Summary of the stress-optic properties measured for a silica fibre doped with 3.4 $^m/o$ GeO_2.

		Signs of B_G and B_S	Sign of B	Trend of $\|B\|$ with increase of temperature
1	$B_S > B_G$	B_G positive B_S positive	positive	decrease
2	$B_S > B_G$	B_G positive B_S negative	negative	decrease
3	$B_S < B_G$	B_G positive B_S positive	positive	decrease
4	$B_S < B_G$	B_G positive B_S negative	positive	increase

Table 6.2 The expected dependence of fibre birefringence on increasing fibre temperature for the various signs and magnitudes of the stress and core-ellipticity contributions.

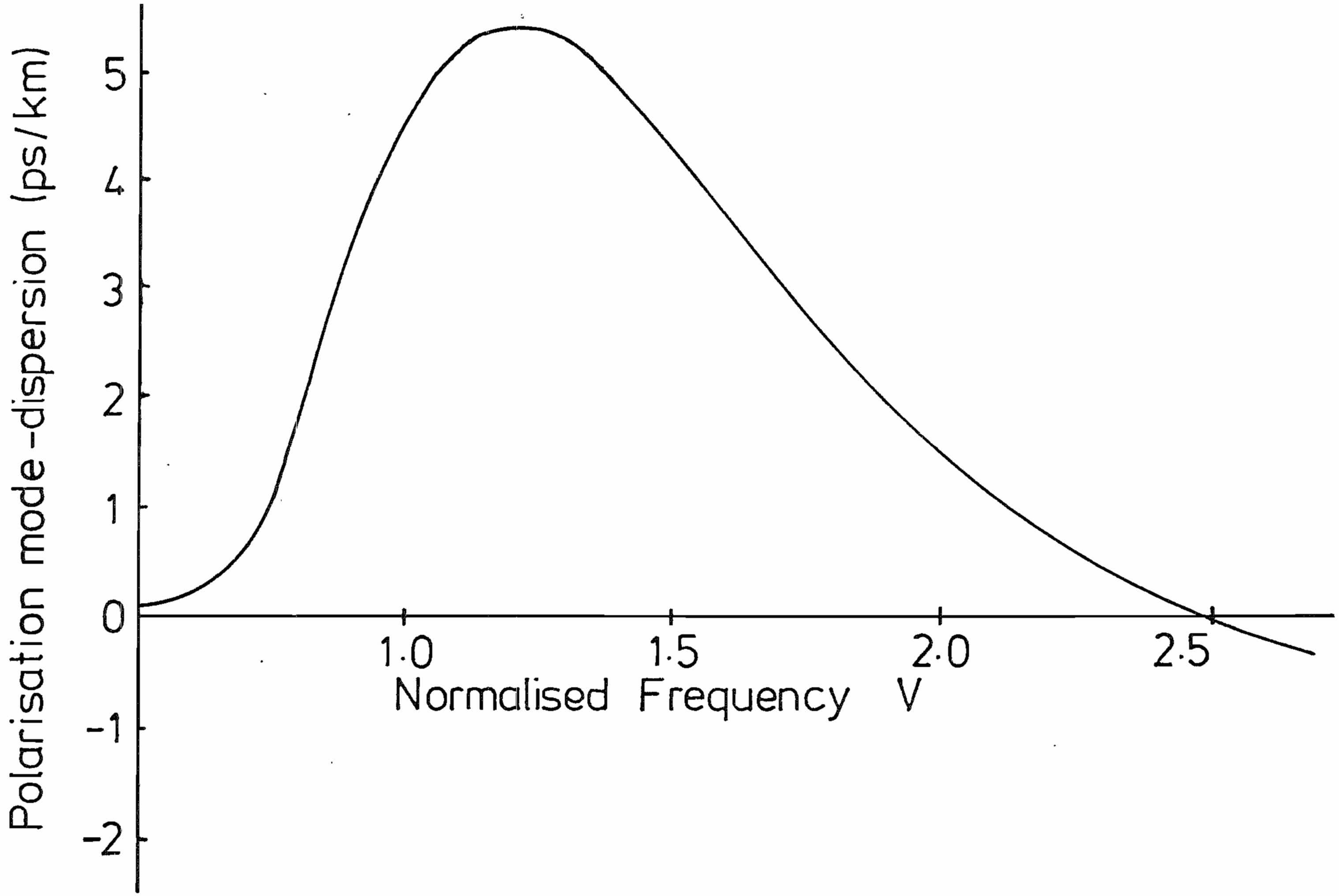

Figure 6.1 Polarisation mode-dispersion due to a core ellipticity (a/b-1) of 4.3%, in a fibre with relative index difference $\Delta' = 0.5\%$.

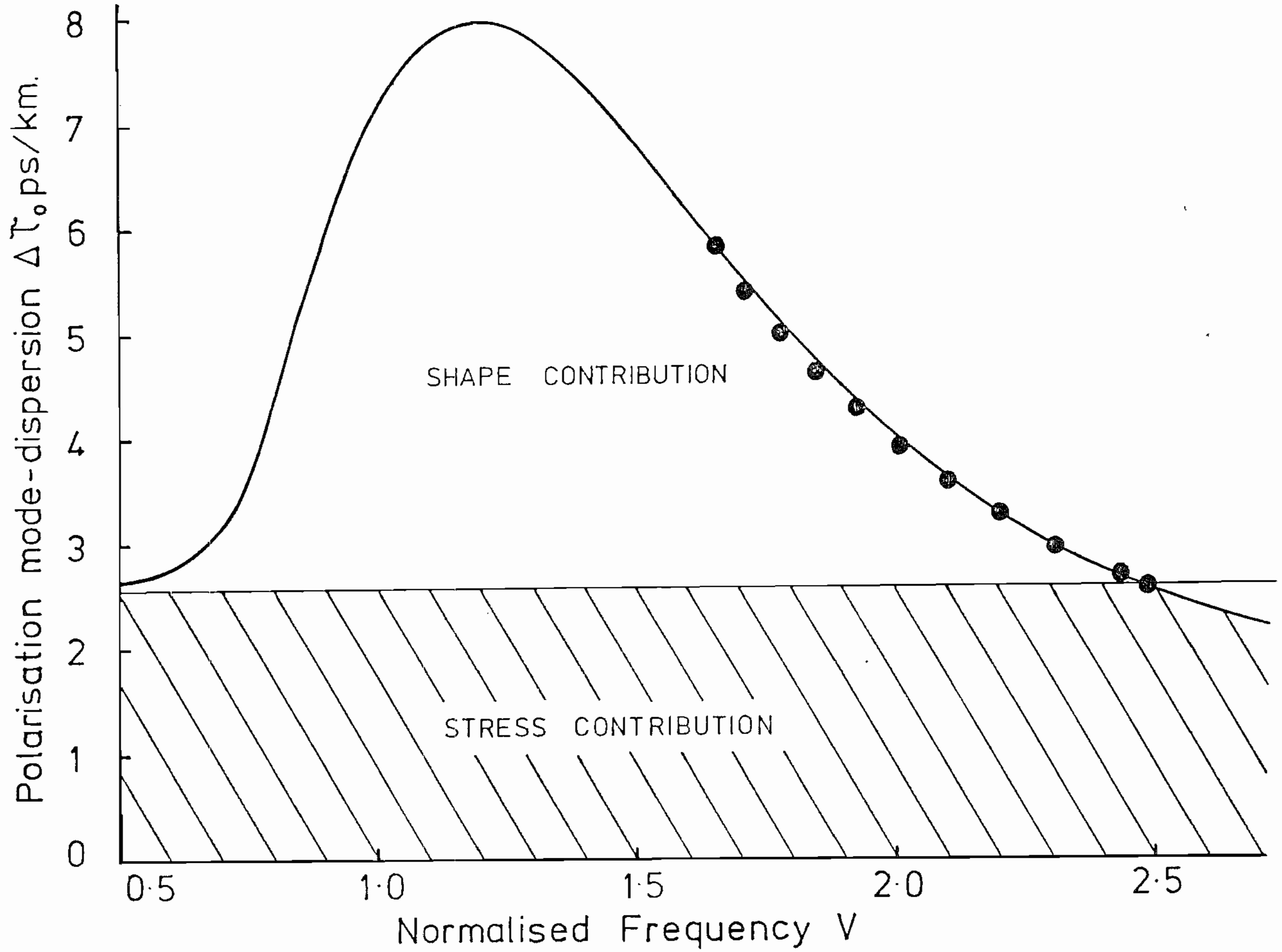

Figure 6.2 Polarisation mode-dispersion calculated in a typical telecommunications fibre with core ellipticity= 4.3% and Δ' = 0.5%, showing the relative contributions of stress and shape birefringence. Dots are experimental values calculated using Figure 6.7.

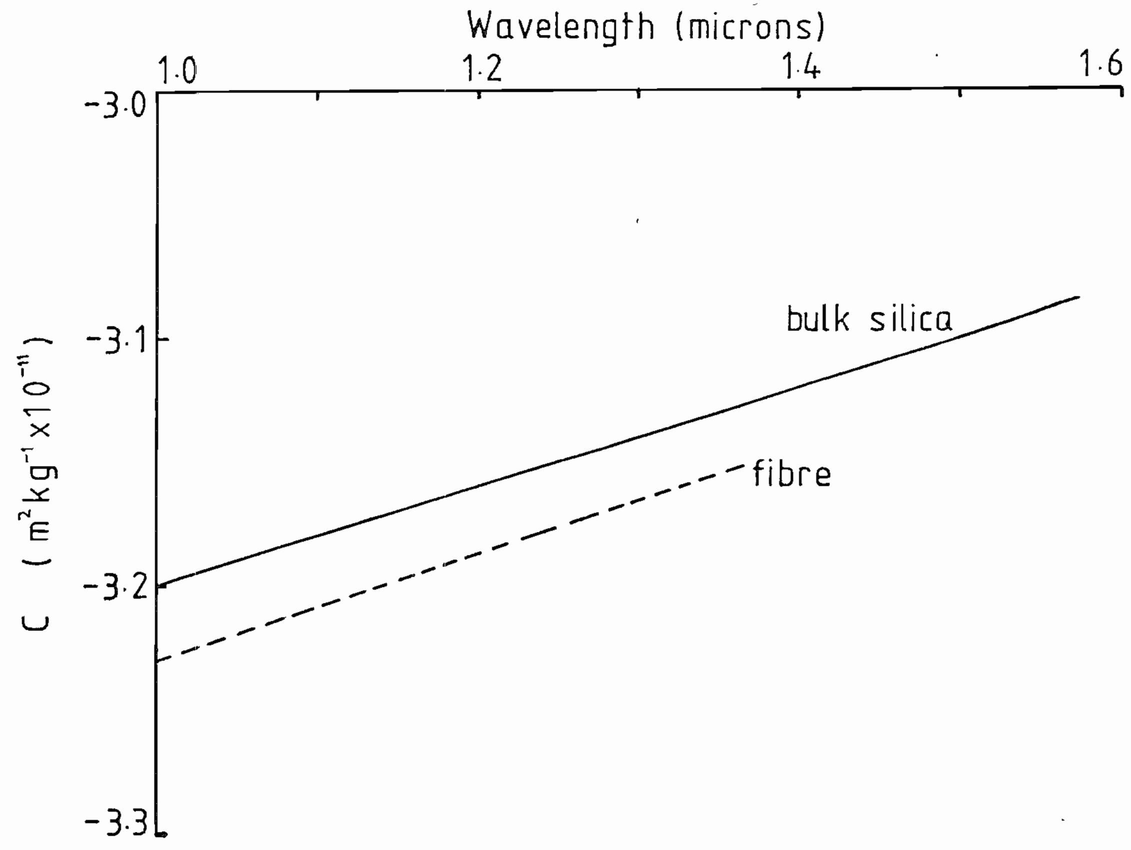

Figure 6.3 Variation of stress optic coefficient C with wavelength. The solid line is the result obtained for pure silica and the dashed line is that measured in a GeO_2-doped fibre.

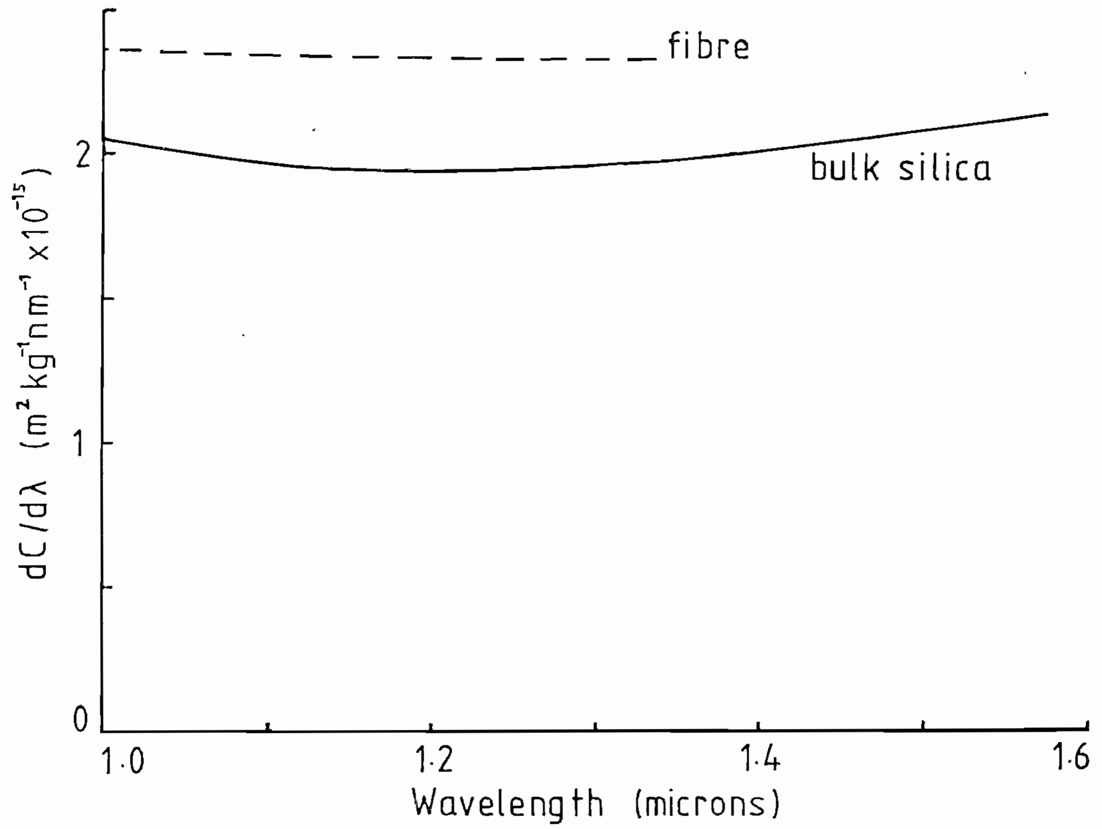

Figure 6.4 The dispersion of the stress-optic coefficient ($dC/d\lambda$) for bulk silica (solid line) and a GeO_2-doped fibre (dashed line).

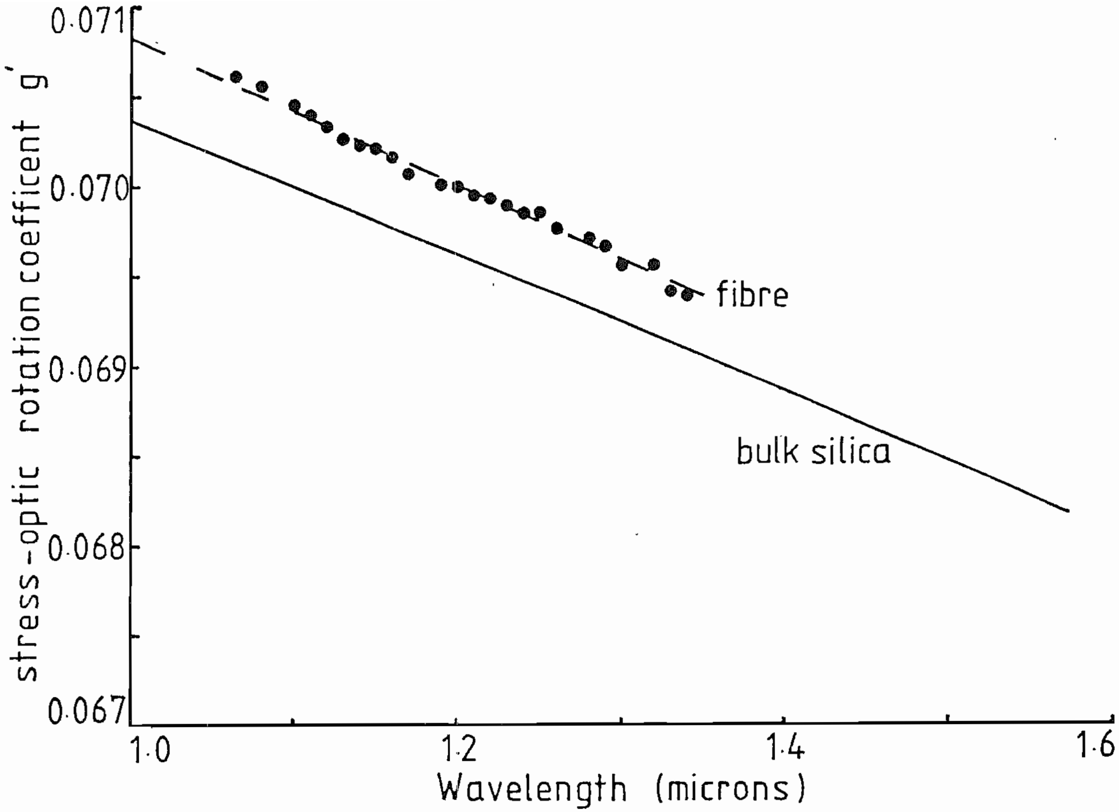

Figure 6.5 The variation of the stress-optic rotation coefficient g' with wavelength for bulk silica (solid line) and that measured in a fibre (dots). Dashed line is fitted to the experimental data.

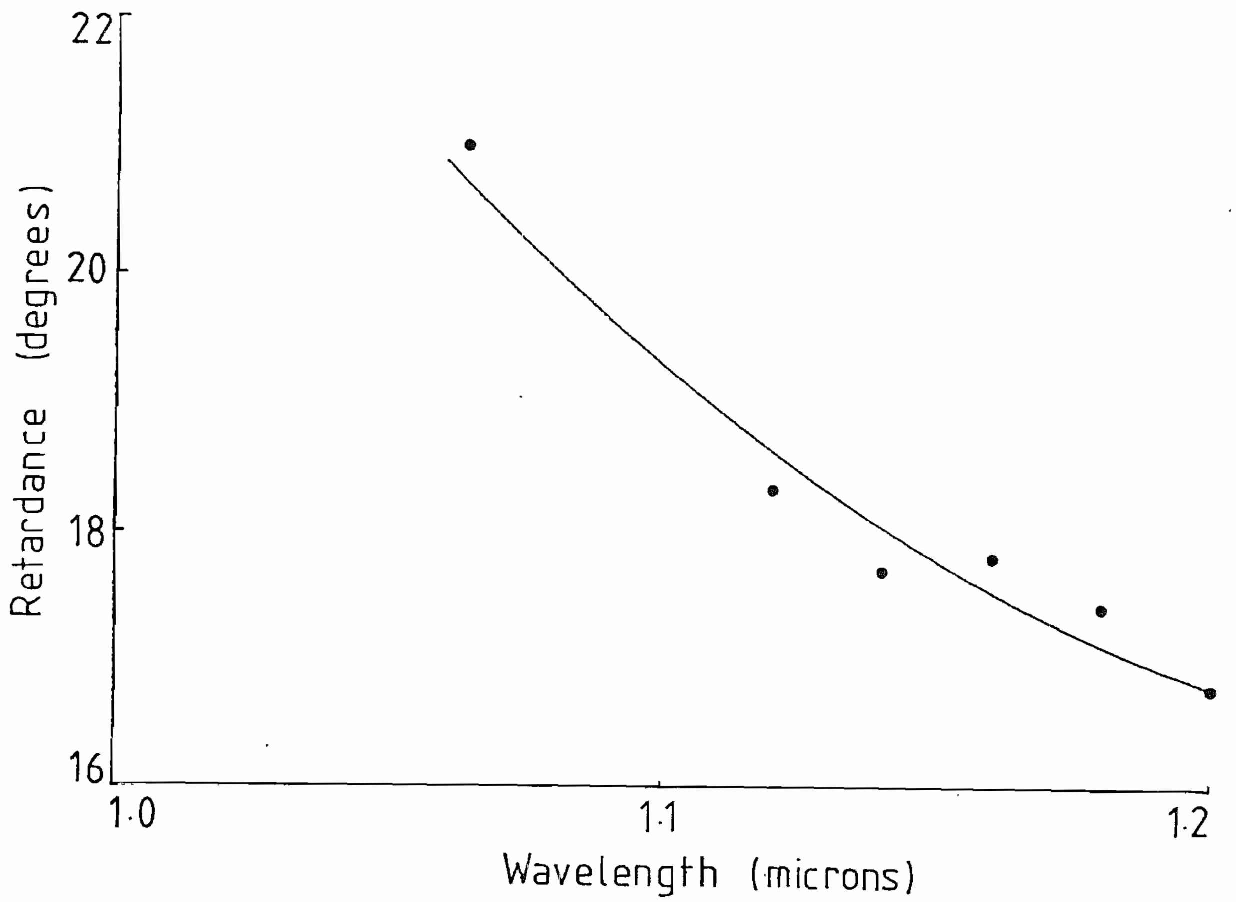

Figure 6.6 Measured variation in retardance with wavelength in fibre BP01 (dots).
Solid line is 2nd-order Chebyshev data fit.

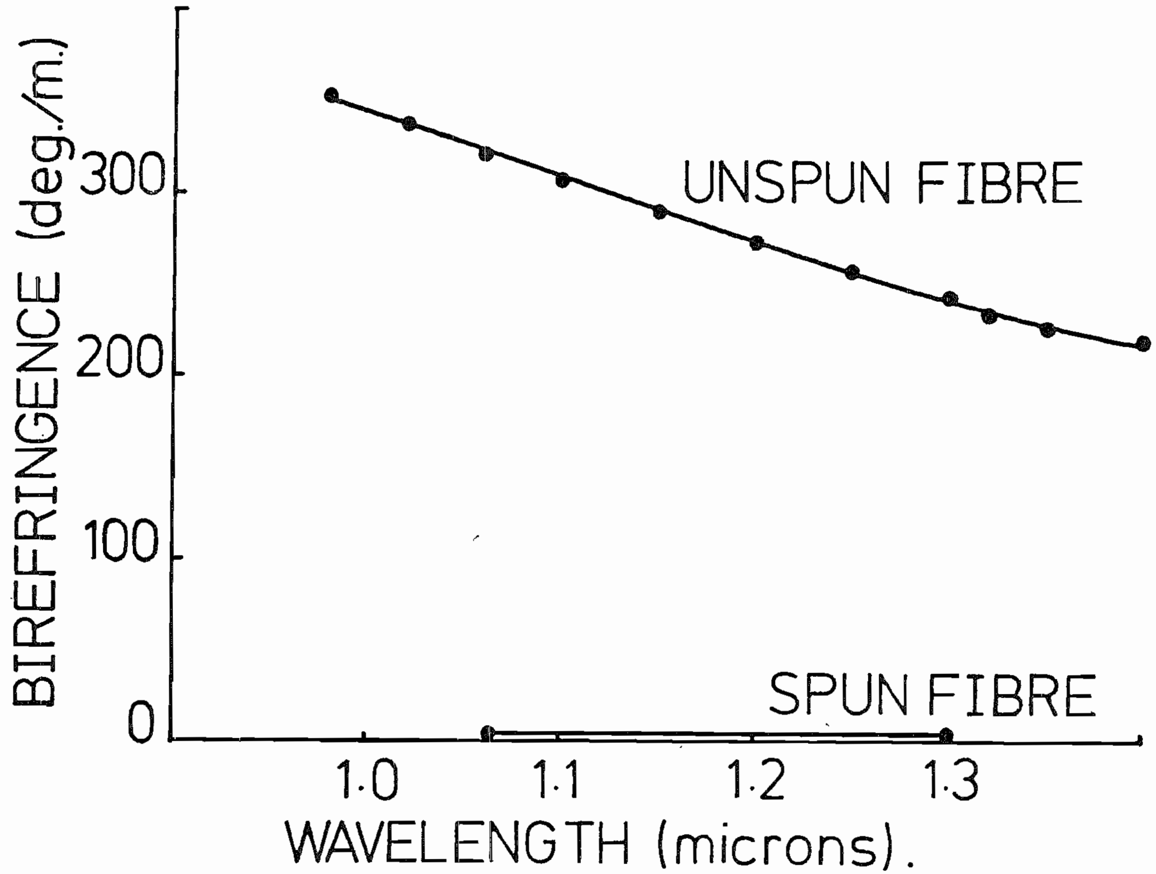

Figure 6.7 Measured variation in birefringence with wavelength for unspun and spun sections of fibre VD319. Solid lines are 2nd-order Chebyshev data fits.

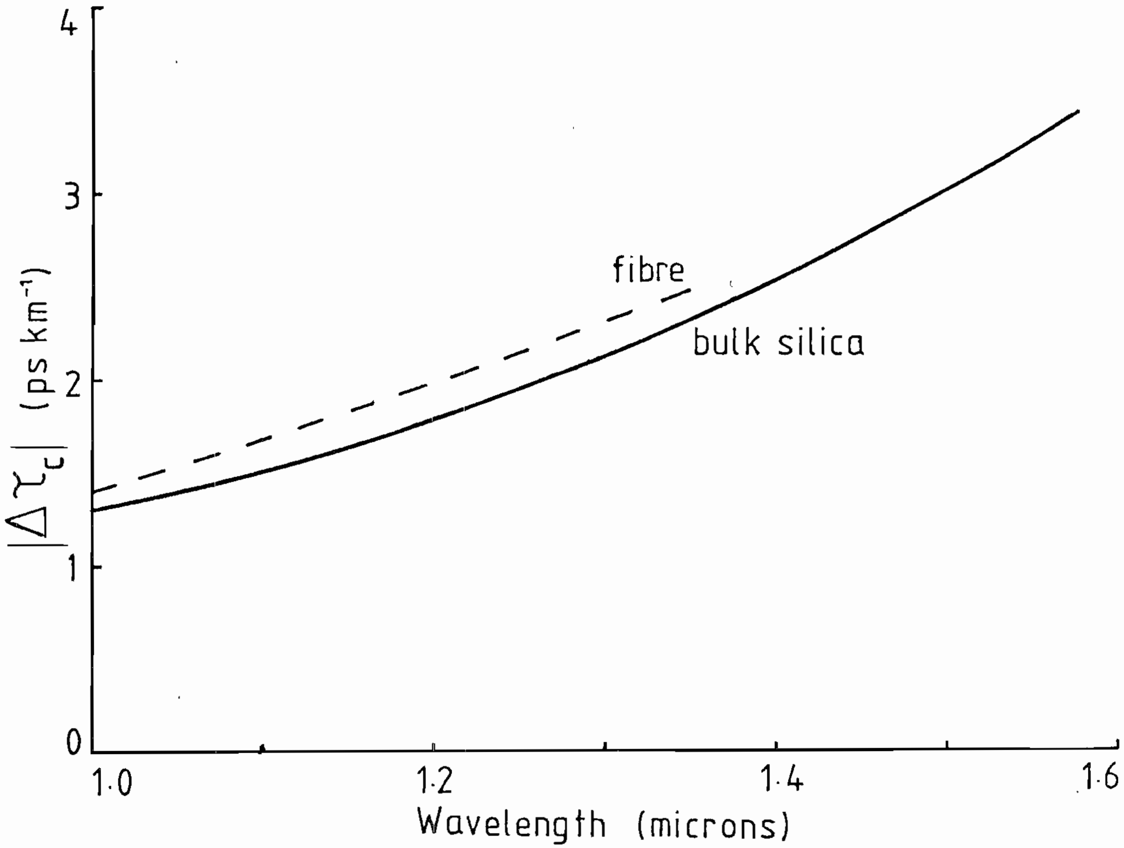

Figure 6.8 Calculated polarisation mode-dispersion in a fibre with 50 turns/m of twist as a function of wavelength; solid line is for bulk silica, dashed line is for GeO_2-doped fibre.

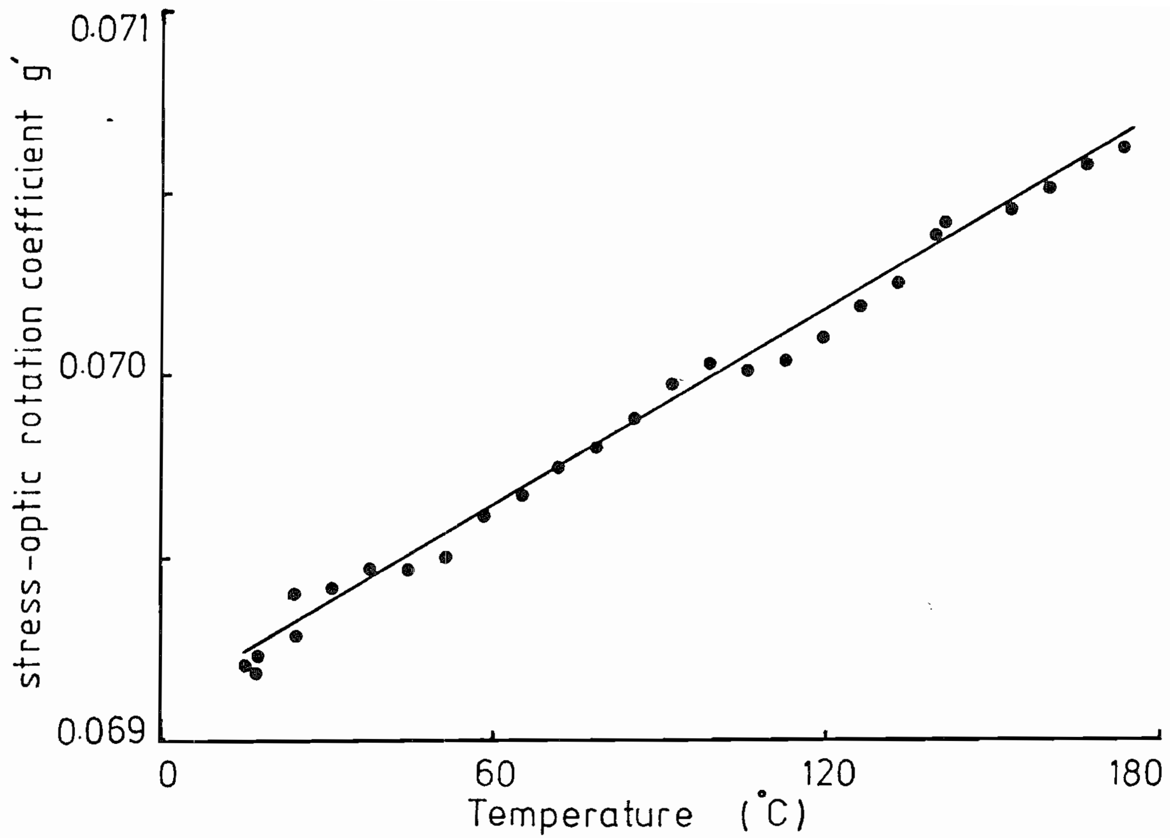

Figure 6.9 Measured variation of stress-optic rotation coefficient g' with temperature at 1.064μm wavelength.

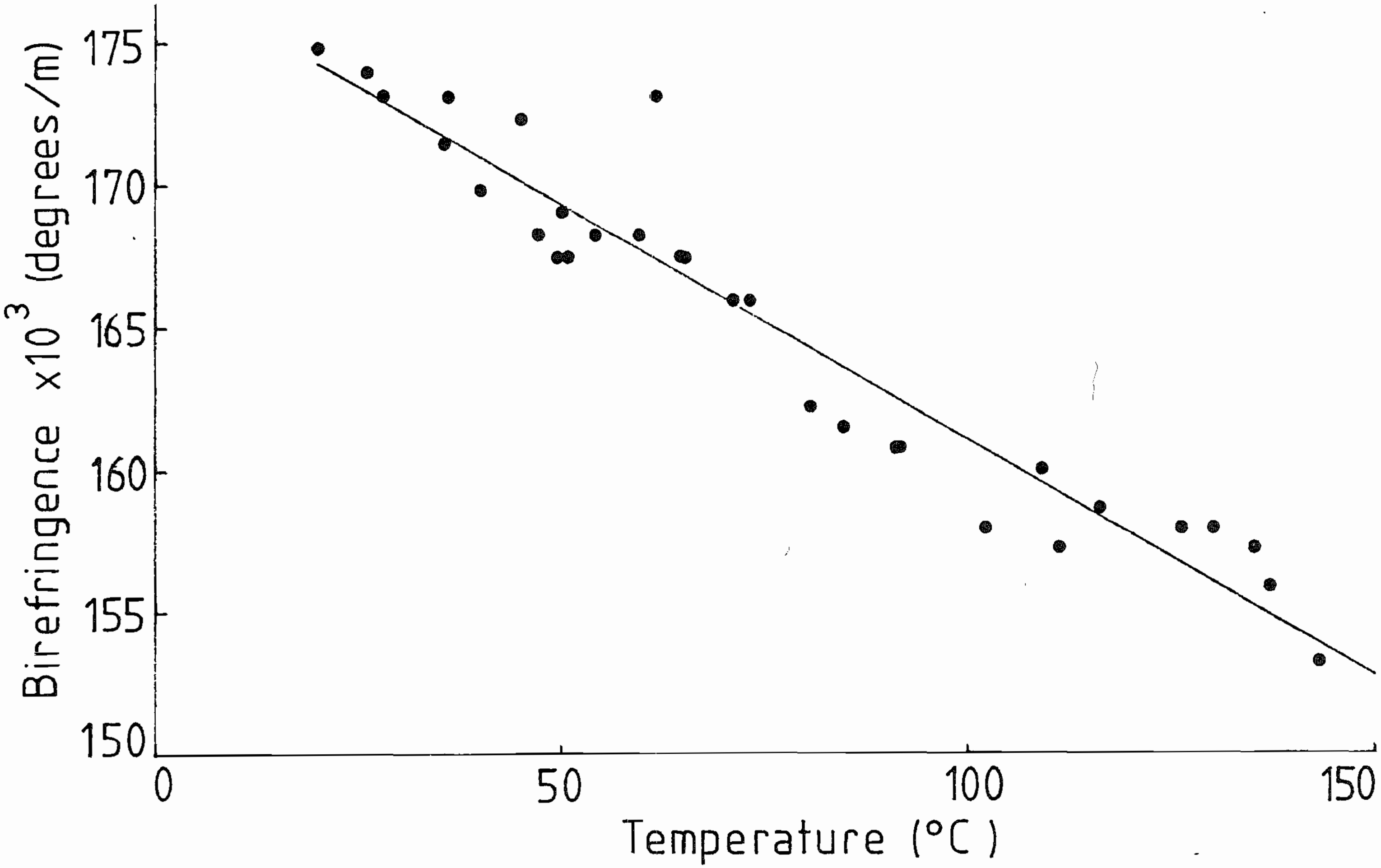

Figure 6.10 Measured variation of birefringence as a function of temperature in a high-birefringence elliptical-core fibre (VD299).

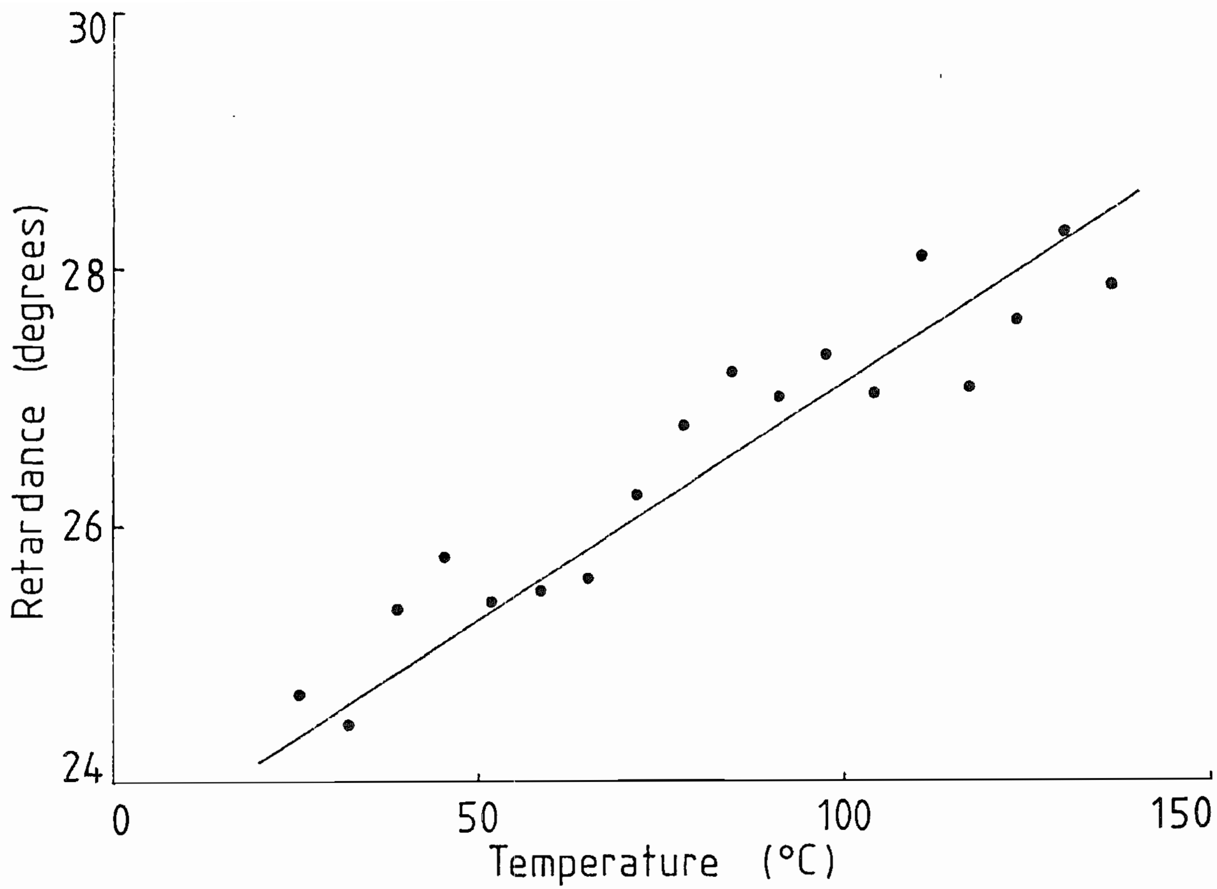

Figure 6.11 Measured variation of retardance as a function of temperature in a low-birefringence fibre (BP01).

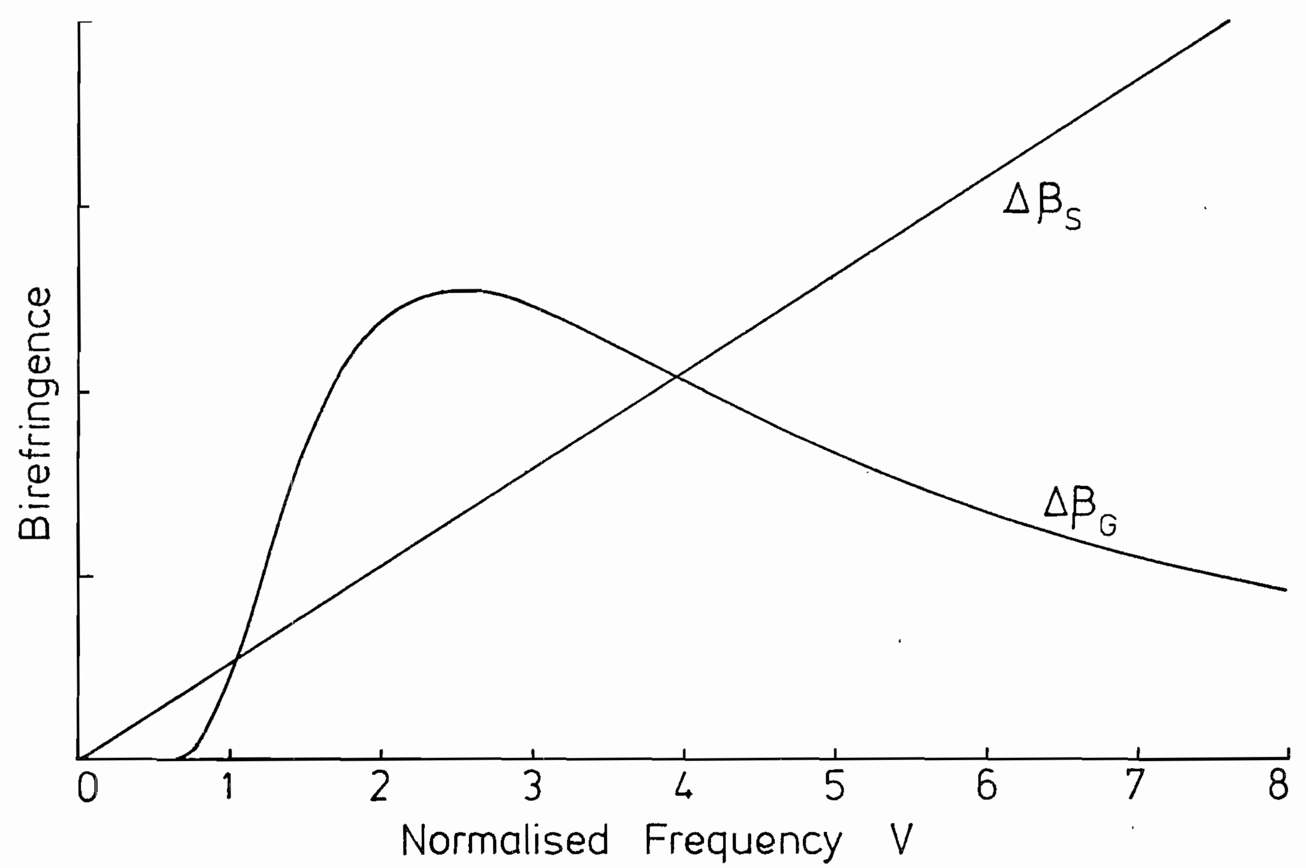

Figure 6.12 Schematic variations of stress and ellipticity birefringence $\Delta\beta_S$ and $\Delta\beta_G$ as a function of fibre V-value.

CHAPTER 7 CONCLUSION

7.1 Summary and Conclusions

The research programme described in this thesis has considered several aspects of birefringence in single-mode fibres. An overall view is now given of the themes of results described in the previous Chapters.

Fibre birefringence arises from intrinsic asymmetry and from extrinsic sources such as bending or twist. The latter results in essentially random fluctuations in the output polarisation state, thus producing polarisation noise in interfometers and polarisation sensitive (e.g. coherent) detectors. In addition, birefringence can introduce polarisation mode-dispersion which limits fibre transmission bandwidth. However, the unique environmental and electromagnetic[1] sensitivity of single-mode fibres can be put to good use in a fibre sensor.

In the systematic study of these effects which was described, the approach has been to make a theoretical study of a given phenomenon and subsequently confirm the results experimentally. By combining Jones Calculus and mode-coupling analysis, a powerful method for predicting the measured birefringence of a fibre has been developed. This method has been used to interpret the effects of bends, side pressure, twist, and magnetic fields on fibres with intrinsic linear or circular birefringence.

The study has repeatedly confirmed a most important concept in the subject of birefringence; "the degree of polarisation immunity from the environment (polarisation-maintenance) depends on the relative magnitudes and spatial periods of the intrinsic fibre birefringence and that produced by the external effects".

Thus high-birefringence fibres can provide stable output polarisation states, with the (usually) small power coupling between their modes avoiding the large polarisation-dispersion generally observed in these fibres. In contrast, a low-birefringence fibre is very sensitive to the environment, because its modes are easily coupled by extrinsic perturbations, but the polarisation-dispersion is small. Between these extremes, mode-coupling is significant and the substantial polarisation-dispersion is brought into play.

In consequence, selecting a fibre for a practical application involves a choice between high-birefringence (polarisation stability) and low-birefringence (environmental sensitivity), and fibre development has concentrated only on these types.

Several different fibre birefringence measurement techniques, to span the enormous range of birefringence observed in fibres, have been evaluated in the present work. Furthermore, a new technique employing a photo-elastic modulator has been adapted from standard ellipsometric methods to cover the entire range and provide faster and more sensitive measurements than previously possible.

The production of ultra-low birefringence fibres has been discussed in detail. A new process called 'spinning' has been developed as a direct consueqence of the investigation of twisted fibres. 'Spin' is a frozen-in twist, applied during drawing by rotating the preform, which averages the local asymmetry to produce near-perfect overall symmetry, and reduces polarisation-mode dispersion to negligible levels. The spinning process is such that low-birefringence may be obtained in any type of fibre with very high yield, and with no significant compromise to other fibre properties such as chromatic dispersion and attenuation. Spun fibres are thus extremely suitable for ultra-high bandwidth polarisation-insensitive communication and being very sensitive to external effects, are eminently suitable for sensors.

The development of high-birefringence fibres however, is by no means as advanced. The analysis of the fibre response to external effects presented here indicates that special cable structures for adequate polarisation-maintenance and beat lengths of ~5mm are necessary for the successful use of these fibres. The latter requirement can be regarded as a target for future production of such fibres.

Polarisation mode-dispersion has been studied by observing the variation of fibre birefringence with wavelength. Mode-coupling can be extremely effective in reducing dispersion with the result that long cable links generally have a much lower dispersion than might be expected from measurements in short lengths. Thus, nominally-round telecommunications fibre cables experience little bandwidth limitation at present 140 Mbit/s data rates. Future bit rates of 1G bit/s may well require the adoption of fibre spinning to reduce polarisation dispersion.

The variation of birefringence with temperature can significantly limit the operating range of fibre sensor devices employing controlled amounts of birefringence, whereas it may be exploited to isolate the intrinsic waveguide and stress birefringence contributions for diagnostic purposes. A similar method using variable wavelength has also been demonstrated.

7.2 Suggestions for Further Work

There are several topics covered in this thesis which still warrant further research.

Although the development of low-birefringence 'spun' fibres is largely complete, further improvements and adaptions of the process for large-scale production are required.

The development of high-birefringence fibres is still underway and the fabrication process is at present complex and unrepeatable. In particular, the analysis of thermal-stress birefringence in asymmetric fibre structures and the role of the cladding stresses need further attention. Evaluation of their attenuation and jointing properties is also required. Considerable research is required to characterise high-birefringence fibres in terms of their polarisation-holding parameters. Improvements in beat-length measurement techniques are urgently needed particularly at wavelengths beyond the visible region. A number of possibilities exist. The periodic variation in the output state as the wavelength is changed (beat-counting) or as a small local birefringence modulation is scanned along the fibre could be utilised. Characterisation of typical extrinsic disturbances in fibre cables is also required. It may be possible to use POTDR (see Chapter Three) to observe the increase of the power in the unwanted mode along the fibre at specific points of disturbance. If the spatial resolution of the technique can be improved, data on the spatial periodicity of natural disturbances may be obtained.

Evaluation of stress and core-ellipticity contributions to fibre birefringence using the methods proposed in Chapter Six will assist the development of high-birefringence fibres. Further improvements in fibre V-value measurements and the evaluation of the thermal and dispersive properties of glasses in fibres are necessary in order to fully exploit the potential of these methods in fibre fabrication diagnostics.

The measurement of birefringence using the photo-elastic modulator has been little more than demonstrated in the text. The system has now been characterised and the performance is as good as that predicted theoretically.

Perfect polarisation-maintenance is unattainable in high-birefringences fibres but this is not the case for single-polarisation fibres[2] since one mode is unguided. Considerable work on the development of single-polarisation fibres is required, however, before they can compete with, or replace, existing high-birefringence fibres.

The field of fibre sensors[3] is another exciting and potentially profitable future research area which was not considered within the scope of the present study. However, a thorough understanding of the polarisation response of fibres to external effects has now been established (see Chapter Five) and fibre sensor design is a logical extension of the work.
This would go hand-in-hand with the development of integrated-optic and single-mode fibre optic components[4] such as couplers, polarisers, modulators, de-polarisers, towards the realisation of solid-state fibre sensor devices.

7.3 Recent Developments

During the preparation of this thesis there have been several advances made in the areas of further study outlined in the previous section. A principal research objective in many laboratories throughout the world is now the production and characterisation of ultra-high birefringence fibres. This follows the achievement of sub-millimetre beat lengths in both stress-birefringent[5] and elliptical-core fibres[6], with reasonably low losses. Both complex numerical methods and simpler analytic treatments[7] have been developed to determine the stress-birefringence in various fibre structures such as the elliptical-jacket fibre[5]. The analytic method mentioned has indicated the existence of an optimum structure to give the highest birefringence for given fibre dopant levels. Very close approximations to this structure can now be routinely obtained in practice. These "bow-tie" structures (so-called because of the shape of the stress-applying jacket region) exhibit beat lengths often around 1mm, the best obtained so far being 0.6mm. Furthermore, losses of 1·8dB/km at 1050 nm have been obtained. Efforts are being currently made to improve the reproducibility and performance of these fibres.

In conjunction with this fabrication programme, methods of characterising the properties of high-birefringence fibres are also being investigated. The measurement of birefringence using the output polarisation state as described in Section 7.2 has been demonstrated[8]. A similar but more sensitive method of "beat counting" employing the photo-elastic modulator described in Chapter Three has been used to study the thermal aging properties of "bow-tie" fibres[9]. Not only has the technique proved extremely accurate, but also the dual retardation outputs allow complex beat length hysteresis effects to be observed.

Development of fibre devices such as the "resonant" Faraday isolator described in Chapter Five has also been undertaken[10]. The performance of this particular device is at present under evaluation but it appears that compact devices with isolation ratios in excess of 40dB can be manufactured relatively easily. Other devices are also being investigated.

The intense activity in the field of fibre interferometric and polarimetric sensors continues[3]. In particular, schemes for reducing the sensitivity of sensors to temperature[11] and also noise and drift in interferometers have been implemented.

7.4 Concluding Remarks

The objective of the research programme has been to extend and broaden the understanding and knowledge of the birefringence properties of single-mode fibres. This objective has been achieved in several areas. Results obtained may be and have been directly applied to practical fibre and sensor design. As a consequence of the present work, it is now possible to manufacture low-birefringence and high-birefringence fibres on a routine basis. Both types are now in great demand for a wide variety of applications.

The understanding of length-invariant extrinsic effects is now such as to produce a sense of direction and make a more theoretical approach to the design and operation of fibre sensors possible. However, the characterisation of non-uniform extrinsic effects in long fibre cables is still in its early stages.

In the future, research into birefringence will undoubtedly shift its emphasis from the basic conceptual groundwork covered so far to the practical application of birefringent fibres in fibre sensors and communications. Continued activity and growth in the subject is inevitable.

7.5 References

1. See for example, Maurer, R. D.: "Glass fibres for optical communications", Proc. IEEE, 61, 1973, pp. 452-462.

2. Okoshi, T., and Oyamada, K.: "Single-polarisation single-mode optical fibre with refractive-index pits on both sides of core", Electron. Lett., 16, 1980, pp. 712-713.

3. Giallorenzi, T. G., et al.: "Optical fibre sensor technology", IEEE J. Quantum Electron., QE-18, 1982, pp. 626-665.

4. Bergh, R. A., Lefevre, H. C., and Shaw, H. J.: "All-single-mode fibre-optic gyroscope", Optics Lett., 6, 1981, pp. 198-200.

5. Katsuyama, T., Matsumura, H., and Suganuma, T.: "Low loss single-polarisation fibres", Electron. Lett., 17, 1981, pp. 473-474.

6. Dyott, R. B., Cozens, J. R., and Morris, D. G.: "Preservation of polarisation in optical-fibre waveguides with elliptical cores", Electron. Lett., 15, 1979, pp. 380-382.

7. Barlow, A. J., Payne, D. N., Varnham, M. P., and Birch, R. D.: "Polarisation characteristics of fibres for coherent detection systems", Paper presented at colloquium on "Coherence in Optical Fibre Systems", IEE, London, 25 May, 1982.

8. Rashleigh, S. C.: "Wavelength dependence of birefringence in highly birefringent fibres", Optics Lett., 7, 1982, pp. 294-296.

9. Ourmazd, A.: University of Southampton, unpublished work.

10. Day, G. W., Payne, D. N., Barlow, A. J., and Ramskov Hansen, J. J.: "Faraday rotation in tuned optical fibre coils", Paper presented at colloquium on "Optical Fibre Sensors", IEE, London, 26 May, 1982.

11. Rashleigh, S. C.: "Fibre-optic sensors with reduced sensitivity to environmental perturbations", Appl. Optics, 20, 1981, pp. 1498-1499.

CHAPTER 8 PUBLICATIONS, CONFERENCE PRESENTATIONS AND PRIZES

The work presented in this thesis has resulted in the following publications, conference papers and prizes which are each listed in chronological order.

8.1 Publications

1. Barlow, A. J., and Payne, D. N.: "Polarisation maintenance in circularly birefringent fibres", Electronics Letters, 17, (11), May 1981, pp. 388-389.

2. Barlow, A. J., Payne, D. N., and Ramskov Hansen, J.J.: "Birefringence and polarisation mode-dispersion in spun single-mode fibres", Applied Optics, 20 (17), September 1981, pp. 2962-2968.

3. Barlow, A. J., Payne, D. N., Hadley, M. R., and Mansfield, R. J.: "Production of single-mode fibres with negligible intrinsic birefringence and polarisation mode dispersion", Electronics Letters, 17, (20), October 1981, pp. 725-726.

4. Barlow, A. J., Ramskov Hansen, J. J., and Payne, D.N.: "Anisotropy in spun single-mode fibres", Electronics Letters, 18, (5), March 1982, pp. 200-202.

5. Payne, D. N., Barlow, A. J., and Ramskov Hansen, J.J.: "Development of low- and high-birefringence optical fibres", IEEE J. Quantum Electronics, QE-18, (4), April 1982, pp. 477-488.

6. Day, G. W., Payne, D. N., Barlow, A. J., and Ramskov Hansen, J.J.: "Faraday rotation in coiled monomode optical fibres: isolators, filters and magnetic sensors", Optics Letters, 7, (5), May 1982, pp. 238-240.

7. Barlow, A. J., and Payne, D. N.: "The stress-optic effect in optical fibres", submitted to IEEE J. Quantum Electronics.

8.2 Conference Presentations

1. Barlow, A. J., and Payne, D. N.: "Birefringence testing in single-mode fibres manufactured with controlled polarisation characteristics", presented at colloquium on "Test Equipment for Optical Fibre Communication Systems" Institute of Electrical Engineers, London, UK, 28th May, 1981.

2. Barlow, A. J., Payne, D. N., Hadley, M. R., and Mansfield, R. J.: "Production of single-mode fibres with negligible intrinsic birefringence and polarisation mode-dispersion" Paper 2.3 presented at Seventh European Conference on Optical Communication, Copenhagen, Denmark, 8-11 September, 1981.

3. Payne, D. N., Barlow, A. J., Hadley, M. R., and Mansfield, R. J.: "Fabrication and properties of low-birefringence spun fibres", presented at "International Conference on Fibre-Optic and Rotation Sensors", Boston, USA, 9-11 November 1981.

4. Barlow, A. J., Payne, D. N., Varnham, M. P., and Birch, R. D.: "Polarisation characteristics of fibres for coherent detection systems", presented at colloquium on "Coherence in Optical Fibre Systems", Institute of Electrical Engineers, London, UK, 25th May, 1982.

5. Day, G. W., Payne, D. N., Barlow, A. J., and Ramskov Hansen, J.J: "Faraday rotation in tuned optical fibre coils" presented at colloquium on "Optical Fibre Sensors" Institute of Electrical Engineers, London, UK, 26th May, 1982.

6. Barlow, A. J., and Payne, D. N.: "Measurements of fibre polarisation properties using a photo-elastic modulator" to be presented at Symposium on Optical Fibre Measurements, Boulder, Colorado, USA, 13-14 October 1982.

8.3 Prizes

The ECOC Prize for 1981 was awarded jointly to Dr. D. N. Payne, Mr. R. J. Mansfield, Mr. M. R. Hadley and myself for the paper "Production of single-mode fibres with negligible intrinsic birefringence and polarisation mode-dispersion" presented at the Seventh European Conference on Optical Communication, Copenhagen, September 1982. The award was made by the Technical Programme Committee for the best presentation at the conference.

8.4 Patent Applications

1. Payne, D. N., Mansfield, R. J., Ramskov Hansen, J.J., Hadley, M. R., and Barlow, A. J.: "Twisted single mode fibre" UK Patent Application No. 8120996 (filed 7th July 1981). Also in USA and Europe (not Italy).

2. Barlow, A. J., Day, G. W., Payne, D. N., and Ramskov Hansen, J. J.: "Faraday rotation device" UK Patent Application No. 8212580 (filed 30th April 1982).

APPENDIX

TRANSFORMATION OF A JONES CALCULUS EQUATION TO OPERATE IN CIRCULARLY-POLARISED MODES

The Jones equation for a circularly-birefringent fibre under the influences of a linear birefringence in terms of linearly-polarised vectors A_x' and A_y' is written (Equation (5.31)):

$$\begin{bmatrix} A_x' \ (z) \\ A_y' \ (z) \end{bmatrix} = \begin{bmatrix} G & -H^* \\ H & G^* \end{bmatrix} \begin{bmatrix} A_x' \ (0) \\ A_y' \ (0) \end{bmatrix} \qquad (A.1)$$

where, in general terms,

$$G = u + i\,v \qquad (A.2)$$

$$H = s + i\,t \qquad (A.3)$$

A_x' (0) and A_y' (0) may be represented as a superposition of two left- and right-circularly polarised components with amplitudes $A_l(0)$ and $A_r(0)$ respectively. The input Jones vector $\begin{bmatrix} A_x' \ (0) \\ A_y' \ (0) \end{bmatrix}$ may be written as:

$$\begin{bmatrix} A_x' \ (0) \\ A_y' \ (0) \end{bmatrix} \equiv \frac{A_l \ (0)}{\sqrt{2}} \begin{bmatrix} i \\ 1 \end{bmatrix} + \frac{A_r \ (0)}{\sqrt{2}} \begin{bmatrix} -i \\ 1 \end{bmatrix} \qquad (A.4)$$

$$= \frac{1}{\sqrt{2}} \begin{bmatrix} i\ A_l\ (0) & - & i\ A_r\ (0) \\ A_l\ (0) & + & A_r\ (0) \end{bmatrix} \tag{A.5}$$

The output vector $\begin{bmatrix} A_x'\ (z) \\ A_y'\ (z) \end{bmatrix}$ may be similarly resolved into circularly-polarised output vectors $A_l\ (z)$ and $A_r\ (z)$. The matrix equation (A.1) becomes:

$$\begin{bmatrix} i\ A_l\ (z) & - & i\ A_r\ (z) \\ A_l\ (z) & + & A_r\ (z) \end{bmatrix} = \begin{bmatrix} G & -H^* \\ H & G^* \end{bmatrix} . \begin{bmatrix} i\ A_l(0) & - & i\ A_r\ (0) \\ A_l(0) & + & A_r\ (0) \end{bmatrix} \tag{A.6}$$

Multiplying out and equating real and imaginary parts yields:

$$A_l\ (z) = \left[A_l\ (0).\ u\ + A_r(0).\ t\right] + i\left[A_l\ (0).\ s - A_r(0).\ v\right] \tag{A.7}$$

$$A_r\ (z) = \left[A_r\ (0).\ u\ - A_l(0).\ t\right] + i\left[-A_r\ (0).\ s - A_l(0).\ v\right] \tag{A.8}$$

i.e.

$$\begin{bmatrix} A_l\ (z) \\ A_r\ (z) \end{bmatrix} = \begin{bmatrix} P & -Q^* \\ Q & P^* \end{bmatrix} \begin{bmatrix} A_l\ (0) \\ A_r\ (0) \end{bmatrix} \tag{A.9}$$

where

$$P = u + i\ s \tag{A.10}$$

$$Q = -t - i\ v \tag{A.11}$$

The matrix equation (A.9) is the new description of the fibre in circularly-polarised modes. The general transformation from linear to circular modes is the transformation equation (A.1) to equation (A.9)[1].

For the specific case under consideration, in equation (5.31) the common phase factor $e^{i\beta_s z}$ is neglected giving:

$$u = \cos\gamma z \tag{A.12}$$

$$v = \frac{\rho}{\sqrt{1+\rho^2}} \cdot \sin\gamma z . \cos 2\Theta \tag{A.13}$$

$$s = \frac{-1}{\sqrt{1+\rho^2}} \cdot \sin\gamma z \tag{A.14}$$

$$t = \frac{\rho}{\sqrt{1+\rho^2}} \cdot \sin\gamma z . \sin 2\Theta \tag{A.15}$$

where γ and ρ are defined in equations (5.34) and (5.35) respectively. From equations (A.10) and (A.11):

$$P = \cos\gamma z \quad - \quad i \frac{1}{\sqrt{1+\rho^2}} \quad \sin\gamma z \tag{A.16}$$

$$Q = \frac{-\rho}{\sqrt{1+\rho^2}} \; i \sin\gamma z \; . \; e^{-i2\Theta} \tag{A.17}$$

Thus the matrix equation (5.37) for a circularly-birefringent fibre subjected to a linearly-birefringent disturbance has been derived.

Reference to Appendix

1. Azzam, R. M. A., and Bashara, N. M.: "Ellipsometry and polarised light", North Holland, 1977, pp. 81-84.